Università di Genova

UNIVERSITÀ DEGLI STUDI DI GENOVA

DOCTORAL THESIS

Compound Impact on Private and Public Transport Network Performance on Integration of New Forms of Mobility

Author:

Muhammad Tabish BILAL

Supervisor:

Prof. Davide GIGLIO

Prof.ssa Angela Di FEBBRARO

A thesis submitted in fulfillment of the requirements

for the degree of Doctor of Philosophy

in the

Curriculum of Logistics and Transport

Dipartimento di Ingegneria meccanica, energetica, gestionale e dei trasporti (DIME)

January 23, 2023

UNIVERSITÀ DEGLI STUDI DI GENOVA

Abstract

Marine Sciences and Technology

Dipartimento di Ingegneria meccanica, energetica, gestionale e dei trasporti (DIME)

Doctor of Philosophy

Compound Impact on Private and Public Transport Network Performance on Integration of New Forms of Mobility

by Muhammad Tabish BILAL

Continued evolutions in autonomous drive technologies and pandemic leading to a boom in micro-mobility usage make these new forms of mobility an integral part of investigative research to assess their impacts on transportation networks. This research thesis examines their impacts in terms of: quantification of the penetration rate of AVs, the influence of physical characteristics of the urban road network on macroscopic fundamental parameters in heterogeneous traffic stream;ù, inequities in travel costs equilibrium, assessment of PuT network vulnerability against random service disruptions and importance of topography for accurate provision of micro-mobility services. Some benefits for 25-35% inclusion of AVs include enhanced network capacity, improvement in travel time, decrement in travel equilibrium costs. Whereas, the integrated micro-mobility modes reduce the commuter's disutility and perceived journey times by 7.14% in case of disruptions. However, the spill-over effects are to watch out for.

Contents

Abstract **iii**

1 Introduction **1**

1.1 **Relevance of research topic** 1

1.2 **Problem statement** 6

1.3 **Scope and objective** 8

1.4 **Research approach** 9

1.5 **Organization of thesis** 12

2 State of the art and practice **15**

2.1 **Introduction** 15

2.2 **An era of Autonomous Vehicles** 15

2.2.1 **Impacts on macroscopic network parameters** 16

2.2.2 **Equillibrium shift in Landuse - Transportation interactions** 22

2.2.3 **Key Takeaways** 25

2.3 **Public transport network vulnerability** 26

2.3.1 **Assessment of the public transport network** 27

2.3.2 **A boom of Micro-mobility** 30

2.3.3 **Key Takeaways** 35

3 Methodological framework **37**

3.1 **Introduction** 37

3.2 **Private transport network supply model setup** 37

3.2.1 **Network Structure** . . . 39
3.2.2 **Quantification of AVs** . . . 41
3.2.3 **Transport supply model** . . . 47
3.2.4 **Travel time and flow relationship** . . . 49
3.2.5 **Covex minimization inequity problem (Lower level optimization problem)** . . . 52
Frank Wolfe assignment algorithm . . . 54
3.2.6 **Bi-level optimization model (Upper level optimization problem)** . . . 55
Genetic algorithm . . . 59
Numerical example of inequity calculation . . . 62
3.3 **Public transport network vulnerability** . . . 63
3.3.1 **Network structure** . . . 64
3.3.2 **Multi-modal public transport model setup** . . . 66
3.3.3 **Shared micro-mobility supply model setup** . . . 71
3.3.4 **Data fusion** . . . 72
3.3.5 **Network structural evaluation** . . . 73
Dynamic Closeness . . . 73
Dynamic Betweenness . . . 74
3.3.6 **Vulnerable components** . . . 75
Based on unsupervised learning . . . 75
Nearest neighbors search via supervised learning . . . 77
3.3.7 **Random service disruptions** . . . 78

4 Inequity analysis for heterogeneous traffic stream on the introduction of AVs **81**
4.1 **Introduction** . . . 81
4.2 **Real network application** . . . 81
4.2.1 **Quantification of penetration rate** . . . 84

4.2.2 Senstivity analysis for quantified penetration rate . . 85
4.3 Macroscopic fundamental characteristics 87
4.4 Inequity analysis 92
4.4.1 Travel equilibrium impacts 102
4.5 Conclusions 109

5 Public transport vulnerability analysis **115**
5.1 Model implementation 115
5.2 Real network application 115
5.3 Network structural evaluation 118
5.3.1 Vulnerable components identification 122
5.4 Impacts of disruptions 134
5.5 Conclusions 140

6 Conclusions **141**
6.1 Potential impacts of the introduction of AVs 141
6.1.1 Private transportation network performance and traffic flows 142
6.1.2 Equillibrium shift in travel equilibrium costs 144
6.1.3 Limitations and future recommendations 144
6.2 Public transport network vulnerability 145
6.2.1 Network evaluation 146
6.2.2 Vulnerability of components against random disruptions 147
6.2.3 Limitations and future recommendations 148

A List of Publications **151**
A.1 Publications during the tenure of Ph.D. 151

Bibliography **153**

List of Figures

1.1 Major research queries of the study 9
1.2 Proposed methodology flowchart 12
1.3 Organization of the study 13

3.1 Bi-level optimization model 57
3.2 Example network 62
3.3 Framework for multi-modal transit network 66

4.1 (A) Area considered for application (B) Network of the considered area 82
4.2 Speed-density relationship for Scenario 0 and scenario A under sensitivity range of AVs 88
4.3 Speed-flow relationship for Scenario 0 and scenario A under sensitivity range of AVs 89
4.4 Decrement in vehicle speed with respect to Saturation grade . 90
4.5 Travel-time flow relationship with a link having physical median and no influence of opposite direction flow under sensitivity range of AVs 91
4.6 Travel-time flow relationship without a link having physical median and influence of opposite direction flow under sensitivity range of AVs 92
4.7 Travel-time flow relationship with physical and functional characteristics of links affecting travel time under sensitivity range of AVs 93

4.8 Fitness curves for GA with Upper inequity bound of 1.05, 1.07, 1.09 and 1.10 94
4.9 Total costs for SUE and SO assignment (Source: (Bilal and Giglio, 2022)) 95
4.10 Mean excess costs comparisons for only TVs and heterogeneous traffic stream scenario (Source: (Bilal and Giglio, 2022)) 96
4.11 Change in travel equilibrium costs for different Upper bounds for Zone 33, 34, 35,38, and 39 103
4.12 Change in volume for different upper bounds for zone 33, 34, 35,38, and 39 103
4.13 Change in travel equilibrium costs for different Upper bounds for Zone 40, 41, 42, 43, and 47 104
4.14 Change in volume for different upper bounds for zone 40, 41, 42, 43, and 47 104
4.15 Change in travel equilibrium costs for different Upper bounds for Zone 61, 62, 63, 64, 65, 66, and 67 105
4.16 Change in volume for different upper bounds for zone 61, 62, 63, 64, 65, 66, and 67 105
4.17 (A) Optimal minimized travel equilibrium costs for Origin zone 33; (B)Optimal minimized travel equilibrium costs for Origin zone 34 (C) Optimal minimized travel equilibrium costs for Origin zone 35 (D) Optimal minimized travel equilibrium costs for Origin zone 38 (E) Optimal minimized travel equilibrium costs for Origin zone 39 106

4.18 (A) Optimal minimized travel equilibrium costs for Origin zone 40; (B)Optimal minimized travel equilibrium costs for Origin zone 41 (C) Optimal minimized travel equilibrium costs for Origin zone 42 (D) Optimal minimized travel equilibrium costs for Origin zone 43 (E) Optimal minimized travel equilibrium costs for Origin zone 47 107

4.19 (A) Optimal minimized travel equilibrium costs for Origin zone 61; (B)Optimal minimized travel equilibrium costs for Origin zone 62 (C) Optimal minimized travel equilibrium costs for Origin zone 63 (D) Optimal minimized travel equilibrium costs for Origin zone 64 (E) Optimal minimized travel equilibrium costs for Origin zone 65 (F) Optimal minimized travel equilibrium costs for Origin zone 66 (G) Optimal minimized travel equilibrium costs for Origin zone 67 111

4.20 (A) Optimal maximized trip generation for Origin zone 33; (B)Optimal maximized trip generation for Origin zone 34 (C) Optimal maximized trip generation for Origin zone 35 (D) Optimal maximized trip generation for Origin zone 38 (E) Optimal maximized trip generation for Origin zone 39 112

4.21 (A) Optimal maximized trip generation for Origin zone 40; (B)Optimal maximized trip generation for Origin zone 41 (C) Optimal maximized trip generation for Origin zone 42 (D) Optimal maximized trip generation for Origin zone 43 (E) Optimal maximized trip generation for Origin zone 47 113

4.22 (A) Optimal maximized trip generation for Origin zone 61; (B)Optimal maximized trip generation for Origin zone 62 (C) Optimal maximized trip generation for Origin zone 63 (D) Optimal maximized trip generation for Origin zone 64 (E) Optimal maximized trip generation for Origin zone 65 (F) Optimal maximized trip generation for Origin zone 66 (G) Optimal maximized trip generation for Origin zone 67 114

5.1 (A) Barcelona PuT network in Visum (B) Line network coded in MATLAB for Barcelona PuT 116

5.2 (A) Genoa PuT network in Visum (B) Line network coded in MATLAB for Genoa PuT 117

5.3 (A) Nodes hierarchy based on inward closeness from other nodes for Barcelona (B) Nodes hierarchy based on outward closeness from other nodes for Barcelona 120

5.4 (A) Nodes hierarchy based on Betweenness for Barcelona (B) Link hierarchy based on dynamic betweenness 122

5.5 (A) Nodes hierarchy based on inward closeness from other nodes for Genoa (B) Nodes hierarchy based on outward closeness from other nodes for Genoa 123

5.6 (A) Nodes hierarchy based on Betweenness for Genoa (B) Link hierarchy based on dynamic betweenness 124

5.7 (A) Weighted dynamic closeness nodal centrality spread for Barcelona (B) Nodes grouped in 2 clusters 125

5.8 (A) Weighted dynamic betweenness link centrality spread for Barcelona (B) Links grouped in 3 clusters 126

5.9 (A) Weighted dynamic closeness nodal centrality spread for Genoa (B) Nodes grouped in 2 clusters 127

5.10 (A) Weighted dynamic betweenness link centrality spread for Genoa (B) Links grouped in 5 clusters 128
5.11 (A)Silhouette plot for k-mean clustering of nodes of Barcelona (B) Silhouette plot for k-mean clustering of Links of Barcelona 129
5.12 (A)Silhouette plot for k-mean clustering of nodes of Genoa (B) Silhouette plot for k-mean clustering of Links of Genoa 130
5.13 (A) High-ranked central nodes marked in red for the Barcelona transit network (B) High-ranked central links marked in red for the Barcelona transit network 131
5.14 (A) High-ranked central nodes marked in red for the Genoa transit network (B) High-ranked central links marked in red for the Genoa transit network 132

List of Tables

2.1 State of the art for Public transport and micro-mobility integration 32

3.1 Quantiles approach 47

4.1 Network data 84
4.2 Quantification of Penetration rate 85
4.3 Senstivity analysis results on the penetration rate of AVs . . . 86
4.4 Inequity model results for 1.05 upper bound. 98
4.5 Inequity model results for 1.07 upper bound. 99
4.6 Inequity model results for 1.09 upper bound. 100
4.7 Inequity model results for 1.10 upper bound. 101

5.1 Dynamic time series-based demand for Barcelona 118
5.2 Dynamic time series-based demand for Genoa 119
5.3 High-ranked candidate central components of the two transit networks selected for vulnerability analysis 133
5.4 Relative perceived journey time and commuter's disutility variations in various scenario combinations for the transit network of Barcelona 138
5.5 Relative perceived journey time and commuter's disutility variations in various scenario combinations for the transit network of Genoa 139

Chapter 1

Introduction

This chapter is a thorough introduction to the research; defining the problem statement, the relevance of the subject, and its scope together with the objectives of this research topic. The approach adopted for attaining the answers to the research question is briefly described followed by the structure of this thesis report describing the contents of each chapter onwards.

1.1 Relevance of research topic

Emerging transportation technologies can expand the way of mobilizing commuters and commodities. Going through the innovations of the last century in particular related to the transportation sector reveals that increased motorized modes elevated mobility by order of enormity, supplying large perks, as well as striking with greater costs on individual commuters and societies. The last century is considered to be the era of automobile paramountcy with the domination of automobiles in transportation systems and societies resulting in growing private car travel instigating a marring effect on the usage of other slow but sustainable modes. Favoritism towards quicker and more expensive modes was given in contrast to those that were rather cost-effective, adaptive, and healthy. All along the twenty-first century, trends became more diverse for many developed countries like the Netherlands, France, Germany, Sweden, China, etc. and more transportation diversity is likely to

be witnessed. Smart adoption for mobility needs based on integrated information models can result in more comfortable, cost-effective, socially inclusive, healthy, and reliable travel. Nonetheless, estimating the future is replete with ambivalence. The forecasts made decades ago related to current travel relying on jet packs, flying cars, moving sidewalks, and common space travel did not come to reality. That is not because of technological infeasibility but due to the change in commuter priorities from fast, farther, and low-effort travel to convenient, healthy, inclusive, and affordable commute.

However, recent technological advancements and transportation innovations in the form of autonomous vehicles (AVs) compelled policymakers and transport planners to re-evaluate their traditional methods of analyzing the impacts of their usage on transportation networks. Furthermore, the pandemic gave rise to a boom in the usage of e-scooters, bicycles, and other forms of micro-mobility. Their usage certainly affects the performance and ride demand of public transport. The dire need of the time is to analyze whether these micro-mobility modes are competing for traditional public transport or are completing them. This opens up a paradigm of possibility to investigate the compound impact of these new forms of mobility considering the priorities of convenience, socially inclusive, equitable, and reliable less vulnerable commute to unwanted halting circumstances in an overall transportation network including both private and public transportation.

As far as the adoption of AVs is concerned, (Carrese et al., 2019) identified that traffic lane usage policy is the most deciding factor among the user for the adoption of AVs. Not only this but their adoption will further increase the urban sprawl. This wave of relocation will consequently cast a positive impact on the central road network of the city of Rome whereas suburban flows will face a negative impact in terms of higher volumes and travel times. The study further suggests that only a shared adoption scheme of AVs can reduce the travel time by up to 19% for the whole network. However, travel

time costs, household costs, residential location, and land user costs are the factors that were completely ignored in this study making them a great limitation in terms of the quoted results. On the other hand, (Patella, Aletta, and Mannini, 2019) performed a noise emission and traffic performance assessment in presence of AVs on the urban mobility level of the city of Rome. Full deployment of AVs improved travel time by reducing it by 33%, increasing the average speed by 51% whereas increasing the total distance travel for highways by 8% and decreasing it by 5% for intra-urban roads. moreover, decreasing the noise levels immensely except for some network links where the condition of noise emissions becomes worse due to increment in traffic volume and speed. the results were promising yet ignored many important parameters of population growth, spatial distribution, mode choice, household travel patterns and budgets. Whereas (Staricco et al., 2018) proposed to utilise transportation quantitative models to analyse the circulation and parking regulatory framework for AVs on the overall modal split of the urban networks. not only that but also visualise the implications on growth and land use patterns through land use and transportation interaction models.

There are uncertainties associated with the large-scale inclusion and impacts of AVs, yet the ambiguities remain there unless we try to cope with them. We need root-level planning for the people by the inclusion of people and their social dynamics. The approach taken in this study consists of more than twenty social-demographic indicators representing the dynamics in social, demographic, urban, and commuter fabric. Limited to no research has been done to quantify the presence of AVs which creates uncertainty when we try to effectuate their effectiveness. Short as well as long-term changes this technology is about to cast on society remain a question.

Often the research (encompassed in Chapter 2) in this particular domain

of technology roams around complex systems, algorithms, models, and machine-learning methods. Concluding outstanding results and enlighting the impacts of AVs on the social fabric as well as traffic systems. Yet these include a random percentage of AVs and TVs, the deficiency lies in the foundation of these studies which here the authors tried to overcome. How could we be so sure about our results if we are just assuming the number of vehicles in absence of some solid evidence or methodology for the quantification? The study tries to minimize the "risk of extent" by adopting classic, simpler, realistic yet effective indices to quantify the amount of AVs for the future scenario. This matrix can be extended with each stage of evolution or change in behaviour by any means. The recent lesson cities learnt from the pandemic was an eye-opener that inclusion of people's preferences and social inclusion is of high importance whether it be a classical or advanced approach to analysis. The pandemic taught the cities that uncertainties are always there thus drawing the planning policies back to basics and disrupting the established patterns of living. Talking about the societal goals of this research, eliminating or keeping the inequity to its minimum itself is a major societal goal that needs to be addressed while developing any policy guides for future scenarios of heterogeneous traffic streams. Although uncertainties are there yet development in technology and testing is at a pace too, coming back to the basic and grass root level planning is of uttermost importance. It is the people no matter from which group for whom the planning and policy-making should be carried out. Inequity is directly related to the social goal of access, inclusion and community well-being. AVs are supposed to contribute to serving the underserved community but at the same time can cause network imbalances too by increment in travelled miles thus it is of prime importance to reveal how much our current networks allow to digest without causing harm to any group of people. That is what is required to be achieved through analysis.

As (Nigro et al., 2022) analysed the shifting potential from personally owned car trips to electric micro-mobility up to 20% of the weekday trips in case of e-bikes (travel distance bound of 6km) and 11.4% in case of e-scooters (travel distance bound of 3km). It reveals the potential trend shift to these new forms of mobility given appropriate infrastructure is provided. Similarly, this potential is up to 7% for e-bikes and 4% for e-scooters in case of weekend trips. For multimodal provision where micro-mobility complements the public transit, they concluded that 6% of the total morning peak trips in Rome record lesser travel time as compared to the car trips for the same origin-destination pair. (Abduljabbar, Liyanage, and Dia, 2021) in their extensive review of the literature on micro-mobility from a sustainability perspective crowns it as an effective low carbon footprint mobility. Not only this but playing the part in deriving the users away from private and high pollutant modes of mobility towards sustainable solutions. they suggest diving deeper into research that aims to assess the urban mobility patterns with micro-mobility through a real-world field and modelling studies. (Christoforou et al., 2021) in a statistical user-based survey of electric scooter users in Paris (pre-pandemic period) revealed that 16% of the e-scooter users have shifted from other motorized modes (private car, taxi, two-wheeler). Moreover, (Comi, Polimenia, and Nuzzolo, 2022) identified by capitalizing on the scope of the floating car data from the city of Trani, Italy that 22% of the car trips can be replaced by the active micro-mobility modes reducing the car demand up to 10%. Also, developed a possible micro-mobility network within the area serving 22% trips and proposed an extension to the analysis for analysing the operation and improvement in the performance of the public transit system. These results immensely illuminate the importance and relevance of evaluation of the public transit systems on integration with these micro-mobility modes.

Not only the potential of a shift from private car trips to the micro-mobility

mode is important but the perspective of micro-mobility complementing the traditional public transit system is as well. It is serving the micro demand. Take it this way, at higher hierarchical levels metro/subway systems serve huge demand but it is the dense bus and tram system that acts as a feeder to the metros. So the disruptions at the metro/subway level are usually catered for by bus transit systems but the disruptions at the bus transit level are not always taken care of by the metro system. It is due to the nature of trips that could be shorter than expected, eliminating the need for the metro or maybe in the area where the metro is not serving at all. In that scenario, it is micro-mobility that complements the ground-level public transit systems. Yet, it is necessary to evaluate the expanse of their serviceability when there is a disruptive scenario disturbing normal operations and creating commuter disutility. In this study, the authors tried to evaluate the effectiveness of micro-mobility provision to assess the vulnerability in light of the above discussion.

1.2 Problem statement

These innovations (autonomous vehicles and micro-mobility modes) and adapting trends will allow commuters of both private and public transportation networks to cycle, scoot, and drive like never before. Nevertheless, they will also cast symbolic outlay on social communities and commuters (Litman, 2021b). This urges transportation planners to adopt innovative analytical and simulative methods for gauging the potential impacts and making informed decisions. The smart usage of these new forms of mobility can help to make communities more liveable, efficient, and fair. For instance, external traffic costs (travel delays, congestion, parking facility costs, etc.) are inequitable but the question of inequity resulting from the introduction of

autonomous vehicles (AVs) is not answered yet. Although, researchers (Fagnant and Kockelman, 2014; Kim and Yook, 2015; Zhao and Kockelman, 2018; Almeida Correia and Arem, 2016; Liu et al., 2017; Mena-Oreja, Gozalvez, and Sepulcre, 2018) concluded the reduction in the number of vehicles serving the demand, vehicle kilometers travel (VKT), and emissions while increasing the road capacity. Albeit, they used various penetration rates (either incremental values from 0-100% or fixed values of moderate to high 0.7-1.0) to evaluate the effects of AVs in various simulative environments and effectively described the possible implications. Yet the variability in conclusions draws our attention to the limitations of studies in terms of quantification of the realistic penetration rate of AVs. So, there is a gap in the current state-of-the-art on quantification of the penetration rate of AVs to be used in transportation models and consequently devising a methodology for analyzing inequity in presence of heterogeneous traffic stream consisting of AVs and TVs (traditional vehicles).

On the other hand, a boom in the usage of micro-mobility modes gave rise to a debate on their impacts on the usage and performance of public transportation networks. Numerous studies evaluated the impacts of integration of micro-mobility with public transportation networks in terms of accessibility of services and stations, economic effectiveness, variation in user costs, policy implications, user perception, and acceptance, modal shifts, change in demand, and health impacts (Cheng and Lin, 2018; Hamidi, Camporeale, and Caggiani, 2019; Wu et al., 2019; Krizek and Stonebraker, 2011; Fan, Chen, and Wan, 2019; Griffin and Sener, 2016; Schröder et al., 2014; Heinen and Bohte, 2014; Marqués et al., 2015; Martens, 2007). Alike, the vulnerability of public transportation systems to random disruptions is an important performance indicator analyzed by (Albacete et al., 2017; Cats and Jenelius, 2014; Chen et al., 2007; Lu and Lin, 2019; Wang et al., 2020; Buijtenweg et al., 2021; Luo, Cats, and Lint, 2020; Yap et al., 2019; Lin and Ban, 2013) using complex

network theory as well as segmentation techniques. Yet, the question of public transportation system vulnerability in presence of micro-mobility service is not explored.

1.3 Scope and objective

As drafted in the problem statement, the main research problem is a collective or compound impact of the new forms of mobility on private as well as public transportation networks. As defined earlier, this research thesis is comprised of two parts; first related to the impacts of the introduction of AVs into the system, and second related to the integration of micro-mobility services with public transportation services. The skimmed gaps in current state-of-the-art pave the way to define the scope of this research thesis which firstly roams around the quantification of the realistic penetration rate of AVs before injecting it into the multi-vehicle assignment models and later performing the inequity analysis. Secondly, appraisal of the vulnerability of public transportation systems against random service disruptions on the integration of micro-mobility services. The objectives can therefore be formulated as:

- Devise a methodology for quantification of the realistic penetration rate of AVs based on a system of indicators depending on the demographic, road network, and land use factors.
- Based on realistic penetration of AVs evaluate the influence of physical characteristics of the urban road network on macroscopic fundamental parameters.
- Analyzing the inequity in travel cost equilibrium caused by the variation in the trip generation on the inclusion of AVs in the private transportation networks.

- Assess the vulnerability of the public transportation network against random service disruptions on integration with micro-mobility services.
- Gauging the improvement or stagnation of public transport network performance on the provision of micro-mobility services based on the topography of the city and the size of the service provided.

1.4 Research approach

As explained in the previous section, multiple objectives both related to private along with public transportation networks are penned down. The thesis report is organized thoroughly into two sub-parts dealing with AVs for analyzing their impact on private transportation networks and micro-mobility for assessing their influence on public transportation network performance. Later, giving a collective picture of the impacts of new forms of mobility on our transportation systems. The highlights of the major research queries being answered in this research work can be seen in 1.1.

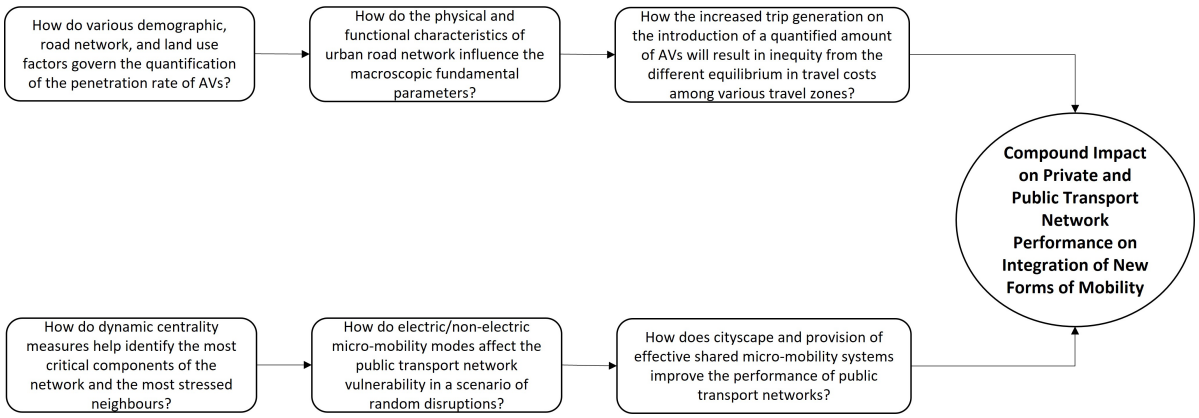

FIGURE 1.1: Major research queries of the study

Below is described briefly the approach adopted to attain each of the drafted objectives in Section 1.3. The schematic visulaization of the propsed methodlogy can be seen in 1.2.

1. Devise a methodology for quantification of the realistic penetration rate of AVs based on a system of indicators depending on the demographic, road network, and land use factors.

    - Depending upon land usage, socio-demographical, and road network classes, indicators are grouped and seven different indices equations are skimmed. All seven indices are integrated to obtain a quantification value of the integrated index following a quantile approach.

2. Based on realistic penetration of AVs evaluate the influence of physical characteristics of the urban road network on macroscopic fundamental parameters.

    - Macroscopic fundamental diagram for an urban network is used to express the change in urban road link capacity and its consequent effect on the travel-time flow relationship by incorporating physical and functional characteristics (such as road link width, non-negative slope, tortuosity, external disturbance, and parking, etc.) of the urban road network

3. Analyzing the inequity in travel cost equilibrium caused by the variation in the trip generation on the inclusion of AVs in the private transportation networks.

    - For the travel equilibrium cost analysis to determine the inequity, the Equilibrium Trip Distribution/Assignment with Variable Destination Costs (ETDA-VDC) model from (Oppenheim, 1995) is used. A bi-level optimization model is used to attain the objective in which the lower level assigns the travel demand to the network following the stochastic user equilibrium (SUE) approach whereas the upper level maximizes the trip generation based on quantified

penetration rate, inequity constraints, and physical constraints of the origin and attraction zones.

4. Assess the vulnerability of the public transportation network against random service disruptions on integration with micro-mobility services.

    - The micro-mobility mode used in this study is the public shared bicycle system. This shared bicycle system supply model is integrated with a multi-modal PuT network model. Later based on the dynamic centrality measures the integrated model is clusterized in the form of hierarchical segments with each cluster having the most vulnerable components highlighted. A mixed machine learning technique is used to highlight the vulnerable components and the most critical neighbors of these vulnerable components in the integrated model. Finally, various random disruption scenarios are assessed in conjunction with micro-mobility usage dependent upon the type of disruption to examine the vulnerability of the PuT system.

5. Gauging the improvement or stagnation of public transport network performance on the provision of micro-mobility services based on the topography of the city and the size of the service provided.

    - The comparison is made between two metropolitan cities of different topographical layouts and sizes of the public shared micro-mobility service. This comparison reveals how different factors in different scenarios cast an impact on the performance of the public transportation system.

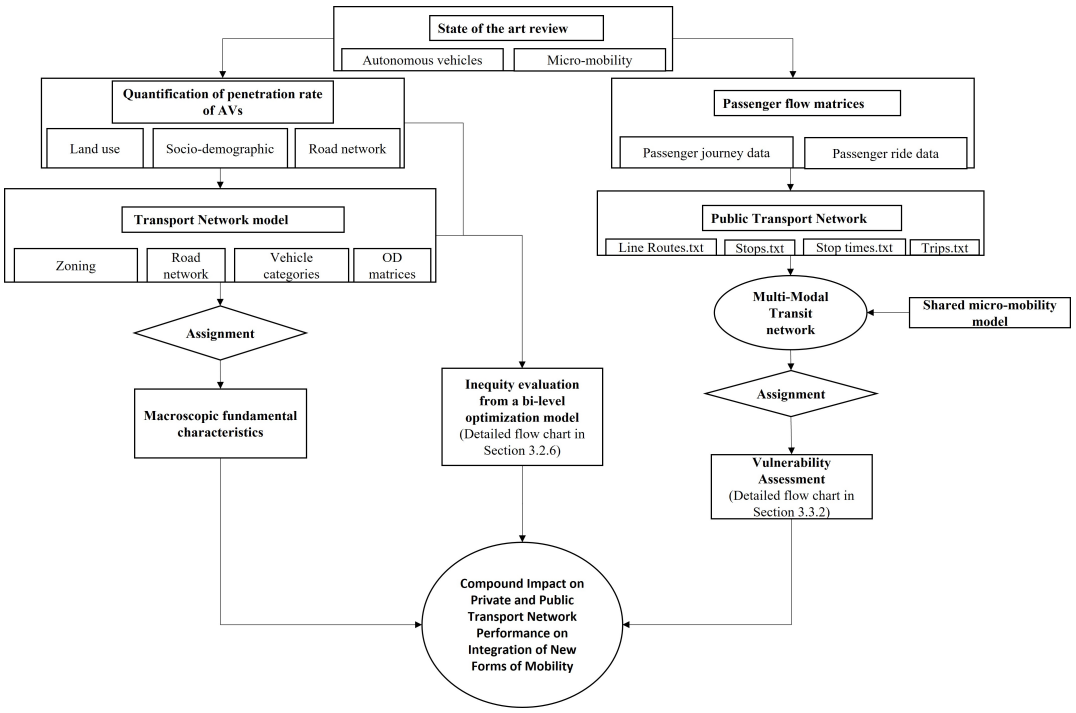

FIGURE 1.2: Proposed methodology flowchart

1.5 Organization of thesis

The next chapters will follow the structure as follows: Chapter 2 describes the state-of-the-art practice and research relevant to the impacts and analysis of new forms of mobility, trying to carve out the opinions of researchers and various studies related to the objectives penned down earlier. Also, revealing the gaps in the research and defining the research questions to be answered via this research thesis. Galvanized by the available methodologies and techniques, Chapter 3 carves out the innovative and detailed methodology to attain the objectives of the compound impact of these new forms of mobilities on transportation systems. The formulated methodology is applied to the city of Genoa, Italy, and Barcelona, Spain in Chapters 4 and 5. All the key objectives and methodology formulated to attain the objectives as well as key findings upon real network analysis are recalled in Chapter 6 to derive the policy implications. It also concludes with the limitations of this work and

directions for future research. The organization of the thesis can be visualized in 1.3.

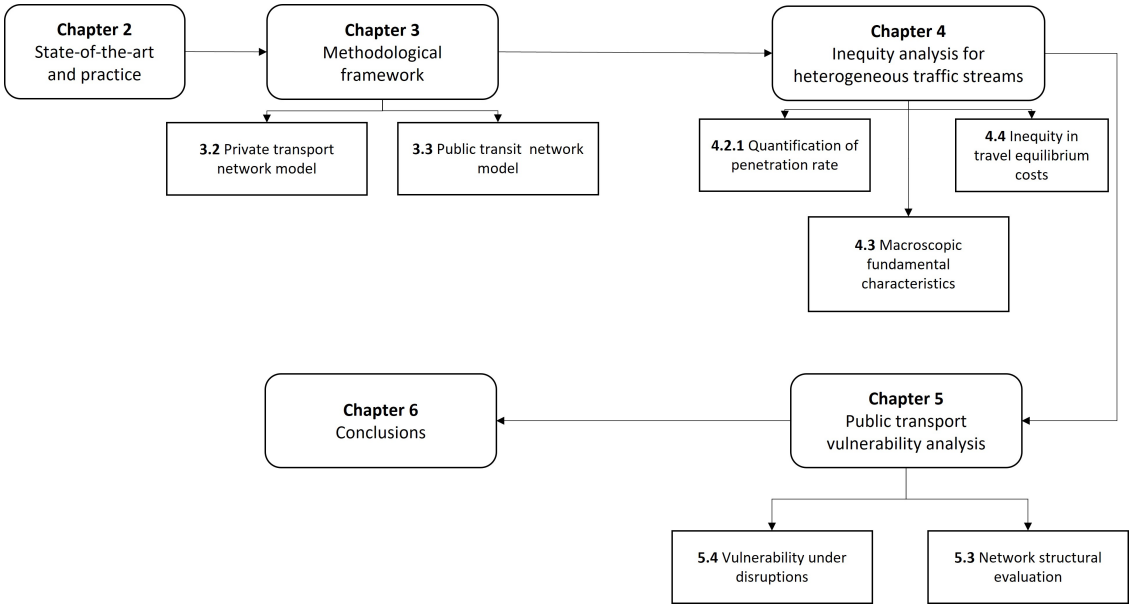

FIGURE 1.3: Organization of the study

Chapter 2

State of the art and practice

2.1 Introduction

This chapter reviews the state-of-the-art in view of the objectives and motivations of this research penned down in Chapter 1 of this research thesis. The organization of this chapter constitutes a thorough review of the current debate related to the impacts of Autonomous vehicles on the performance of transportation networks and urban land usage patterns in terms of travel costs equilibrium. Later, it also summarizes the existing theories, and empirical as well as statistical studies related to the integration of micro-mobility modes with traditional public transportation networks. This extensive review reveals the gap in the existing literature forming a conceptual map of research questions that are studied, worked upon, and answered by this novel research.

2.2 An era of Autonomous Vehicles

The concept of a person driving behind the steering was always accompanied by a vision of a car bringing its passengers to their destinations without a driver controlling the vehicle. However, the accomplishment of this vision continually remained somewhat 20 years away from becoming a reality (Wetmore, 2003). Self-driving vehicles played a vital role in visualizations of

technology albeit their translation into reality largely remained pictorial until recent times.

The technological boom in the vehicle industry arose with the invention of autonomous vehicles (AVs) in the late 1920s (Kröger, 2016). From the first driverless car tested on McCook airforce base in Ohio, USA to the American Wonder on Broadway, New York, technically these vehicles were remote-controlled but theoretically driverless self-driving wonders (Kröger, 2016). From the period when they were called phantom auto (Sentinel, 1926) or robot cars (O, 1936) up to recent times with the development of fully autonomous vehicles (AVs) and connected automated vehicles (CAVs), their prototypes are being tested on common roads. The latest example of this is a 22-mile long network of urban streets augmented for self-driven vehicle testing in Turin, Italy (*Car and Driver* 2019). These test runs attested to the replacement of traditional vehicles (TVs) whether they are privately or commercially owned. Furthermore, through test runs, it is revealed that introducing AVs into the system generates an evolutionary change in vehicle usage norms while at the same time impacting the transportation systems.

2.2.1 Impacts on macroscopic network parameters

The capacity of urban networks and traffic flow has always been a topic of interest for planners, policymakers, government authorities, and statistical physicists in recent decades (Chowdhury, Santen, and Schadschneider, 2000; Yoshioka et al., 2019; Yoshioka, Shimada, and Ito, 2017). Repetitive travel patterns of commuters make it difficult to mitigate congestion as increased induced travel demand and population growth rapidly consume any added network capacities (Loder et al., 2019). Traffic yields three macroscopic parameters namely speed, flow, and density of vehicles on the network. These

parameters generate two conditions of the traffic which either becomes saturated or unsaturated. A saturated condition is when the addition of a vehicle to the network further moves the system towards congestion decreasing the speed and flow of traffic. Whereas, in an unsaturated condition any addition of vehicles to the network also increases the flow of vehicles (Cascetta, 2009). The critical point decides the boundary between the network's saturated and unsaturated conditions. This critical point is the capacity of the urban traffic network to yield the maximum traffic flow that can be accommodated without causing congestion. Although one-dimensional and expressway traffic flows are detailed in studies like (Castrillon and Laval, 2018), some of them (Daganzo and Geroliminis, 2008; Geroliminis and Daganzo, 2008) also studied urban traffic networks.

The rapid testing of AVs and the impact of these technological advancements on transportation systems need to be investigated. In this regard, researchers (Cantarella et al., 2019; Payre, Cestac, and Delhomme, 2014; Talebpour and Mahmassani, 2015) analyzed and evaluated the problem of introducing autonomous vehicles into the transportation networks and highlighted the opportunities and gains that could be achieved in terms of macroscopic fundamental traffic network characteristics. Despite improved mobility and safety to the highest level expected from these technologies, concerns about their long-term impact on transportation systems are also there (Fakhrmoosavi et al., 2020; Shao and Sun, 2021; Mahmassani, 2016; Jiang et al., 2021; Ghiasi, Li, and Ma, 2019; Zmud et al., 2018). Yet, there is no evidence of quantification of the penetration rate of AVs in urban network evaluations but some predictive studies (Milakis et al., 2017; Research, 2020; Litman, 2020; Ben-Haim, Ben-Haim, and Shiftan, 2018; Lavasani, Jin, and Du, 2016) for penetration rate are present.

Milakis et. al. conducted a scenario analysis following an intuitive logic

approach around the most impactful technologies and policies towards supportive and refuting implementation of AVs. Four scenarios of AVs in standby, in bloom, in demand, and in doubt were analyzed for the future developments track in the Netherlands and their potential impacts over the time up to 2030 and 2050. The analysis revealed that fully automated vehicles will be available in twenty years thus increasing the penetration rate of AVs up to 61% in 2050. This inclusion is expected to enhance the capacity of the motorway from 5% to 25% and vehicle kilometers traveled from 3% to 27%. Following the analysis, the results are validated in a logical workshop of fifteen field experts.

Litman used previous analysis to predict the market penetration of AVs for 2020-70 based on the factors like the pace of technological developments, regulatory and testing approvals, incremental costs, land usage and travel preferences at the user end, service quality, and affordability, public policies for swift inclusion and safety. This theoretical analysis predicts the increase of market penetration of AVs based on improvement in performance, decrement in price, and increment in user confidence such that by 2045 half of the new vehicle sales would be autonomous albeit market saturation will not be the same. This trend can result in a faster shift towards AVs in dense urban environments considering sharing services but unlikely to switch to private travel in suburban and rural areas. Although, this study predicts that AVs travel between 50-80% by 2060 albeit highly dependent on theoretical predictive studies.

Ben-Haim et. al. developed a qualitative approach for estimating the penetration rate of AVs for 2030-50 to evaluate their impact on travel behavior and user activities. They used the Delphi method in combination with scenario analysis to construct two rounds of survey analysis. Again the approach of expert-based surveys was used which concluded significant

progress in AV technology and usage till 2050 thus increasing the penetration of these vehicles into the traffic network. The penetration rate of AVs touches 23% for the year 2030 whereas jumps up to 60% by the year 2050. Similarly, Lavasani et. al. developed a market diffusion model based on the data of previous technologies adoption. Considering the adoption patterns of previous advancements, an indicator of innovation factor and imitation factor were deduced to evaluate the market penetration of AVs. The study concluded that a market saturation might occur in 35 years given that fully autonomous vehicle is available by 2025. To the best of the knowledge of the authors, no state-of-the-art quantitative method for AV penetration rate was found except for Lavasani et. al. with limited indicators considered. This certainly is a gap since without a precise penetration rate the impacts of AVs cannot be synthesized as they are not part of the real-time networks yet.

Furthermore, various researchers penned down the impacts on travel and mode choices, travel behavior, traffic patterns, environmental effects, and road safety. As per (Fagnant and Kockelman, 2014), a system of shared AVs reduces 10 times the number of vehicles to serve the existing travel demand as well as appreciable emission savings but suffers 11% more empty vehicle kilometers travel (VKT) to reach the next passenger. Effective roadway capacity increased three times with 100% deployment of AVs on the roads consequently incurring travel time savings (Kim and Yook, 2015), while (Zhao and Kockelman, 2018) suggests that increasing the induction of AVs with more travelers opting for them over TVs and public transport will result in a 10% increase in VKT with consequent congestion and almost a 3% drop in average speed. Nevertheless, (Almeida Correia and Arem, 2016) concludes after solving a traffic assignment and vehicle routing problem for user optimum scenario of privately owned AVs that this new form of intelligent vehicles can serve more trips as compared to TVs while causing only a little increase in congestion regardless of extra VKT. They also concluded that if in

conjunction with this technology user perceives a lower value of travel time this can further serve even more trips without any cost of congestion.

On the other hand, (Liu et al., 2017) revealed the increase in road capacity up from 2000 veh/h at 0% AVs to 3070 veh/h by replacing all the TVs with AVs in a transportation network that is with 100% of the penetration rate of AVs. Similarly, an increment of 46% in the free flow speed from 78.85 km/h to 115.20 km/h, whereas improving the critical density slightly shows the property of AVs to make the entire traffic flow stable. However, (Mena-Oreja, Gozalvez, and Sepulcre, 2018) shows that large safe gaps in the platoon of mixed vehicle streams reduce the impacts of AVs in the traffic. In over conservative scenario even with a 100% penetration rate of AVs the traffic flow only increases to 9.39% as compared to the scenario with no AVs in the traffic stream, whereas for aggressive and neutral gap configuration the flow increases up to 39.21% and 26.09% respectively (Liu et al., 2017). (Stern et al., 2018) in a thorough real-life experiment with a circular mixed traffic stream of AVs and TVs, claims the augmented capacity of a mixed traffic stream for a penetration rate as low as 5% of intelligently controlled AVs. Overall, (Stern et al., 2018) shows that the deviation of velocity between vehicles in a mixed stream is reduced up to 80% and braking events from 9 events/veh/km decreased to 2.5 events/veh/km. (Friedrich, 2016) after macroscopic traffic flow analysis involving AVs shows a significant increase in capacity leading to the efficient use of transport infrastructure, reduction of traffic loss time and jams due to shortening of headways, and higher speed at constant density in presence of AVs.

However, (Little, 2019) came up with a different conclusion stating that the capacity increases and the urban congestion reduce drastically in a setting of 100% AVs but a mix of TVs and AVs on the contrary reduces the capacity of an urban traffic system. They discovered that in a mixed traffic stream scenario with a 50% penetration rate of AVs the traffic capacity decreases up

to 16.3% as compared to the current capacity. This volatility in conclusions from the literature creates room for questions and still, the answers are uncertain. (Narayanan, Chaniotakis, and Antoniou, 2020) reviewed and summarized the state-of-the-art literature on the consequences of CAVs and AVs on road network capacity, traffic flow stability and safety, travel time, congestion, changes in VKT, and policy recommendations for the inclusion of this new form of mobility. According to (Narayanan, Chaniotakis, and Antoniou, 2020), one of the key constraints in current literature recounts the factors and assumptions being used in the modeling studies analyzing the impacts of AVs on transportation networks, users, and society. Although testing of this new form of mobility is at pace; studies except for (Martin-Gasulla, Sukennik, and Lohmiller, 2019) do not often take into account the real-world parameters and factors affecting the inclusion of AVs on transportation networks. The study (Martin-Gasulla, Sukennik, and Lohmiller, 2019), uses realistic network parameters to evaluate the impacts of AVs on traffic flow parameters using a microsimulation analysis of a simplified four-leg intersection. But do not consider any realistic parameters for the inclusion of AVs thus calculating the impacts on various penetration rates from 0-100%. Studies (Ye, Yamamoto, and Morikawa, 2018; Zheng et al., 2019; Sagir and Ukkusuri, 2018; Anis and Csiszár, 2019; Kutgun, Duc Pont, and Janzen, 2018; Xie et al., 2019) used various penetration rates (either incremental values from 0-100% or fixed values of moderate to high 0.7-1.0) to evaluate the effects of AVs in various simulative environments and effectively described the possible implications.

For evaluating the implications of this new technology macroscopic fundamental diagram (MFD) offers a simplified yet holistic approach to systematically examining urban traffic at both link and network levels (Loder et al., 2019). It effectively allows determining the critical point between two traffic conditions of an urban network consequently revealing overall capacity.

As (Leclercq, Chiabaut, and Trinquier, 2014) presents a cross-comparison of various MFD estimation methods both for a link and network level and describes its possible usage for simulation purposes. This makes it a useful tool to analyze the operation of urban transportation networks in heterogenous traffic scenarios with AVs.

The MFD gives an overall link/network capacity and corresponding critical density and flows after which the saturation starts. Later, they are used to determine the travel-time and flow relationship for the link or the entire network. Researchers (Di Febbraro and Sacco, 2016; Maximcsuk, Lu, and Tettamanti, 2019; Karbasi, Mehrabani, and Saffarzadeh, 2020) evaluated the influence of introducing this new form of mobility into urban transportation networks by using MFDs. Although they (Maximcsuk, Lu, and Tettamanti, 2019; Karbasi, Mehrabani, and Saffarzadeh, 2020) showed that AVs have significant impacts on traffic flow, their consequences on travel time are still missing. Also, they do not take into account the physical and functional parameters of the network links (disruption, road bends, number of non-signalized crossings, etc.) which certainly influence link and overall network performance. The variability in conclusions also draws our attention to the limitations of studies in terms of quantification of the realistic penetration rate of AVs.

2.2.2 Equillibrium shift in Landuse - Transportation interactions

Given the law of physics, any new addition to the existing system shifts its equilibrium. Similarly, this new form of self-driven form of mobility raised a question of changes in transportation system equilibrium including all different classes of autonomous vehicles as explained in J3016 Information Report (SAE, 2014). Albeit, it is also a fact that a complete transition and 100% a shift

from the TVs to AVs could take many years or a couple of decades to be true and massively reliant on huge investments from the tech giants for developing full-proof technology (A, 2018). Such a level of technological advancement makes it necessary to get done a thorough evaluation of functionalities and impacts on the user, society, and overall system.

In a scenario of a heterogenous traffic stream with TVs and AVs, the interactions on a transportation network for studying mobility patterns in polycentric urban dwellings need a comprehensive analysis of user demographics, road network characteristics, and land usage. Henceforth, following realistic quantification of the penetration rate of AVs, it appears lucrative to highlight and investigate the impacts of AVs in terms of land use and transportation interaction (LUTI) for effective planning of future transportation networks. Although effective studies of spatial interactions date back to 1931 albeit the articulation of urban-dwelling models for land use and transportation interactions came into existence in the early 1950s and 1960s (Wilson, 1998). Theoretical advancements in the field of land use and transportation interaction models are comprehensively penned down by (Wilson, 1998). Going through the land use and transportation interaction patterns, it is observed that they are dependent on each other in a cyclic pattern. The interaction patterns are most probable and consistent with the state of the intensity of transportation services availability and land usage pattern (Wilson, 1998). Since the start of urbanization, the location of the population remained dependent on the location of their workplaces, then with the era of powered mobility, the urban population started to expand alongside the major roads, tram lines, etc. (Cordera et al., 2019). In turn, land use and settlement decisions contributed towards trip generation with the continued increase resulting in congestion and consequent high trip costs.

However, some of the research (Erlander, 1977; Fisk, 1979) proved that incremental trips do not necessarily become a reason for high trip costs for all

the paths in the network. (Fisk, 1979) showed via extensive sensitivity analysis of travel costs in Wardrop's equilibrium problem that both origins to destination and overall travel cost can be decreased for an increasing input flow but not necessarily for the same OD pair. In such a case, the travel cost for the same network does not remain equitable for all the network users. For evaluating the amount of inequity resulting from the higher inflows in the network there have been many examinations (Meng and Yang, 2002; Rodier et al., 2010; S, 2013) in continuous network design problems for LUTI. (Meng and Yang, 2002) analyzed equity after the network design project for different OD pairs of the network via continuous network design problems by implementing it on the Sioux Falls network. (Rodier et al., 2010) investigated the equity issue for different transport and land usage policies on travel time and travel costs using advanced aggregate travel models and activity-based models. (S, 2013) used a regional activity-based travel model for transportation equity analysis involving distributional comparisons of individual-level equity indicators and societal scenario-based equity analysis.

Similarly, (Litman, 2021a; Fan et al., 2019) detailed the disparities and unfair distributional gains of transportation systems, services, and policies collectively impacting the part of communities. Not only this but providing methods for determining the inequity for various transportation enhancements. (Kassens-Noor et al., 2020) after an extensive review of current literature on AVs astoundingly identified the gaps in research on the social impacts of AVs and concluded that the challenges are being overlooked. No evidence was found of inequity analysis on the inclusion of AVs into real transportation systems creating heterogeneous traffic streams up to the author's knowledge except (Bilal and Giglio, 2021) which involves the analysis of an example network with an independent penetration rate of AVs.

2.2.3 Key Takeaways

The extensive review of state-of-the-art related to the impacts of AVs on transportation networks as well as land-use interactions reveals a gap for us to fill via this novel research. It brings us to the first objective of our research to define a methodology that extensively and realistically quantifies the penetration rate of AVs to be used in modeling and analyzing traffic flow characteristics. The first goal is to identify the factors converted into indices for the inclusion of AVs into the network based on the socio-economic and demographical characteristics of the study area. Secondly, by using this realistically quantified penetration rate, evaluate the impacts of this new form of mobility on urban road link capacity via macroscopic fundamental diagrams and its consequences on the travel-time flow relationship by incorporating physical and functional characteristics of the urban road link. Later, using the realistic penetration rate of AVs, carrying out the inequity analysis on a real transportation network to analyze the resultant change or imbalance in travel equilibrium costs.

The quantification in this research is based on three major classes: user demographics, road network, and land use which will be responsible for the adoption and consequently get influenced by the impacts of AVs. For the consistent and reliable evaluation of extracted data, different researchers (Frei, 2006; Bergström and Magnusson, 2003; Hensher, Stopher, and Bullock, 2003; Dios Ortúzar, Iacobelli, and Valeze, 2000; Keegan and O'Mahony, 2003) used a system of indicators for evaluating the quality of services, social equity improvement, transport network assessment for pedestrian mobility, and temporal and spatial comparisons. Here we grouped various indicators into already mentioned three major classes to quantify the penetration rate of AVs for the city of Genoa, Italy in the first part of our research for analyzing

the impacts of the state-of-the-art form of mobility on the transportation network in terms of private mode commuters. Major research questions to be answered for the part of private transport network evaluation are as follows;

- How do various demographic, road network, and land use factors govern the quantification of the penetration rate of AVs?
- How do the physical and functional characteristics of urban road network influence the capacity and travel time flow relationship in presence of a realistically quantified amount of AVs?
- How the increased trip generation on the introduction of a quantified amount of AVs will result in inequity from the different equilibrium in travel costs among various travel zones?

2.3 Public transport network vulnerability

The public transport network (PuT) is vital for the mobility of people and goods within and between cities. Components of this system that are serving the purpose of connecting the evolving polycentric urban dwellings are the backbone of the system (Louf and Barthelemy, 2013; Zhong et al., 2014). The daily commute of users on this system creates a natural urban mobility pattern inherently linked with the set-up of public transport networks. Moreover, urban settings with extensive multi-modal transportation networks form a complex system of mobility giving rise to mobility patterns of passenger flows. In this scenario, commuters demand the least fluctuations in terms of travel time and travel quality while commuting toward their destination point (Bilal, Sarwar, and Giglio, 2021).

As much as the system is complex, more vulnerable is it to unwanted disruptions. So before dealing with the disruptions it is important to skim out the vulnerabilities of the system. For a public transportation system to

be an alluring option for people with daily mobility needs, it has to be up to the mark in terms of efficacy and robustness. Efficacy refers to the ability of the system to allow its users to reach their destinations in a rapid, calm, reasonable, and accessible manner. Moreover, robustness depicts the capability of the public transport system to withstand and recover from unwanted and unexpected disruptions in terms of network, vehicle, or infrastructure (Cats and Jenelius, 2012). It should be noted that vulnerability is defined for the transportation network but that doesn't mean the network is the least robust but certain components (nodes and links) and locations are. Identifying the locations of public transport networks where the failure could impose the worst consequences on urban mobility is of prime importance. The likelihood of failure of various network components is usually the same but the effect isn't. There are critical components precisely links and nodes in the public transport network which upon failure cause immense disruptions in public transport operations consequently affecting users' mobility (Mouronte-López, 2021). A trustworthy public transport system should be of high tolerance to disruptions for keeping the commuter journey by the plan. Very few researchers (Bilal, Sarwar, and Giglio, 2021; Berche et al., 2009; Albacete et al., 2017; He, Guo, and Xu, 2019; Cats and Jenelius, 2014) focussed on assessing the vulnerability of a public transport network where multiple modal services superimpose to serve the demand.

2.3.1 Assessment of the public transport network

(Berche et al., 2009) tested the public transport network resilience of 14 different cities under 16 different attack scenarios. The scenarios range from random disruptions to targeted removal of critical nodes based on the operational characteristics and various centrality indicators leading to the removal

of all the links; starting or ending at that node. Apart from deviation in response to attacks of the considered transport networks, high resilience results in the high value of the Molly-Reed parameter in L-space and a small value of mean shortest paths in P-space. (Albacete et al., 2017) in their comparison of various public transport network accessibility methods implied the structural accessibility layer and public transit and walking accessibility methods in the multi-modal public transport network of Helsinki. This research aimed to analyze the policy implications of various accessibility measures for public transport systems considering traffic conditions instead of timetables. (Albacete et al., 2017) concluded that the methodologies for accessibility measures are sensitive to the type of inputs, demographics, space, and time. (Bilal, Sarwar, and Giglio, 2021) studied the impact of travel time reliability in multi-modal public transport route assignment. Various scenarios based on perceived journey times including reliability constraints deduced from the Poisson parameters in the optimization model were generated. Based on these scenarios (Bilal, Sarwar, and Giglio, 2021) concluded that line routes with longer lengths, fewer stops, and the least disruptions are the most reliable routes chosen by the maximum users in the simulative environment.

(He, Guo, and Xu, 2019) applied cascade failure theory to analyze the risk propagation in a multi-modal freight transport network. The study revealed that when the proportion of risk source nodes is greater than 60% the network leads to a state of failure with average network efficiency being zero. (Cats and Jenelius, 2014) developed centrality measures based on dynamic and stochastic settings from the perspective of both users and service providers to study the vulnerability of the network in case of disruptions. Application of devised measures on the public transport network of Stockholm, Sweden revealed that real-time information provided to the users of the public transport system not only has positive but negative impacts in case of disruptions depending upon the nature and extent of information

provided. Moreover, (Cats and Jenelius, 2014) also concluded that betweenness centrality is not the best indicator of link importance.

(Chen et al., 2007) proposed a methodology of combined demand and supply change model for evaluating network vulnerability against disruptions. The formulated combined travel demand model used accessibility measures to quantify the impacts of disruptions. A numerical example showed that the derived measures are capable of estimating the disruption consequences on both demand and supply changes. Similarly, (Lu and Lin, 2019) applied the accessibility-based vulnerability assessment method to an urban rail transit network considering passenger flow characteristics for the city of Shenzhen, China. Also, (Lu and Lin, 2019) concluded that besides network topology, passenger flow yields a more authentic and realistic approach to studying the impact of disruptions where stations with higher passenger flow pose a huge impact on network accessibility in the event of a disruption.

For effective and inclusive analysis of the public transport network and to identify the vulnerable network components; segmentation of the network is a valuable tool. There have been studies (Wang et al., 2020; Buijtenweg et al., 2021; Luo, Cats, and Lint, 2020; Yap et al., 2019; Lin and Ban, 2013) implying complex network science factors like the position of network hubs, passenger transfer flows, accessibility analysis, and topological analysis to unravel the hierarchy of public transport networks. This hierarchical segmentation of the public transport network can help understand the vulnerable clusters in the network with susceptible components. (Wang et al., 2020) used passenger flows in complex network theory to cluster the public transport network of the city of Hague, The Netherlands. By using Louvain community detection in combination with the self-sufficiency ranking method to determine the hierarchy of the public transport network (Wang et al., 2020) concluded that the hierarchy changes for different time sets.

(Buijtenweg et al., 2021) used a metrics approach to quantify the hierarchy in public transport networks on a nodal basis with its application to the city of Amsterdam and Rotterdam. The metric used topological, transfer potential, and redundancy measures of a public transportation network to yield a single measure. One of the important conclusions of this study was the fact that the degree of spatial distribution in node-based public transportation network hierarchy defines the robustness against random disruption events. Not only this but (Luo, Cats, and Lint, 2020) used reversed engineering approach to approximate the passenger flow distribution across the public transport networks of two Dutch cities solely based on certain network topological indicators through network hierarchy. Whereas, (Yap et al., 2019) used passenger flow clustering to identify the transport hubs and their spatial distribution to solve the transfer synchronization problem thus providing specific locations to be prioritized for transfers consequently reducing the complexity. (Lin and Ban, 2013) after an extensive theoretical review of complex network theory based on topological measures revealed that each advancement in transportation technology generates a unique behavior of user mobility giving rise to movement patterns. Exploring the relationships of these patterns with underlying public transportation systems is of utmost importance.

2.3.2 A boom of Micro-mobility

With cities accepting and including new forms of electric/non-electric micro-mobility options in the traffic networks it is an important aspect to re-evaluate and think about the effects of these emerging forms of mobility on public transport. Various studies as listed in Table 1 analyzed the potential use of micro-mobility modes and evaluated the impacts of the built environment

properties in the surroundings of PuT stations. Characteristics like population density and land usage significantly influence the propensity of choosing micro-mobility as a first/last mile option for public transport, both in the case of private and shared micro-vehicles (Cheng and Lin, 2018; Hamidi, Camporeale, and Caggiani, 2019; Lee, Choi, and Leem, 2016; Zuo et al., 2020). Also, necessary for optimal planning of several parking spaces for this mode or the area and position of docking stations.

The presence of greenery around the PuT station is also considered in studies (Ji et al., 2018; Lin et al., 2019; Liu et al., 2020; Wu et al., 2019; Zhao and Li, 2017; Chan and Farber, 2020; Geurs, La Paix, and Van Weperen, 2016; Pritchard et al., 2019; Sagaris, Tiznado-Aitken, and Steiniger, 2017; Guo and He, 2020) which in turn leaves a positive impact on the usage of micro-mobility. Another important factor analyzed in studies (Hamidi, Camporeale, and Caggiani, 2019; Wu et al., 2019; Geurs, La Paix, and Van Weperen, 2016; Zuo et al., 2020) is the accessibility of PuT stations when micro-mobility modes are integrated with public transportation. It is analyzed how well sharing services, micro-mobility infrastructure, and facilities can be accessed and how well these provide access to services and opportunities within a given time. It is an important factor when evaluating mobility patterns, inequity of access, and user behavior analysis. Some of the mentioned studies (Cheng and Lin, 2018; Li et al., 2020; Krizek and Stonebraker, 2011) also included cost-benefit analyses for various integration measures to determine the economic effectiveness of micro-mobility and public transport integration. Not only this but researchers (Adnan et al., 2019; Fan, Chen, and Wan, 2019; Griffin and Sener, 2016; Li et al., 2020; Miramontes et al., 2017; Qin et al., 2018; Schröder et al., 2014; Heinen and Bohte, 2014; Marqués et al., 2015; Martens, 2007) studied the cost of users, policy implications in favor of micro-mobility, user preferences, modal choices, user perception, and acceptance, modal shifts, change in demand, health and economic impacts, safety and

TABLE 2.1: State of the art for Public transport and micro-mobility integration

Research	Type of micro-mobility	Integration with	Area of application	Type of analysis
(Cheng and Lin, 2018)	Shared service	Metro rail	Kaohsiung, Taiwan	A survey in which respondents are asked about their possible usage patterns and stated preferences for the inclusion of Micro-mobility services in the vicinity of metro stations. Later, GIS and cost-benefit analysis for possible incorporation.
(Hamidi, Campo-reale, and Caggiani, 2019)	Shared service	All PuT	Malmo, Sweden	Analysing the transport-related social issues by using a bicycle as a feeder mode for PuT accessibility. Usage of Theil index to picturise the distribution and inequality of bikeability at a spatial and non-spatial level for policy evaluation of investments.
(Zuo et al., 2020)	Private owned	Bus	Hamilton, USA	Transit accessibility study by comparing walk and bicycle and first-and-last mile access modes. Examining the benefits and distribution inequalities of transit among various social groups in terms of ethnicity.
(Ji et al., 2018)	Docking bicycle service	Metro rail	Nanjing, China	Mining of smart card data to explore the possibility of bike-share mode as a feeder for the metro transit.
(Lin et al., 2019)	Shared service	Metro rail	Shanghai, China	Evaluating the catchment area capacity of metro stations in presence of a dockless shared bicycle system. Statistical and spatial analysis for discovering the distribution patterns for urban planning regarding the size of a shared system.

(Liu et al., 2020)	Shared service	Metro rail	Nanjing, China	Statistical and spatial analysis to discover the influence of socio-demographics, travel patterns, and built environment on the usage of bike-share as a feeder mode for the metro transit.
(Wu et al., 2019)	Shared service	Metro rail	Shenzen, China	Destination accessibility analysis from big data of bicycle usage of the public bike-sharing system in conjunction with the metro transit system.
(Zhao and Li, 2017)	Docking service	Metro rail	Beijing, China	Statistical study to determine the factors for the promotion of bicycle usage as a transfer mode to and from metro transit stations.
(Chan and Farber, 2020)	Private	Commuter rail	Toronto, Canada	Preliminary statistical investigation for defining the indicators influencing the active mode of travel (walking and cycling) as access to the transit system.
(Geurs, La Paix, and Van Weperen, 2016)	Private	Railways	Randstad, Netherlands	Simulative study to examine the impingements of bicycle and train integration on work accessibility and train ridership.
(Pritchard et al., 2019)	Private	Metro and railways	Sao Paulo, Brazil	Bike-and-ride model to evaluate the potential benefits in terms of job accessibility by transit.
(Sagaris, Tiznado-Aitken, and Steiniger, 2017)	Private	Bus & Metro transit	Santiago, Chile	Conceptual framework in terms of social and spatial perspective for various formats of bicycle and public transport integration based on the type of land use.

(Adnan et al., 2019)	Single Docking service	Railways	Belgium	Providing a user-based stated preference survey technique to evaluate their choices for selecting shared bicycle systems as the first-last mile travel mode in a multi-stage rail trip.
(Fan, Chen, and Wan, 2019)	Shared service	All PuT	Montreal, Canada	Examining the effects of user attributes, trip properties and built environment on travel mode choices for first-last mile trips through multinomial logit mode choice model before and after the implementation of the shared bicycle system.
(Griffin and Sener, 2016)	Shared Docking service	Railways	Austin & Chicago, USA	A review study of policy and planning documents by using mixed method datasets by combining empirical data from bike-share system operators.
(Miramontes et al., 2017)	Intermodal Hub	Tram, Metro rail, Bus	Munich, Germany	Survey-based study to examine the user acceptance and perception as well as the mobility impacts of micromobility stations at particular public transport nodes.
(Qin et al., 2018)	Docking shared service	Metro rail	Beijing, China	Stated preference survey-based study to read the user choice behavior on the provision of public bike and ride systems
(Schröder et al., 2014)	Electric Micro vehicle	Rail PuT	Germany	A multi-method approach proposes a customer-oriented intermodal sharing service and integrates it with a macroscopic model for the economic evaluation of e-sharing services.
(Marqués et al., 2015)	Private	PuT	Seville, Spain	An extensive study for determination of main catchment areas of PuT by using GIS and variable demand of usage.

(Martens, 2007)	Private	PuT	Netherlands	A review study to summarize the experience, impacts and possible policy implications of various Dutch initiatives for the integration of shared bicycle systems with public transport networks
(Tavassoli and Tamannaei, 2020)	Shared Docking service	BRT	Isfahan, Iran	A numerical study for an optimal hub network design for Bike-and-Ride services to reduce car usage.
(Guo and He, 2020)	Dockless shared service	Metro rail	Shenzen, China	A study to analyze the impacts of the built environment on integrated use of dockless bike sharing system with metro rail.

liveability effects upon integration of public transport and micro-mobility.

2.3.3 Key Takeaways

Even though extensive work is present in the literature related to the integration of public transport and micro-mobility, no evidence of the impacts of this micro-mobility on the vulnerability of public transport networks was found except for (Geurs, La Paix, and Van Weperen, 2016). Albeit, (Geurs, La Paix, and Van Weperen, 2016) extensively modeled the public transport network but only analyzed vulnerability in terms of accessibility on integration with micro-mobility. Segmentation of public transport networks in presence of micro-mobility and analyzing detailed dynamic vulnerability is something missing from the current state of the art. As cities have witnessed a boom in the usage of micro-mobility options while recovering from the pandemic it is a dire need to work in this direction. Certainly, the integration of micro-mobility with public transport generates interesting facts and impacts overall user mobility but the absence of its impacts on the whole public transport network in terms of vulnerability assessment paves way for our research questions as follows;

- How do dynamic centrality measures help identify the most critical components of the network and the most stressed neighbors?
- How do electric/non-electric micro-mobility modes affect the public transport network vulnerability in a scenario of random disruptions?
- How does cityscape and provision of effective shared micro-mobility systems improve the performance of public transport networks?

Chapter 3

Methodological framework

3.1 Introduction

Given the objectives laid in Chapter 1 and research questions defined in Chapter 2, this chapter includes a methodological framework formulated to find the answers. Section 3.2 constitutes the methodology formulated for the quantification of the realistic penetration rate of AVs, transport supply model setup for macroscopic fundamental parameters evaluation, and later a convex minimization problem for the inequity analysis in transportation equilibrium costs. Section 3.3 is composed of a multi-modal public transportation setup, share micro-mobility model formulation, dynamic centrality measures for vulnerable network components identification, and random disruption scenarios definitions.

3.2 Private transport network supply model setup

In this section, the main assumptions, notations, and definitions of the involved constants related to the model settings are presented. Moreover, realistic quantification of the penetration rate is done in this section followed by the setup of the transportation supply model leading to solving the convex minimization problem. Major assumptions of the methodology of private transport network supply model are as follows:

1. a macroscopic model is considered for two different classes of privately owned vehicles i.e. TVs and AVs. Initial OD demand is fixed and remains stable.

2. AVs are further grouped into two categories, Level 1 to 2 in the first group and Level 3 to 5 in the second group, particularly for reaction times and deceleration rates.

3. a constant safety policy for AVs is considered for forming the platoon of vehicles.

4. incremental trips generation is following the quantified penetration rate while keeping the already present demand intact.

5. a stable regime network is considered with stationarity conditions for the macroscopic fundamental relationships.

6. MFD is strictly concave holding only one maximum.

7. the network is considered to be congested with an assignment to the network based on the stochastic user equilibrium (SUE) principle.

8. given already stored algorithms for path choice in AVs, the choice processes are assumed to be deterministic; whereas for TVs path choice is done via logit model with the least variance parameter.

9. no inter-period dynamics are considered, as steady-state conditions with only one transport mode is deemed.

It must be noticed that in seventh assumption, the network considered is congested however for the initial setup the network is always non-congested or in other words they are sometimes referred to as network loading model. It is intended to visualize the effects of increasing link loads instead of full range demand-supply interaction at once. Later with a fully loaded network,

the assignment is done based on stochastic user equilibrium approach. Now to be clear about the question of path choice processes (path identification for any generalized OD), the explanantion is given in Section 3.2.1.

It is to be noted that concerning the societal, economical, and user-demographical characteristics, house maintenance and lodging costs are considered to be fixed depending upon the number of residents on a condition of a single city center having services of interest amassed in selected zones as in the case of many European cities e.g. Genoa, Cagliari, Porto, Timisoara. Although MFD is majorly dependent upon the road network topology, choices for route and mode, and signal controls (Loder et al., 2019), we are considering here uninterrupted conditions with a network topology as a major factor.

3.2.1 Network Structure

In the context of the considered scenario under the abovementioned assumptions, the traffic network is represented by a synchronic graph of nodes N and directed links L; $G = \{N, L\}$. Let $P \in Z$ and $Q \in Z$ be the set of origin and the set of destinations, respectively, for the considered network where Z is the set for all zones consisting of all the origin-destination pairs. All the links are connected by a set of paths R for all origin-destination pairs. $R_{pq} \subset R$ is the subset of all the paths connecting origin $p \in P$ to destination $q \in Q$. Moreover, an incidence matrix I is set up with all probable or possible paths connecting any generalized origin-destination pair (pq). It should not be confused with path choice probability functions which are followed to choose a path to travel among the various alternatives. This matrix involves all the paths (set of connected links and nodes in the network) with which a user can travel between its origin and destination. Each link $l \in L$ weighs depending on flow-based travel cost $c_l(flow_l)$ where $flow_l$ is link flow. Deviation in the flows on all the links is affecting the travel cost of a generalized

link. c_l is assumed to be monotonically continuous and directly proportional to $flow_l$. The parameters for possible paths search is dependent on the path impedances which in turn are dependent upon the path volumes (the sum of all the link volumes involved in the path). A parameter for the AVs-ready infrastructure is used for defining the impedances of network links. This is then used to search all the possible paths between an OD pair. A different number of extra iterations in each search iteration is defined for the best possible paths. To avoid overlapping paths, a detour test is also executed which defines that a new path is eliminated if the travel time is greater than 44% of the travel time to an existing path and the entire impedance is greater than that of an existing path.

As assumed, initial OD demand is fixed and remains stable denoted as m_{pq}, and distributed over the network following the SUE principle. Newly generated trips/demand m^{n}_{pq} follow the path choice process of the combination of logit and kirchoff model (more formaly known as Box-cox model) among various destinations independent from the irrelevant alternatives. This makes the attraction cost c_q an increasing function i.e. $c_q = c_j(m^{\mathrm{n}}_{pq})$.with the increment of flow under newly generated demand.

Parameters for the quantification are defined for routes set S, activities set AC, age groups set AG and households set H. Keeping in view the proposed enhancement for AVs, ceteris paribus, a quantification equation (QE_{AV}) is defined by aggregating various parameters from three classes: user demographics, road network, and land use, to generate seven indices. These indices together result in the penetration rate (PR_z) of AVs to be used in the formulated model.

Notations	
$DLP_{u,t}$	Discounted land owner profit for the land u in time t with inflation i.
$LR_{u,t}$	Rent of the land u in a time t.
$MC_{u,t}$	Maintenance cost of the land u in a time t.
$NOR_{u,t}$	Number of residents lived in land u over time t.
h_s	household size.
RL_z	The total length of roads in a zone z.
PS_z	The total population in the zone z.
$L_{r,prt}$	Length of route r from the route set RS using a private vehicle .
$e_{tr,h}$	total household income expenditure for transport in a month.
I_h	Total household monthly income.
B_{prt}	Binary index for private vehicle ownership. if a household owns a car it is 1 otherwise 0
$dc_{t,h}$	User discounted generalized cost for a time period t in each household h from set H for inflation i.
$\alpha_{q,a}$	Number of opportunities for activity a from set AC in destination zone q from set Z.
β_q	Binary index. 1, If an opportunity to carry out an activity is available in zone q or 0 otherwise.
$NTR_{g,a}$	Number of trips by the special group g from AG for an activity a from AC
$NTR_{tot,a}$	Total number of trips by all population of the respective zone for an activity a from AC
$AT_{\text{prt},r}$	Average travel time on route r using private transport.
ΔVKT_5	Relative growth of vehicle kilometers travelled over 5 years.
ΔGTI_5	Relative growth of the total covered area by transportation infrastructure for over 5 years
ω_{NMS}	Weight for the provision of non-motorized streets such as car-free zones and streets.
ω_{SF}	Weight for the number of services in the zone such as work, leisure, education.
ω_{R}	Reliability factor

3.2.2 Quantification of AVs

The first research objective as defined earlier is to obtain a realistic value of the penetration rate of AVs as an input to the private transport network analysis model. Depending upon land usage, socio-demographical, and road network classes, indicators are grouped and seven different indices equations are skimmed. These indices relate to the adaptation of AVs in a systematic and quantitative perspective instead of including a random percentage of these vehicles to identify the outcomes of introducing this new form of

mobility to the urban transportation networks. Furthermore, this quantification explains the diversity of the impacts and dependence of the usage of AVs in the coming decades. Not only does it allow to indicate various influences of different urban sub-systems on the usage of AVs but also illustrates the reverse impacts. This also realistically inputs the value of AVs into the system while avoiding divergent solutions at the same time.

1. In terms of demographical indices, the economical prospect of land usage is of prime importance while choosing a residential location (Putman, 2013). A variance of landowner profit over a period keeping in view the inflation reveals the extent of inequity in the vicinity type (Szeto et al., 2015). This inequity is a consequence of the population's choice to reduce the time spent to get to work and daily utilities. As (Wegener and Fürst, 2004) explains the slow relationship between land usage and transportation activities which gives a proposition of location choice near to the point of activities. This gives a proposition of adaptation AVs to reduce the inequity by renting or buying at farther places yet using time of commuting for productive tasks instead of driving. We use the index from (Szeto et al., 2015) to compute the landowner profit index $(LI_{u,t})$ as in (3.1) normalized to attain a value from 0 to 100. Where i is the inflation rate in a given period t and the rest of the attributes are defined in **Notations** table.

$$LI_{u,t} = \sum_{u} \frac{DLP_t}{(1+i_t)^{t-1}} \tag{3.1}$$

$$DLP_{u,t} = LR_{u,t} \cdot \frac{NOR_{u,t}}{h_s} - MC_{u,t} \tag{3.2}$$

2. As (Janasz, 2017) states that higher population density does not guarantee a higher number of services, but higher services do guarantee higher population density. This gives us the insight to evaluate the

density of transportation links which can be depicted by an index of transportation land usage (TI) as in3.3. Both land usage type and infrastructural provision are important for a new service to be welcomed as the era of the pandemic taught us and we witnessed it in the case of new electric micro-mobility provision. Also, (Litman, 2020) describes private vehicle ownership as being dependent on the infrastructure provider for a region as long as it remains sustainable which gives a proposition of direct relation for adaptation of AVs. An index is devised by taking a ratio of the weighted road link density to the weighted population density for an area. Whereas the attributes of the index are defined in **Notations** table.

$$TI = \frac{1}{|Z|} \sum_{z \in Z} \frac{RL_z \cdot \omega_{\text{NMS}}}{PS_z \cdot \frac{1}{\omega_{\text{SF}}}} \tag{3.3}$$

3. Land coverage (LC) by transportation network infrastructure is also indexed in terms of vehicle miles traveled throughout a certain period. Indexed as in (Kaparias, Bell, and Tomassini, 2011), long-term adaptation times for land usage is a property that is also common for the adaptation of AVs and them to be part of the traffic stream. The value for this index from 3.4 is in the range from [-100 to 100]. Whereas the attributes of the index are defined in **Notations** table.

$$LC = \frac{\Delta VKT_5}{\Delta GTI_5} \tag{3.4}$$

4. Urban mobility index (UI) formulated by (Kaparias, Bell, and Tomassini, 2011) represents the mobility condition of users within an urban transportation network by calculating travel time per kilometer. If a user is experiencing less or more precisely affordable travel time per kilometer

then the probability of adaptation of AVs is less and vice versa thus giving an indirect relation for the penetration rate. This index is upgraded as in 3.5 by using the route reliability factor which is the percentage of travel time not more than 10% higher than the average travel time on a certain route. Also, the value of the travel time $VOTT$ parameter is induced in the index which signifies a potential loss of productive hours for the commuter. The index calculated for a route r in route set S. Whereas the ω_{prt} is a binary operator having value of one if the trip is being carried out with a privatly owned car. Morever, the attributes of the index are defined in **Notations** table.

$$UI = \omega_{\text{prt}} \cdot \frac{1}{|S|} \cdot \sum_{r \in S} \frac{AT_{\text{prt},r} \cdot VOTT}{L_{\text{prt},r} \cdot \omega_{\text{R}}} \tag{3.5}$$

5. On the socio-economic side, (Nicolas, Pochet, and Poimboeuf, 2003) presented an effective index considering household transportation expenditure that is converted into household transportation budget index (HBI_t) considering the inflation rate over a certain period. The user generalized cost as in (Szeto et al., 2015) is used as an inclination towards adaptation of AVs in case a household owns a private vehicle controlled by a binary operator B_{prt} in determining the economic expenditure state on transportation for a household as in (3.7). The economic expenditure ratio EES_h for a household h is the ratio of total household income expenditure for transport in a month to the total household monthly income. Whereas the attributes of the index are defined in **Notations** table.

$$EES_h = \frac{e_{\text{tr},h}}{I_{\text{h}}} \tag{3.6}$$

$$HBI_t = \frac{1}{|H|} \sum_{h \in H} EES_h \cdot B_{\text{prt}} \left[\frac{dc_{t,h}}{(1+i_t)^{t-1}} \right] \tag{3.7}$$

6. Social inclusion index (SI_p) is explained in (Kaparias, Bell, and Tomassini, 2011) through an accessibility index on a spatial level for different activities. Activities represent the opportunities to undergo a task for the commuters of one zone concerning other zones. This index as in 3.9 is superimposed with trip propensity assumption $PF_{p,q}$ as in 3.8 from (Putman, 2013) in form of skewed peak form with a gamma distribution, with $d_{p,q}$ is the distance between any OD pair (p, q). The difference of minimum and maximum factors can reveal vacant developable space which in terms of (Wegener and Fürst, 2004) is a proposition for adaptation of AVs as a result of equitable development of land as in landowner profits inequity scenario. Whereas the attributes of the index are defined in **Notations** table.

$$PF_{p,q} = \frac{d_{p,q}^{-1.330}}{\sum_q d_{p,q}^{-1.330}} \tag{3.8}$$

$$SI_p = \frac{1}{|AC|} \sum_{a \in AC} \left(\sum_{q \in Z} \beta_q \cdot \alpha_{q,a} \cdot PF_{p,q} \right) \tag{3.9}$$

7. Similarly, (Kaparias, Bell, and Tomassini, 2011) defined an opportunity index (OI) at the social level for the special group of society (elderly, disabled, etc.) to quantify their movement. A reformed index is generated as in (3.11) by creating weighted values concerning each age group weight ω_g where is the special group g from age groups set AG since they rely on public transport systems having special allocations, demand responsive transit, or a family member to drive them off. Quantification of mobility of a special group is checked against the mobility of all other users.

$$MSG_g = \sum_{a \in AC} \frac{NTR_{g,a}}{NTR_{\text{tot},a}} \cdot \omega_a \tag{3.10}$$

Where MSG_g is the mobility of a special group for all activities in AC withe each activity a given a weight of importance in ω_a. Furthermore, the attributes of the index are defined in **Notations** table.

$$OI = \frac{1}{|AG|} \sum_{g \in AG} MSG_g \cdot \omega_g \tag{3.11}$$

Conforming to our first objective, all seven indices are integrated under all assumptions defined in Section 3.2. To obtain a quantification value of the integrated index as in (3.12), The weights of each index in the QE_{AV} are defined by passing the indices through a regression analysis over a choice of upgrading or buying a new vehicle. This willingness of users affects the user class indicators thus deciding the weight for each of them, particularly for the household transportation budget index. For instance, the data for each of the indicators included in the above-mentioned seven indices are analysed for the time t against the willingness of the stakeholders which in this case is the user to upgrade or buy a new vehicle. This suggests the importance of each of the indicators involved thus giving weightage to each of the seven defined indices. The weights $(\omega_1, \omega_2, \omega_3)$ given can be adjusted according to the area or city of application of the formulated QE_{AV}. Thus the cumulative or aggregated value of the final index can be a maximum of 600. This value is analyzed against the penetration rate according to Table 3.1 to be incorporated into the urban transportation network as below following quantile approach as per (Frei, 2006). The methodology of (Frei, 2006) is simple yet very practical to be implemented in indicator systems. In it, we made quantiles or groups of the penetration rate with an interval of 5% increment from 0 to 100%. Similarly, making intervals of the formulated QE_{AV} remaining in the bound of maximum value that is 600. Thus giving us 20 quantiles. The value of the formulated index falls in one of the intervals consequently revealing the

penetration rate of the AVs.

$$QE_{AV} = LI_{u,t} + TI + LC - UI + \omega_1 HBI_t + \omega_2 SI_p + \omega_3 OI \tag{3.12}$$

TABLE 3.1: Quantiles approach

QE_{AV}	PR_z (%)	QE_{AV}	PR_z (%)	QE_{AV}	PR_z (%)	QE_{AV}	PR_z (%)
0 - 30	5	151 - 180	30	301 - 330	55	451 - 480	80
31 - 60	10	181 - 210	35	331 - 360	60	481 - 510	85
61 - 90	15	211 - 240	40	361 - 390	65	511 - 540	90
91 - 120	20	241 - 270	45	391 - 420	70	541 - 570	95
121 - 150	25	271 - 300	50	421 - 450	75	571 - 600	100

3.2.3 Transport supply model

Moving onwards to the second objective of this research, macroscopic fundamental relationships are formulated for the heterogeneous traffic stream. Following the assumptions defined in Section 3.2, the fundamental relationship is determined by calculating the inter-vehicle spacing of heterogeneous traffic streams. The inter-vehicle spacing as in (Di Febbraro and Sacco, 2016) is evaluated as a weighted sum of the spacing of TVs and AVs as follows:

$$SP_{\text{mix}} = PR_{\text{z}} \cdot SP_{\text{AV}} + (1 - PR_{\text{z}}) \cdot SP_{\text{TV}} \tag{3.13}$$

where

$$SP_{\text{AV}} = v \cdot t_{\text{rec,AV}} + \frac{v^2}{2\, a_{\text{d,AV}}} + l \tag{3.14}$$

$$SP_{\text{TV}} = v \cdot t_{\text{rec,TV}} + \frac{v^2}{2\, a_{\text{d,TV}}} + l \tag{3.15}$$

Where SP_{mix}, SP_{AV}, SP_{TV}, $t_{rt,AV}$, and $t_{rt,TV}$ are spacing of heterogeneous traffic stream, spacing in case of only AVs, spacing in case of only TVs, reaction time in the case of AVs and TVs respectively. $a_{d,AV}$ and $a_{d,TV}$ is the minimum guaranteed deceleration rate in case of emergency for AVs and TVs respectively. v is the average vehicle velocity and l is the vehicle length. The governing parameters here i.e. the reaction time (a combination of human

reaction time to hurdle and brake actuation time) and deceleration rate are computed as in (Maximcsuk, Lu, and Tettamanti, 2019)and (Transportation and Administration, 2022). Since AVs are further divided into two groups as per our assumptions in Section 3.2, two reaction times for both of the classes are calculated. Thus AV_1 and AV_2 have different reaction times.

Moreover, aggregated reaction time for AVs is based on the dynamic weighted average dw_{avg} where weights are based on the concentration of the two sub-classes in the total amount of AVs. Calculation of the reaction time for two sub-classes of AVs is based on detailed propositions from (Litman, 2021b). For the first ten-year periods of the futuristic scenario of the heterogeneous traffic stream, AVs of Level 1-2 AV_1 are given the weight of 0.9 and for Level levels 3-5 AV_2 the weight is 0.1. For the next 5 years of the futuristic scenario, the AVs of Level 1-2 AV_1 are given the weight of 0.8 whereas Level levels 3-5 AV_2 class of AVs is given the weight of 0.2. The weights are represented by α_1 and α_2 for AV_1 and AV_2 classes as shown below. Following (Transportation and Administration, 2022) the brake actuation time is kept constant i.e. 0.35 sec considering the latest vehicle technology irrespective of automation, whereas, human reaction time to hurdle varies. The time to hurdle is the highest i.e. 0.65 sec for non-automated (traditional) vehicles and zero for the fully automated ones taking into account the constant safety policy in case of a brick-wall stopping.

$$t_{\mathrm{rt,AV}} = \textit{brake actuation time} + \textit{human reaction time} \tag{3.16}$$

$$t_{\mathrm{rt,AV}} = dw_{\mathrm{avg}} = \frac{\alpha_1 \cdot t_{\mathrm{rt,AV_1}} + \alpha_2 \cdot t_{\mathrm{rt,AV_2}}}{,} \alpha_1 + \alpha_2 \tag{3.17}$$

On integrating the quantified penetration rate of AVs PR_z into the inter-vehicle spacing relationship following the reaction time evaluation criteria mentioned above, macroscopic fundamental relationships can be defined for

the heterogeneous stream of traffic. Given the conventional inverse relationship of density of traffic stream with inter-vehicle spacing, the density of heterogeneous traffic stream d_{mix} involving AVs is formulated as a function of velocity and penetration rate according to the spacing as in 3.18.

$$d_{\text{mix}}(PR_{\text{z}}, v_{\text{mix}}) = \frac{1}{\begin{array}{c} PR_{\text{z}} \cdot \left(v_{\text{mix}} \cdot t_{\text{rt,AV}} + \frac{v_{\text{mix}}^2}{2a_{\text{d,AV}}} + l \right) + \\ (1 - PR_{\text{z}}) \cdot \left(v_{\text{mix}} \cdot t_{\text{rt,TV}} + \frac{v_{\text{mix}}^2}{2a_{\text{d,TV}}} + l \right) \end{array}} \tag{3.18}$$

Consequently, the flow as a function of the average velocity and the quantified penetration rate of AVs in the heterogeneous stream is presented in 3.19.

$$flow_{\text{mix}}(PR_{\text{z}}, v_{\text{mix}}) = \frac{v_{\text{mix}}}{\begin{array}{c} PR_{\text{z}} \cdot \left(v_{\text{mix}} \cdot t_{\text{rt,AV}} + \frac{v_{\text{mix}}^2}{2a_{\text{d,AV}}} + l \right) + \\ (1 - PR_{\text{z}}) \cdot \left(v_{\text{mix}} \cdot t_{\text{rt,TV}} + \frac{v_{\text{mix}}^2}{2a_{\text{d,TV}}} + l \right) \end{array}} \tag{3.19}$$

3.2.4 Travel time and flow relationship

Following the formulation of macroscopic fundamental relationships for capacity, the next phase is to pass this capacity to define the flow-dependent travel time tt_r function by incorporating the physical and functional parameters of the urban road network. Three different scenarios have been used to determine the travel-time flow relationship for an urban road link. Firstly the upgraded BPR function from (Cascetta, 2009) is used as in 3.20 which defines the link with a physical median so independent of the effects on the flow of the opposite direction in the traffic stream, then 3.21 (Cascetta, 2009) gives the travel-time flow relationship with an impact of opposite direction flows, and lastly the major function in 3.22 (Carteni and Punzo, 2007) which gives the travel time as a function of the flow of the heterogeneous traffic stream and the physical characteristics of the urban road link.

$$tt_{r_1}(flow_{\text{mix}}) = \frac{L_x}{v_o} + \gamma_1\left(\frac{L_x}{v_c} - \frac{L_x}{v_o}\right) \cdot \left(\frac{flow_{mix}}{Q_x}\right)^{\gamma_2} \tag{3.20}$$

$$tt_{r_2}(flow_{\text{mix}}, flow_{\text{mix}^o}) = \frac{L_x}{v_o} + \gamma_1\left(\frac{L_x}{v_c} - \frac{L_x}{v_o}\right) \cdot \left(\frac{flow_{mix} + flow_{\text{mix}^o}}{Q^o_{mix}}\right)^{\gamma_2} \tag{3.21}$$

$$tt_{r_3}(flow_{\text{mix}}) = \frac{L_x}{29.9+3.59W_x-0.58S_x-13.86Tor_x-10.8Dis_x-6.38Po_x+ 4.73Pv_x+\frac{-1.05\left(\frac{q^n}{W_x}\right)^2}{1+Tor_x+Po_x+Dis_x}} \tag{3.22}$$

In 3.20 and 3.21, L_x, Q_x, v_o, v_c are the length of the link, the capacity of the link, free-flow speed and critical speed for the urban road link x; γ_1 and γ_2 are the model parameters. It must be noticed that the variation of behavior between the human-driven vehicle and autonomous vehicle, calibrated γ_1 and γ_2 parameters are used for AVs following (Qiu et al., 2022). In 3.21, $flow^o_{mix}$ and Q^o_{mix} represent the flow in opposite direction and overall capacity respectively. Consideration of opposite direction flow is important to be as realistic in defining the travel-time relationships as possible. As in the case of many European cities, the urban road links are influenced by the opposite direction flow due to non-median separation between the two directions. In 3.22, W_x is the useful road link width; S_x is the non-negative slope of the link; Tor_x is the tortuosity of the link; Dis_x is the disturbance to traffic from external factors like pedestrian crossings, irregular parking, and side entries; Po_x is the percentage of links occupied by parking; Pv_x is a pavement type variable. The function from (Carteni and Punzo, 2007) is modified by multiplying the flow by the percentage increase in capacity from the speed-flow relationship in 3.19 and defined as q^n. Overall, these travel-time relationships

are dependent on the flow of heterogeneous traffic streams which is in turn dependent upon the quantified penetration rate.

AVs are modelled in PTV Visum (a macroscopic travel deman modeling software) to create a heterogenous traffic scenario and use the resulting data for optimization purposes. Things to take into account while modelling a heterogenous stream of vehicles in Visum are AVs-ready infrastructure, driving behaviour selection (normal, vigilant, aggressive) according to road category, and penetration rates. With a fixed initial demand according to the assumptions in Section 3.2, AVs are introduced into the network using the scenario management capability of Visum. The number of scenarios was equal to the quantified penetration rate calculated in Section 3.2.2 with each scenario consisting of 10 iterations in terms of modifications. So each scenario gives an increment of 1% of AVs in the network to assign the demand over the network following the algorithm defined in Section 3.2.5. In the AVs scenario, 50% of the network links are provided with an AVs-ready infrastructure modelled in scenario modifications. The characteristics of the links are updated by introducing user-defined attributes in the volume-delay (VD) function. The VD function is updated with user-defined attributes of reaction times, deceleration rate, and free flow speed for AVs using the methodology of our previous work (Bilal and Giglio, 2022). Also, the user-defined attributes for modelling heterogeneous traffic streams on the AV-ready links are based on the type of follower-leader vehicle. At the end of each assignment period, the flow-dependent link costs and zonal attraction costs are calculated given the constraint set up at a lower level. This is then passed on to the Genetic algorithm at the upper level of the model to maximise the traffic flow remaining into the inequity bounds. The algorithm goes on until the equilibrium is reached between volume and costs revealing the inequity values for the optimal solution at each introduced upper bound of inequity.

3.2.5 Covex minimization inequity problem (Lower level optimization problem)

Once the impacts on transportation network performance are evaluated, the quantified penetration rate is utilized to analyze the inequity in travel equilibrium costs on the inclusion of AVs. The increased trip generation on the introduction of AVs certainly shifts the equilibrium of travel costs so in the following section a methodology is devised to assess that inequity.

As defined in Section 3.2.1, link travel equilibrium cost $c_l(flow_l)$ is dependent on the flow of that link. Following the ETDA-VDC approach (Oppenheim, 1995), this cost function is differentiable concerning flow $flow_l$ consequently leading to defining the convex minimization transportation problem. The constraints for the lower level of the optimization model i.e. convex minimization problem are defined by following the approach of (Bilal and Giglio, 2021). The lower level minimization function as in 3.23 comprises three parts; flow-dependent travel link cost, zonal trip attraction cost and path choice function based on logit parameter ρ involves in the assignment procedure.

The cumulative flow over the network is constrained in 3.24, which is the cumulative sum of the existing path flows from the previous iteration plus the newly generated path flows of the current iteration for all the OD pairs p, q true for all the paths r connecting them. δ_{lr} is a binary operator whose value is 0 if the link l is not included in path r for an OD pair p, q, otherwise 1 if the link is included in the path. Not only this but the existing path flows $flow_{exis,r}$ and newly generated path flows $flow_{n,r}$ are also constrained as in 3.25 and 3.26 respectively. For any OD pair p, q and path $r \in R_{pq}$ the existing path flows $flow_{exis,r}$ should be equal to the existing demand m_{pq} so as the newly generated path flows $flow_{n,r}$ should be equal to the newly generated demand m^{n}_{pq}. As the newly generated demand m^{n}_{pq} from the inclusion of AVs into the system is quantified; it is constrained in 3.27 by the penetration

rate of AVs i.e. PR_z. The boundary conditions for existing path flows, newly generated path flows and newly generated demand made sure that the network remains under stable state conditions. By defining the lower level of the optimization model it is possible to distribute demand matrix X on the transportation network keeping in view the assumptions of Section 3.2. After distributing the initial demand over the network following the SUE principle based on zonal attraction costs $c_q(m^{\mathrm{n}}_{pq})$, the assignment algorithm reveals the link travel costs for the user choices. So, this part of the model is responsible for assigning the trips over the network while keeping the travel equilibrium cost to a minimum.

$$\min_{flow,m} TC(flow,m) = \sum_{l\in L}\int_0^{flow_l} c_l(x)dx + \frac{1}{\rho}\sum_{\substack{(p,q)\\ p\in P, q\in Q}} m^{\mathrm{n}}_{pq}(\ln m^{\mathrm{n}}_{pq} - 1) + \sum_{q\in Q}\int_0^{\sum_{p\in P}(m_{pq}+m^{\mathrm{n}}_{pq})} c_q(x)dx \quad (3.23)$$

subject to:

$$\text{(Cumulative Network flow constraint)} \quad flow_l = \sum_{\substack{(p,q)\\ p\in P, q\in Q}} \left[\sum_{r\in R_{pq}} (flow_r + flow_{exis,r})\delta_{lr}\right], \quad \forall l \in L \quad (3.24)$$

$$\text{(Existing path flows constraint)} \sum_{r\in R_{pq}} flow_{exis,r} = m_{pq}, \quad \forall p \in P, \forall q \in Q \quad (3.25)$$

(New path flows constraint) $$\sum_{r \in R_{pq}} flow_{n,r} = m^{n}_{pq},$$

$$\forall p \in P, \forall q \in Q \quad (3.26)$$

(New demand constraint) $$\sum_{q \in Q} m^{n}_{pq} = PR_z,$$

$$\forall z \in Z, p \equiv z \quad (3.27)$$

Boundary conditions:

(New path flow boundary) $flow_{n,r} \geq 0,$

$$\forall r \in R_{pq}, \forall p \in P, \forall q \in Q \quad (3.28)$$

(Existing path flow boundary) $flow_{exis,r} \geq 0,$

$$\forall r \in R_{pq}, \forall p \in P, \forall q \in Q \quad (3.29)$$

(New demand boundary) $0 \leq m^{n}_{pq} \leq PR_z,$

$$\forall p \in P, \forall q \in Q \quad (3.30)$$

Frank Wolfe assignment algorithm

As explained in the previous section, the lower-level convex minimization problem functions to assign the demand on the network while keeping the link travel equilibrium cost to a minimum. The assignment procedure follows a stochastic user equilibrium approach in which path choices for AVs are considered to be deterministic whereas for the TVs a general constrained

distribution logit model is followed with logit parameter $\rho = -0.03$. Following the incidence matrix I, for each path connecting an OD pair p, q the link cost vector is calculated and passed to the minimization function. For this purpose, an updated convex combination algorithm i.e. the Method of Successive Averages – Frank Wolfe (MSA-FWA) algorithm, is used. At each iteration, the link flows are calculated based on the generalized link cost function following the Taylor polynomial of first order yielding recursive equations thus giving the new link costs. Consequently updating the path choice probabilities at each iteration. the convergence to the solution is checked with a gap threshold of 0.001. According to the assumptions, the considered network is non-congested initially but as the iterations go on link cost and flows become mutually dependent. So, the assignment to the network is performed to obtain mutually consistent link costs and flows. Flow-dependent link costs are defined as in 3.31. Also, attraction costs are defined as in 3.32.

$$c_l = c(flow_l(Q_l^p, \psi)) \tag{3.31}$$

$$c_q = c(m_{pq}^n, C_p) \tag{3.32}$$

Here Q_l^p is the capacity of link l and ψ is the vector of the link's physical and functional characteristics. Moreover, in attraction cost c_q for any destination $q \in Q$, C_p is the maximum parking capacity of the attraction zone.

3.2.6 Bi-level optimization model (Upper level optimization problem)

In this section, a bi-level optimization model is formulated specifically defining the upper-level problem for it. Concerning the objective of assessing the inequity, we are clear that two agents are trying to optimize at the same time;

first the link travel cost minimization in the lower-level of bi-model and second the maximization of the newly generated demand bounded by inequity thresholds and quantified penetration rate at the upper level. So, a multi-objective function serves the purpose.

As defined earlier, user equilibrium is reliant on two things the minimization of the total link costs based on the distribution and assignment of trips following MSA-FWA and the maximization of the newly generated trips after introducing AVs into the system among various attraction zones. The scenario for attaining two objectives simultaneously and mutually at the same time is ideal for the bi-level optimization model. In the lower-level convex minimization problem, the distribution of trips over the network is dependent on $m^{n}_{p,q}$ as in 3.27 which in turn is dependent on the quantified penetration rate PR_z. Also, $m^{n}_{p,q}$ is a decision variable of the upper level of the model which is maximizing this M^{n}_{z}. Moreover, the distribution at the lower level is also serving as an input for inequity threshold constraint giving us Stackelberg Nash equilibrium condition (Liu, 1998). At the upper level, the maximization of newly generated trips is constrained by network physical characteristics, attraction zone, and essential inequity thresholds. The pictorial visualization of Bi-level optimization model is given in 3.1.

In the upper level of the bi-level model, the objective function is the maximization of total newly generated trips TG which is a function of total growth vector M^{n}_{z}. The function in 3.33 is weighted by ω_z which is the weight of opportunities in a zone z i.e. if a zone has fewer service opportunities the weight will be higher showing that the generation of trips to other zones will be higher and vice versa. The weights are adjusted to shift the system towards equilibrium with the proposed development in line with the maximum potential of development keeping the constraints defined active. As in 3.34, the lower and upper threshold of inequity is shown by θ_U and θ_L values respectively, $\boldsymbol{M^{n}_{z}} = (M_1, M_2, \ldots, M_{|Z|})$ is the vector of the total growth

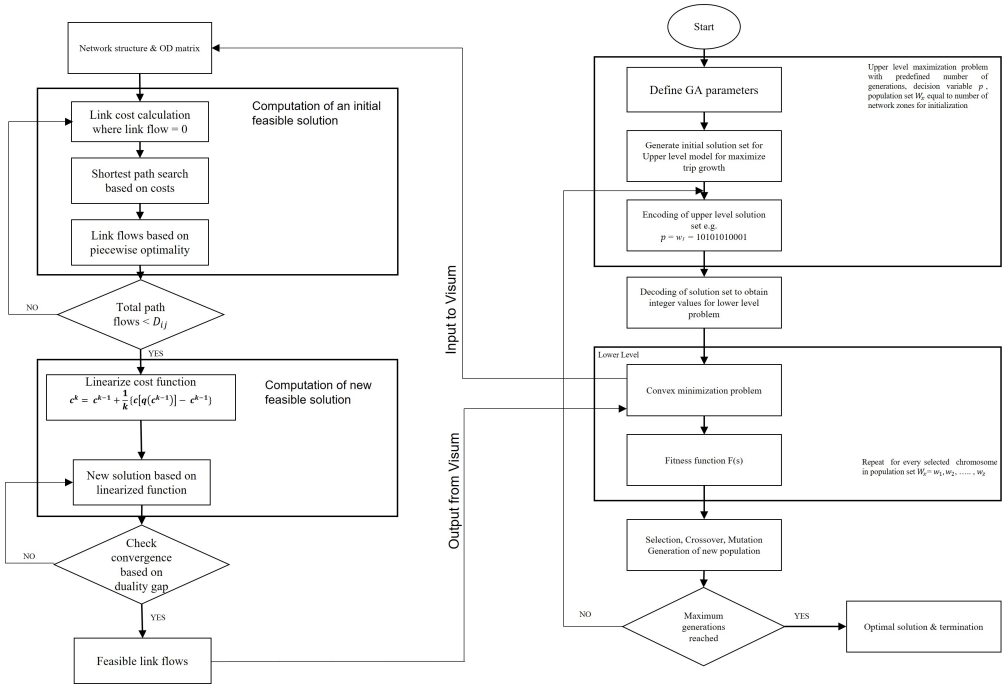

FIGURE 3.1: Bi-level optimization model

of trips (newly generated demand) on introducing AVs into the transportation network bounded by the quantified penetration rate for all the zones. $TC^{n}_{pq}(\boldsymbol{M}^{n}_{z})$ shows the user equilibrium travel cost supplied by the lower level of the model. This cost serves as an implicit function of the vector of newly generated demand $\boldsymbol{M}^{n}_{z}$ between OD pairs (p, q). 3.35 depicts that the flow on any generalized link $flow_l$ must not be greater than the link's capacity Q^{p}_{l} providing sufficiency to the assumption of the non-congested network. Also in 3.37, the total number of trips generated from all the zones for all destinations $\sum_{q \in Q} m^{n}_{pq}$, must be less than or equal to the maximum allowed growth for that zone $m^{n,max}_{z}$. Similarly, 3.38 shows that the amount of newly generated demand attracted by each zone from all the origin zones $\sum_{p \in P} m^{n}_{pq}$ must not b greater than the maximum attraction potential $m^{n,max}_{q}$. This attraction potential should be less than or equal to the parking space of the attraction zone C_q as in 3.39. Link constraints in 3.35 and 3.36 control the convergence of solutions for the formulated problem.

$$\max TG(\boldsymbol{M}) = \sum_{z \in Z} \omega_z M_z \tag{3.33}$$

subject to:

$$\text{(Inequity thresholds constraint)} \ \theta_L \leq \frac{TC^{\mathrm{n}}_{pq}(\boldsymbol{M})}{TC_{pq}} \leq \theta_U, \quad \forall p \in P, \forall q \in Q \tag{3.34}$$

$$\text{(Link capacity constraint)} \quad flow_l(\boldsymbol{M}) \leq Q^p_l, \forall l \in L \tag{3.35}$$

$$\text{(Link occupancy constraint)} \quad \frac{PCE_l(g)}{Q^p_l} \leq 1, \forall l \in L \tag{3.36}$$

$$\text{(Trip generation constraint)} \quad \sum_{q \in Q} m^{\mathrm{n}}_{pq}(PR_z) \leq m^{\mathrm{n,max}}_z - m^{\mathrm{cur}}_z, \quad \forall z \in Z, p \equiv z \tag{3.37}$$

$$\text{(Trip attraction constraint)} \quad \sum_{p \in P} m^{\mathrm{n}}_{pq}(PR_z) \leq m^{\mathrm{n,max}}_q - m_q, \quad \forall q \in Q \tag{3.38}$$

$$\text{(Attraction zone parking space constraint)} \quad m^{\mathrm{n}}_q \leq C_q, \forall q \in Q \tag{3.39}$$

Boundary conditions:

$$m^{\mathrm{n}}_{pq} \geq 0, \forall p \in P, \forall q \in Q \tag{3.40}$$

$$m_z^{max} = \sum_{q \in Q} m_{pq}^{\mathrm{n}},\ m_z^{\mathrm{cur}} = \sum_{q \in Q} m_{pq}, \forall z \in Z, p \equiv z \tag{3.41}$$

$$m_q^{\mathrm{n}} = \sum_{p \in P} m_{pq}^{\mathrm{n}},\ m_q = \sum_{p \in P} m_{pq}, \forall q \in Q \tag{3.42}$$

Here the point to ponder is that the constraints of link capacity, link occupancy, and attraction zone can be introduced both in the lower and upper levels of the problem. Nevertheless, the reason for introducing them to the upper level along with the inequity threshold is their behavioral results. They are introduced into the upper level of the model to avoid any divergence from the solution. Since we mentioned that the upper level of the model is acting as a decision-maker for the lower level, the latter itself is acting as a major constraint for the prior (Lee, Wu, and Meng, 2006). To solve the bi-level optimization model, a Genetic algorithm is used as explained in the next section. To summarise, the overall multi-objective fitness function of the model is given by (3.43)

$$\begin{aligned} FT(s) = \sum_{z \in Z} M_z - \mathcal{L}\Bigg[& \max_{(p,q)p \in P, q \in Q} \left\{0, \theta_L - \frac{TC_{p,q}^{\mathrm{n}}(\boldsymbol{M})}{TC_{p,q}}, \frac{TC_{p,q}^{\mathrm{n}}(\boldsymbol{M})}{TC_{p,q}} - \theta_U\right\} \\ & + \max_{l \in L}\left\{0, flow_l \breve{} Q_l^p\right\} + \max_{l \in L}\left\{0, \frac{PCE_l}{Q_l^p} - 1\right\} + \\ \max_{\substack{z \in Z \\ p \equiv z}} & \left\{0, \sum_{q \in Q} m_{p,q}^{\mathrm{n}} - m_z^{\max} + m_z^{\mathrm{cur}}\right\} + \max_{q \in Q}\left\{0, \sum_{p \in P} m_{p,q}^{\mathrm{n}} - m_q^{\mathrm{n,max}} + m_q\right\} + \\ & \max_{q \in Q}\left\{0, m_q^{\mathrm{n}} - C_q\right\}\Bigg] \end{aligned} \tag{3.43}$$

Genetic algorithm

To solve the formulated bi-level optimization model which is innately non-convex, the genetic algorithm approach is followed. Since two agents are trying to obtain the indirect global optimums; minimized equilibrium costs at the lower level of the problem and maximized newly generated trips at

the upper level; the genetic algorithm is ideal for obtaining the solution considering that link flows are nonconvex and continuous but they are non-differentiable function concerning the newly generated trips. In a nutshell, the decision variable for the upper-level problem; the vector of newly generated trip growth is coded as finite strings and for each string, the fitness is calculated by solving the lower-level problem. The process goes on until the optimal string is found under defined constraints and boundary conditions for both upper and lower-level problems.

The algorithm starts with random initial solutions as a population set for all the zones in the network. This population set consists of decision variables that are the maximum newly generated trips vector M comprising of $m^{n}_{p,q}$ values for each OD pair within a range of quantified penetration rate $\mathcal{P} = [m_z^{\min}, m_z^{\max}]$. This initial set $\boldsymbol{M}_{\boldsymbol{z}}^{\mathbf{n}} = (M_1, M_2, \ldots, M_{|Z|})$ is encoded in the form of binary strings to form a set of initial chromosomes. For encoding, we followed (Bilal and Giglio, 2021). Here the set of chromosomes is called a population. Following that random chromosomes are picked equal to the number of zones in the traffic network for mating and decoded using binary bit conversion to decimal technique. These decoded chromosomes are passed to the lower-level problem to obtain the fitness value from the fitness function. At the lower level, a sub-algorithm is implied to distribute and assign the demand on the network following the SUE principal as described in sub-section 3.2.5. After evaluating the fitness of the current population, the genetic algorithm applies three operators to generate new chromosomes from the existing mating ones. These new chromosomes are called offspring which replace the chromosomes they are made from. These operators are called selection, crossover, and mutation. This process is a single generation of genetic algorithms. After generating a new population the process repeats until the optimum set of the population is discovered. This whole procedure is described in the *Algorithm*. It should be noted that in the fitness function

Algorithm

STEP 1 Initialization.

1.1 In initialization, encode the random population set for the decision variable of the upper-level problem $(M_1, M_2, \ldots, M_{|Z|})$ in the form of finite binary $(0, 1)$ strings representing chromosomes for the first population set. For mating (assigning values of a number of trips for each zone) in initial iteration $(G_x, x = 1)$, pick the chromosomes equal to the number of zones in the network.

STEP 2 Using the technique mentioned above, decode the chromosomes in G_x to real numbers and pass it to the lower-level problem.
STEP 3 Evaluate the fitness function by solving the lower-level problem.

3.1 Determine the shortest path for all OD pairs (p, q).

3.2 Calculate the link flows for the network for all OD pairs based on the piecewise optimal step size distributing all present demands.

3.3 Linearize the generalized link cost function and find the new solution following the procedure as explained in sub-section 3.2.5.

3.4 If no convergence is reached go to Step 3.2 otherwise Step 4.

STEP 4 After obtaining the solution set for the fitness values, using the roulette wheel-based method eliminates the least probable solution from the solution set and keeps the solution with the highest probability, and reproduces the population set G_x.
STEP 5 Perform the crossover operation on the reproduced population set by giving a crossover probability of 0.5 (Bilal and Giglio, 2021) on the encoded population set. Replace the column entries of one chromosome with others yielding new offspring.
STEP 6 Perform the mutation operation after the crossover operation on the reproduced population set by selecting a random chromosome from the set based on mutation probability equal to $\frac{1}{\text{population size}}$ as per (Bilal and Giglio, 2021) and (Carroll et al., 1996). Replace the gene values from 1 to 0 and vice versa to generate new offspring revealing a new population set $(G_x, x = x + 1)$.
STEP 7 If the maximum number of generations for the genetic algorithm is reached the population set with the highest value of fitness results as an optimal solution otherwise go to Step 2.

in 3.43 a penalty function $\mathcal{L}$ is introduced to cater to the infeasibility of the solution set.

Numerical example of inequity calculation

In this sub-section, we try to illustrate the methodology of inequity evaluation with a simple numerical example. Let us consider the following simple network as seen in 3.2 having two origin zones 1 and 2 and one destination zone 4. Such that our OD pairs are 1 to 4 and 2 to 4. The demand from zone 1 is 400 and that from zone 2 is 600.

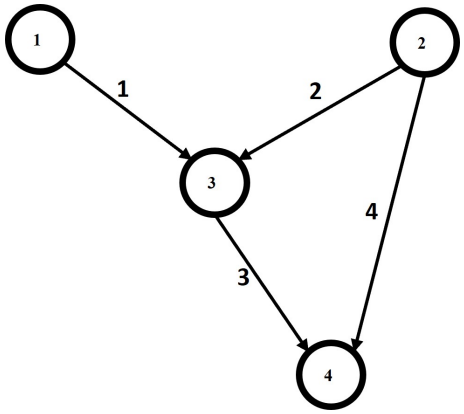

FIGURE 3.2: Example network

Let's assume that from the three indicator classes, the quantification of penetration rate is carried out and comes out to be 20% of AVs on the network. Only links 1, 2 and 3 are with AVs ready infrastructure. For the OD pair 1 to 4 only one possible path is identified whereas for the OD 2 to 4 two different paths are possible. Following the stochastic equilibrium approach, after the network is loaded with demand and reaches equilibrium: the flow-dependent link costs are accumulated to give path costs according to equation (3.31) as follows:

$$R_{1,4} = 44.605 \tag{3.44}$$

$$R_{2,4} = 57.135 \tag{3.45}$$

On the introduction of AVs into the network, the new demand from the

two zones becomes: from zone 1 is 480 and from zone 2 is 720. Once a heterogeneous traffic stream is formed. It is again assigned to the network to analyse the change in travel cost equilibrium. Once SUE has reached the new path costs are as follows:

$$R^{n}_{1,4} = 88.809 \tag{3.46}$$

$$R^{n}_{2,4} = 70.2197 \tag{3.47}$$

The corresponding ratios of OD travel path costs reveal the situation before and after the introduction of AVs and the impact it has on both zones.

$$\frac{R^{n}_{1,4}}{R_{1,4}} = 1.991 \tag{3.48}$$

$$\frac{R^{n}_{2,4}}{R_{2,4}} = 1.23 \tag{3.49}$$

It shows that the impact of AVs deployment has more impact on travellers from zone 1 with increased path costs as compared to those from zone 2. This means that zone 1 commuters are not attaining any positive outcome but rather facing negative implications as shown by the inequity ratio. Here we need to understand and estimate through optimizing the situation how much of these new forms of vehicles can these zones accommodate without creating any negative impact on the rest of the network users.

3.3 Public transport network vulnerability

After an extensive review of the existing literature, it revealed that a significant contribution is made to the assessment of public transport vulnerability (Cats and Jenelius, 2012; Mouronte-López, 2021; Berche et al., 2009; Albacete et al., 2017; He, Guo, and Xu, 2019; Cats and Jenelius, 2014; Chen

et al., 2007; Lu and Lin, 2019). Yet, no evidence was found in evaluating the vulnerabilities of a micro-mobility integrated public transport system apart from accessibility and conceptual analysis (Hamidi, Camporeale, and Caggiani, 2019; Zuo et al., 2020; Geurs, La Paix, and Van Weperen, 2016; Sagaris, Tiznado-Aitken, and Steiniger, 2017). This propels us to devise a methodology traversing through the definition of the network structure, setting off public transport and a shared micro-mobility model involving a data fusion method and mathematical construct of network vulnerability characteristics. The proposed methodology assumes that:

1. Departure rates of commuters are inelastic concerning the change in travel times.

2. The number of commuters is elastic representing day-to-day dynamics whereas their arrival at the stop points is modeled as Poisson random process.

3. Choice behavior of commuters is pre-trip/Enroute choice mixed based on the prior knowledge of transit timetables and headways while no knowledge about network conditions for the considered high-frequency urban transit system.

4. The disruptions occur in an emergency and commuters cannot change their origin or destination but the choice of mode and route. Moreover, no replacement service is provided by the operators.

5. Commuters have full flexibility in returning the rented bicycle to any of the docking stations.

3.3.1 Network structure

The public transport network structure is defined by a line-based graph $GP(N, L)$ with underlying nodes set NS and links set LS skeleton. N represents the

stop areas for public transport whereas, L shows the direct connection between any two stops traversed by public transport lines. Also, each link $l \in L$ can be used by several public transport lines where a line p from the public transport lines set P is defined by a continuous sequence of stops between an origin and destination terminals. Such that a line is $p = (np_1, np_2, \ldots np_{|P|})$ where np_1 and $np_{|P|}$ showing the first and last stops of the line p depicting the origin "o" and destination "d" terminals respectively. The subset of stop areas set N consisting of all origins and destination terminals is defined by $N_{ter} \subseteq N$. All the lines for which the origin and destination terminal is in N_{ter} are represented by a set POD which also is a subset of lines set P. By analogy each link belongs to a line i.e. $l \in p$, consequently consisting of a stop area pair $l = (np_1, np_2)$. Moreover, each stop and link belongs to a set of lines P_l and P_n respectively i.e. $(l \in p \forall p \in P)$ and $(n \in p \forall p \in P)$.

As depicted in (Bilal, Sarwar, and Giglio, 2021), each link in a public transport network is associated with a post-run time which is the time to traverse the link on a specific mode from the predecessor to the successor stop. This run time depends upon the type of public transport mode, time of day, characteristics of the road network, and traffic conditions. Similarly, each stop is also linked with a time when a public transport vehicle stops and commuters board and alight the vehicle known as dwell time. Precisely, dwell time starts from the opening of vehicle doors till they are closed. This also depends on the type of vehicle, number of dedicated entrances, time of day, and the number of commuters. For any link l at any time of day t the post-run time is defined by $TR_l(t)$ and for any stop n, line p, and any time of day t the dwell time is defined by $TD_{n,p}(t)$.

3.3.2 Multi-modal public transport model setup

A multi-modal public transport model is set up with a detailed time-table-based assignment for evaluating the interactions of supply and demand. Consequently, revealing the vulnerabilities in the network and impacts on micro-mobility integration as shown in 3.3. Public transport service is defined in terms of lines, line routes, and vehicle journeys with dynamic headways based on the time of day. Each vehicle journey for a certain line makes up a timetable which is a sequence of vehicle trips controlling its operation as well as performance evaluation. Apart from headway, successive vehicle journeys are a function of departure and arrival times according to the timetable thus giving a stochastic function since dependent upon the end of the previous trip.

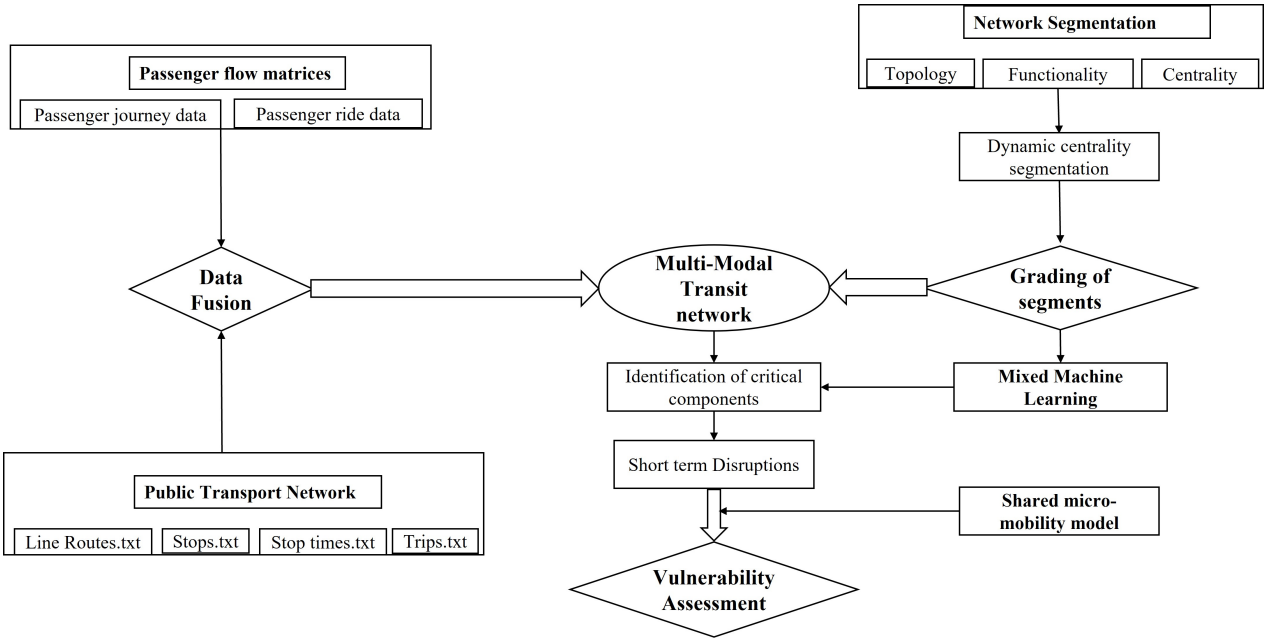

FIGURE 3.3: Framework for multi-modal transit network

For any line p, the set of departures of vehicle journeys in any time interval $(t, t+1)$ is represented as $F_p(t, t+1)$. The departure time $dep^f_{n,p}$ for any trip $f \in F_p$ using any line p at a particular stop n is a function of post-run time between the current stop n and previous stop $n-1$ together with the dwell

time at stop $n-1$ as shown in 3.50. Here, the post-run time $TR^{f}_{p,(n,n-1)}$ includes the congestion impedance parameter ζ incorporating the traffic state of the link. Similarly, the dwell time $TD^{f}_{p,(n,n-1)}$ since dependent on the number of alighting and boarding commuters is also stochastic. Moreover, a stop-blocking parameter ω is incorporated into the function. The number of commuters using the public transit network is modeled as stochastic showing daily variations and inelastic according to the assumptions. This demand is connected to the underlying transport network via a subset of stops N including all origin and destination pairs as N_{OD}. Whereas the number of commuters for any time interval $(t, t+1)$ for any origin and destination (OD) is represented as $T_{OD}(t, t+1)$. As the line follows a path of a sequence of stops, similarly, a commuter path in the form of traversed stops is represented as $r_{OD} = (n_{r,1}, n_{r,2}, \ldots, n_{r,|R|})$ for any OD pair. All paths of the commuters are represented by a path set R_{ab} for any origin a and destination b.

$$dep^{f}_{n,p} = (TR^{f}_{p,(n,n-1)} * \zeta) + (TD^{f}_{p,(n,n-1)} * \omega) \tag{3.50}$$

As per the above-mentioned assumptions in Section 3.3, the choice of a path by a given commuter is based on Pre-trip / Enroute mixed choice behavior as in (Bilal, Sarwar, and Giglio, 2021) and demand is assigned to the network via timetable-based assignment considering the precise departure and arrival times of all available lines. This choice varies considering the time of day, the lines available, and the purpose of the trip. Assignment of demand to the network consists of two parts; first the search of all possible/convenient paths for any OD pair based on the Branch & Bound method and second the choice of path based on commuter utility and perceived journey time. For an OD pair ab, all the good paths are branched based on the quality of a path $QP^{f_{ab}}_{r}$ as in 3.51 for any trip $f \in F_p$ and path r without involving fare parameters for simplicity. Here, $N^{f_{ab}}_{tr,r}$ is the number of transfers

included in path r factorized by a transfer penalty parameter γ. Also, $\delta_r^{f_{ab}}$ is the reliability parameter as used and detailed in (Bilal, Sarwar, and Giglio, 2021).

$$QP_r^{f_{ab}} = \sum_{n=n_a}^{n_b} dep_n^{f_{ab}} + (\gamma * N_{tr,r}^{f_{ab}}) + \delta_r^{f_{ab}} \tag{3.51}$$

Based on the quality of all the paths branched for an OD pair, the less favorable paths are eliminated. Apart from the quality, paths are compared for elimination based on the time interval of the trip, discomfort, and wait time in case of missed line. The maximum number of transfers allowed for branching and bounding is kept to 3. After the branching of favorable paths, the demand is assigned based on the probability of choice for all path alternatives between an OD pair. The probability of choice of a certain path out of all the present alternatives depends on perceived journey time and temporal utility. Perceived journey time involves the path length d_r, post-run time factorized by a mode type parameter μ_m, a factor of slopes and bends on the path σ_r, a factor of actual stops on the path $h_p^{'}$, and transfer walk time TW_p as seen in 3.52. For simplicity, the origin wait time is assumed to be half of the mean headway for a line $p \in P$.

$$PJT_r = d_r + \sigma_r + \sum_{p \in P} \left[(\mu_m * TR_p) + \frac{h_p^{'}}{h_p} + TW_p \right] \tag{3.52}$$

The demand between an OD pair consists of commuters which are distributed among various alternatives. Given our assumptions each commuter chooses the paths based on pre-trip / Enroute choice mixed behavior, so with evolving network conditions the PJT-dependent probability of path choice changes consequently the decision of the commuter to traverse a certain path $r \in R_{ab}$ between the origin a and any destination b. The decision of path choice out of all the alternatives is based on three components i.e. diversion,

alighting, and boarding at a particular transfer stop. These decisions represent the subsets of original path sets and are known as hyperpaths sets Y which is a subset of paths set R. The restriction of the initial path alternatives to the subsets is based on the decision components that are detailed in (Bilal, Sarwar, and Giglio, 2021). The probability of choice of the path then depends upon the path utility UT_r^t which is a function of perceived journey time as in 3.53 following the Box-cox model. This distribution principle is based on box-cox transformation. The transformation parameter φ is set to 0.5 and the beta parameter β to 1. The preference for using the Box-cox distribution model is that it not only takes the decision based on PJT-based impedances but also incorporates the impedance ratios thus generating a realistic distribution.

$$UT_r^t = f((b(\varphi) * PJT_r), t) \tag{3.53}$$

Hence the choice probability $Pr_u(r)$ of a commuter u to choose an alternative path $r \in Y$ is given by 3.54.

$$Pr_u(r) = \frac{e^{-\beta \cdot UT_r^t}}{\sum_{r_1 \in Y} e^{-\beta \cdot UT_r^t}} \tag{3.54}$$

This choice probability function is upgraded to accommodate the interaction between various branched alternatives to present more realistic results. To model the impact of other alternative paths r_1 on a path $r(r, r_1 \in Y \& Y \subseteq R)$ an independence factor $\rho(r, r_1)$ as in 3.57 is used in (Cascetta, 2009) which involves temporal proximity $t_p(r, r_1)$ of the two alternative paths as in 3.55 and perceived journey time advantage $adv_{PJT}(r, r_1)$ as in 3.56. Here $maxt_p(r, r_1)$ is the maximum temporal difference for a commuter u in which the path r_1 can affect r. α is the control constant for the absolute effect of the second part of the independence factor. $\varepsilon(r, r_1)$ is the maximum temporal advantage or disadvantage according to the evaluated PJT for various path

alternatives.

$$t_p(r, r_1) = \frac{\mid dep_{r_1} - dep_r \mid + \mid arr_{r_1} - arr_r \mid}{2} \tag{3.55}$$

$$adv_{PJT}(r, r_1) = PJT_{r_1} - PJT_r \tag{3.56}$$

$$\rho(r, r_1) = \left(1 - \frac{t_p(r, r_1)}{max t_p(r, r_1)}\right) * \left(1 - \alpha * min\left\{1, \frac{adv_{PJT}(r, r_1)}{\varepsilon(r, r_1)}\right\}\right) \tag{3.57}$$

Where;

$$\varepsilon = \begin{cases} \varepsilon^+ \forall & adv_{PJT}(r, r_1) \geq 0 \\ \varepsilon^- \forall & adv_{PJT}(r, r_1) < 0 \end{cases} \tag{3.58}$$

The range of $\rho(r, r_1)$ is $[0, 1]$ showing no impact of an alternative path to a completely overlapping path. This independence factor yields an independence function as seen in 3.59. Thus the upgraded probability function can be represented as in 3.60.

$$IF_r = \frac{1}{1 + \sum_{r_1 \in Y, r_1 \neq r}^{|Y|} \rho(r, r_1)} \tag{3.59}$$

$$Pr_u(r) = \frac{e^{-\beta \cdot UT_{r_1}^t} * IF_r}{\sum_{r_1 \in Y} e^{-\beta \cdot UT_{r_1}^t} * IF_r} \tag{3.60}$$

This linear reliance on the independence function confirms that m concurrent, identical but overlapping alternatives are treated as a single connection. According to the definition of IF_r, the independence of each of such m alternatives is precise $\frac{1}{m}$ (if no other connections with temporal proximity have an effect).

3.3.3 Shared micro-mobility supply model setup

A docking station-based shared bicycle system is modeled beside the public transport network. All the docking stations have a fixed number of docking places as well as the number of vehicles depending upon the time of day and place. The station is linked to the underlying public transport network via an access node which can be a transit stop and vice versa. The set of docking stations is represented as dS which is a subset of the nodes set NS thus $dS \in NS$. Similarly, bicycle lanes are modeled as a separate subset of links set as $bL \in LS$. The capacity of each station is represented as Q_{dS} and the optimal occupancy is represented as O_{dS}. The number of bicycles is represented by a set B. Similar to the public transportation model, when used in combination with transit, the commuter experience an extended impedance. The perceived journey time thus includes extra time and effort to retrieve and park the vehicle from/to the stations. The extended PJT thus includes the detour factor ϑ, rejection rate $\mathbb{R}$ in case of no vehicle available at the origin station or no parking space available at the destination station, journey time τ and wait time including the access and return procedures Ψ. The extended PJT as seen in 3.61 thus impacts the commuter utility and route choice behavior.

$$PJT_r = d_r + \sigma_r + \sum_{p \in P} \left[(\mu_m * TR_{p,r}) + \frac{h'_{p,r}}{h_{p,r}} + TW_{p,r} \right] + (\vartheta_r * \mathbb{R}) + \Psi_r + \tau_r \tag{3.61}$$

Where;

$$\mathbb{R} = \mathbb{R}_a + \mathbb{R}_e \tag{3.62}$$

$$\mathbb{R}_a = c_1 * e^{-c_2 * b_a} \tag{3.63}$$

$$\mathbb{R}_e = c_1 * e^{-c_2(Q_{dS_1} - O_{dS_1})} \tag{3.64}$$

Here, $\mathbb{R}_a$ and $\mathbb{R}_e$ are the rejection rate for accessing and returning a bicycle to the station respectively. b_a is the number of bicycles available for rent. Q_{dS_1} is the total capacity and O_{dS_1} is the occupancy at time interval t of station dS_1.

3.3.4 Data fusion

The proposed methodology uses a general transit feed specification (GTFS) data set to represent the public transportation network. The GTFS includes the required information to define the transit network considering the stochasticity of the methodology. Although having detailed data about various components of the network our focus was on extracting the transit routes with their frequencies $(T_routes.txt, frequencies.txt)$, system paths defined for each route $(vehicle_trips.txt)$, the stops defined for each route $(stops.txt)$ and the arrival/departure times at each stop $(stop_times.txt)$. Additionally, demand data for the usage of the public transportation network is represented in the form of origin-destination matrices A. It involves the data collected from the public surveys as well as the smart card readers thus revealing the commuters' journey and ride data. Next, the data for sharing stations of micro-mobility (bicycle) as well as the capacity and occupancy at different times of day is imported in $.txt$ format and merged with GTFS data to reveal the detailed network. This allows us to visualize which sharing stations are overlapping the transit stops and vice versa. Following the approach of (Buijtenweg et al., 2021), these two data sets are fused to be fed to the formulated methodology for analyzing the vulnerability of the multi-modal public transportation network. The fusion is done by the stop i.d. thus revealing the details of stop-wise passenger demand.

3.3.5 Network structural evaluation

The components of a network are critical for the vulnerability of a public transportation network both in terms of infrastructure and services. Many indicators had been designed and used to portray unique aspects of the network components. Once the multi-modal public transport model is set up next step in the proposed methodology involves the formulation and application of centrality indicators considering both infrastructures as well as services incorporating the stochastic nature of the realistic transit networks. The aim of devising the centrality indicators is to reveal the vulnerable components. This property of stochasticity leads to the dynamic clustering of the network as in Section 3.3.6 revealing not only the critical components of the network but also the neighboring critical components thus allowing for analyzing an evolving state of the network in case of disruptions

Dynamic Closeness

As the inherited meaning from the name, closeness represents the proximity of a certain node to all other nodes in the network topologically. For any pair of nodes (OD pair), the number of links on the shortest path between them yields the topological distance. If a node is capable of connecting to a maximum number of nodes in a network via a few links it is considered to be central thus closeness can be defined as an inverse of the shortest path length. For the directed graphs the closeness must be calculated separately for the incoming and outgoing links thus revealing in-closeness for paths coming toward the node and out-closeness for paths going out of the node. Since in the proposed methodology the public transportation model is stochastic the closeness of nodes is weighted by the number of line transfers to reach that node, the weight of links traversed in terms of vehicle journey time and the

number of commuters thus yielding a dynamic closeness function DC_{n_1} for any node n_1 as seen in 3.65.

$$DC_{n_1} = \Big[\frac{1}{\sum_{n_2 \neq n_1} e_{n_1 n_2} + dep_{n_1 n_2} + (\gamma * N_{tr,n_1 n_2})} * \Big(\frac{g_{n_1}}{N-1}\Big)\Big] \tag{3.65}$$

Where g_{n_1} is the number of reachable nodes from a node n_1 and $e_{n_1 n_2}$ is the Euclidean distance between nodes n_1 and n_2.

Dynamic Betweenness

A link is said to be central if it is a part of many shortest paths between any pair of nodes/stops to reach from origin to destination commonly referred to as betweenness (Freeman, Borgatti, and White, 1991; Crucitti, Latora, and Porta, 2006). Consequently, it becomes a critical component of the network in case of disruptions. To avoid the limitations of traditional node betweenness centrality measure as in (Cats and Jenelius, 2014), we here define a dynamic betweenness centrality DB_l for any link l. The DB_l considers weighted time series demand for any time interval $(t, t+1)$ between all OD pairs distributed over transit lines in terms of the number of commuters $T_{OD}(t, t+1)$ showing the inherent stochasticity. It is weighted by the stop centrality over a chosen path depending upon the choice probability $Pr_u(r)$ of a commuter u. To identify the presence of the concerned link l in a path r, a link-path incidence matrix I is generated. An element $i(r,l) = 1$ indicates that the link is present in the path and vice versa.

$$DB_l = \frac{\sum_{n \in r} C_n}{\sum_{n \in R_{OD}} C_n} * \frac{\sum_{r \in R_{OD}} \{\sum_{u \in T_{OD(t,t+1)}} Pr_u(r)\} * i(r,l)}{\mid T_{OD(t,t+1)} \mid} \tag{3.66}$$

3.3.6 Vulnerable components

Following the evaluation of network centrality, the next step is to cluster the network to better understand the hierarchy of its components revealing the vulnerable spots. Based on the dynamic closeness and betweenness functions the nodes and links of the public transport network are clusterized. Thus this hierarchical clusterization inherently takes into account the infrastructure and service characteristics of the transit system. This segmentation consists of two steps; the first is to divide the network into a suitable number of clusters based on the dynamic centrality measures and expose the most vulnerable components following an unsupervised machine learning approach. Second, after the clustering is complete, a supervised machine-learning approach is used to reveal the nearest neighbors of the most vulnerable nodes and links.

Based on unsupervised learning

Taxonomy analysis or clustering of the network based on centrality measures involves an unsupervised learning approach. *Taxonomy* is the clustering method used to draw inferences and hidden patterns in the evaluated centrality for links and nodes. It clusters the data into k exclusive groups treating each centrality value for link and node as an object that has a precise location in space. Operating on actual observations it finds the objects which within an identical cluster are near to each other and farthest from the objects of other clusters. To find the optimal number of clusters *hitandtrial* method is used starting from 2 to 5 clusters. The distance metric is set to be $city - block$ to compute the centroid in $p - dimensional$ space. It is the summation of the absolute difference between the centroid and each cluster point location as seen in 3.67. Here *obs* is the location of a data point in a cluster, *cent* is the centroid location, and $\mid q \mid$ is the total number of observations in a respective

cluster. The maximum iteration is set to be 100 whereas the replicate is set to be 5. $kmeans++$ algorithm is used for cluster centroid initialization.

$$cb(obs, cent) = \sum_{q=1}^{|q|} \mid obs_q - cent_q \mid \tag{3.67}$$

The method also known as Lloyd's algorithm goes along with the following steps;

1. Choose k being the number of groups the data set Z is meant to be clusterized in.

2. Initialize by selecting k starting clusters following the $kmeans++$ algorithm as:

   (a) Randomly select an object from the data set and assign it as a first centroid $cent_1$.

   (b) Calculate the distances of each observation obs_1 from centroid $cent_1$ and assign them to $d(Z_{obs_q}, cent_1)$.

   (c) Choose the next centroid $cent_2$ from Z based on the weighted probability of the previous centroid's distance i.e.

$$\frac{d^2(Z_{obs_q}, cent_1)}{\sum_{h=1}^{z} d^2(Z_h, cent_1)} \tag{3.68}$$

   (d) Evaluate the distance of each object in set Z to each centroid and assign the object to the consequent nearest centroid.

   (e) Select each center with probability proportional to the calculated distance from this center to the centroid is already chosen.

   (f) Go to Step 2.4 until k number of centroids is chosen.

3. Calculate the distance of the cluster centroid to each point in a data set.

4. Assign each point in the data set to the respective cluster with the relative closest centroid.

5. For the first replicate, determine the average of all the points in each cluster yielding k number of new centroids locations.

6. Go to step 3 until the cluster observations do not change or the maximum number of iterations is reached.

This results in an optimal number of clusters with the most vulnerable component in each of them revealed. To validate the clustering results a *Silhouette plot* method which identifies the most suitable value of clusters for the present dataset.

Nearest neighbors search via supervised learning

Once the vulnerable component in each one of the clusters is highlighted, the next step is to find the nearest neighbors of that critical component based on evaluated centrality. Now here we do not skim out the topological nearest neighbors. The reason for this is that during the analysis of public transportation assignments with and without disruptions, the topologically affected nearest neighbors are also identified as explained in Section 3.3.7.For identifying the nearest neighbors, the $k - nearest\ neighbors(knn)$ algorithm is used which skims out the nearest data points within a specified distance considering the distance metric. For producing efficient results a searcher object is created first using the $kd - treesearcherobject$. $kd - tree$ model segmentizes the *mbyk* data set (k-mean clustered data) by repeatedly splitting it into m points in the form of a tree. Once the tree is formed it includes the training data set (the centrality data for the nodes and links), the distance metric with its parameters, and the data points in each leaf of the tree which is also known as the bucket size. After creating the tree object, the *knn* search algorithm is used to find the all nearest neighbors of the query data point

which in our case is the most vulnerable component of each cluster from Section 3.3.6. This method is ideal and most effective when the number of clusters is *leq* 10. For comparisons, two different distance metrics are used in *knn* is $Minkowski(md_{ij})$ as seen in 3.69 which for a special case of Minkowski exponent $v = \infty$ becomes $ChebyChev\ (cd_{ij})$ as seen in 3.70.

$$md_{ij} = \sqrt[v]{\sum_{q=1}^{|q|} \mid x_{iq} - y_{jq} \mid^{v}} \tag{3.69}$$

$$cd_{ij} = max_q\{\mid x_{iq} - y_{jq} \mid\} \tag{3.70}$$

The bucket size is kept to 50 representing the number of data points in each leaf with $v = 5$.

3.3.7 Random service disruptions

Randomly generated service disruptions are modeled to evaluate the change in the system reflecting any unforeseen and short-term event (accident, protest, signal malfunction, vehicle breakdown, etc.). The disruptions are targeted at certain vulnerable segments skimmed out in previous steps of the proposed methodology. Following the assumptions described above, the disruptions at one vulnerable segment or stop create two possibilities $(S1\ and\ S2)$ whereas the non-disruptive normal state is considered to be the base scenario $(S0)$ for comparisons;

S1 a disruption on a stop means the line continues to traverse on the defined vehicle route but does not allows commuters to board/alight at the disrupted stop.

S2 a disruption on a link of the network implies that the line de-routes from its original path skipping all the stops from a de-route start point to the

endpoint and thus does not allows commuters to board/alight on the de-route course.

This reflects the real situation when commuters on board and those waiting at the non-served stops can re-plan and revise their travel decisions, however, their origin and destination remain the same. This creates a spill-over effect on the rest of the network when this induced demand interacts with the transit supply consequently creating delays, failed boardings, discomfort, etc. In the present study, the usage of a micro-mobility (Bicycle) sharing system is analyzed to evaluate the vulnerability of a public transport system in case of two disruption scenarios $(S1,\ S2)$ thus generating the following three combinations;

B1 Disruptive access to the origin stop: Ride a bicycle from sharing station to the accessible transit stop, use public transport, and alight at the destination stop.

B2 Disruption on some part of a trip: Alight at the non-disruptive stop, ride a bicycle to the next accessible stop, board the public transportation available, and alight at the destination stop

B3 Disruptive access to destination stop: Board public transportation to the last accessible stop before the destination, alight at the stop, and ride a bicycle to the nearest station to the destination.

The combination of disruption and bicycle usage scenarios is analyzed to determine the impacts of disruptions thus answering the questions of vulnerability. Since our multi-modal public transportation model is stochastic showing day-to-day variations and demand depending upon the time interval of the day the disruptions and their impacts are also dynamic. Considering the assumptions and aims of this study the vulnerability of the transit network is presented in terms of the commuter's disutility $CD_{r(t,t+1)}(S,B)$

for a different combination of scenarios $(S,\ B)$ at any time interval $(t, t+1)$ in terms of productive hours (time used in travel which if used for work could result in production). The disutility is a combination of total ride time TRT_r (including post-run times and dwell times at each stop on the path), the number of actual stops $h_r^{'}$, the total number of transfers, the total wait time TWT_r considering all events and total walk time including the transfer walk time.

$$CD_{r(t,t+1)}(S,B) = TRT_r + \frac{h_r^{'}}{h_r} + N_{tr,r} + TWT_r \tag{3.71}$$

This stochasticity of this proposed methodology reveals a realistic complete situation of the transit network under different disruption scenarios with and without mitigation by the provision of micro-mobility options. This also results in the most affected links, lines, and stops apart from the disrupted ones thus revealing the spill-over effect too.

Chapter 4

Inequity analysis for heterogeneous traffic stream on the introduction of AVs

4.1 Introduction

This chapter includes the application of the extensive methodology formulated in Chapter 3 on real transportation networks for the city of Genoa, Italy. Section 4.2 involves the definition of the study area and the data resources used for extracting the data to be adopted for the analysis. The penetration rate of AVs is quantified based on real network data in Section 4.2.1 followed by the impacts of the inclusion of AVs in the network on macroscopic fundamental characteristics in Section 4.3. The detailed inequity analysis is carried out in Section 4.4 to highlight the variations in travel equilibrium costs.

4.2 Real network application

For real network implementation of the private network transportation model, a part of the transportation network of the city of Genoa in northern Italy is used as can be seen in Figure 4.1.

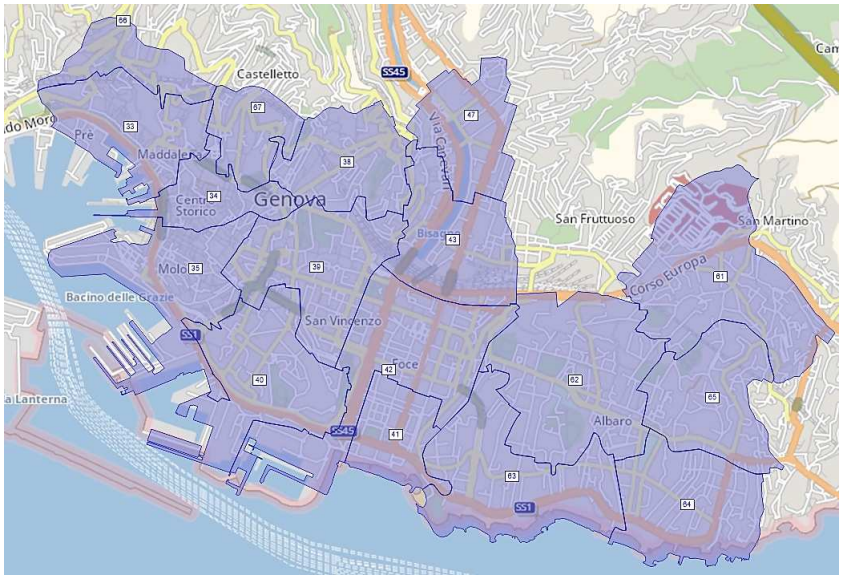

(A)

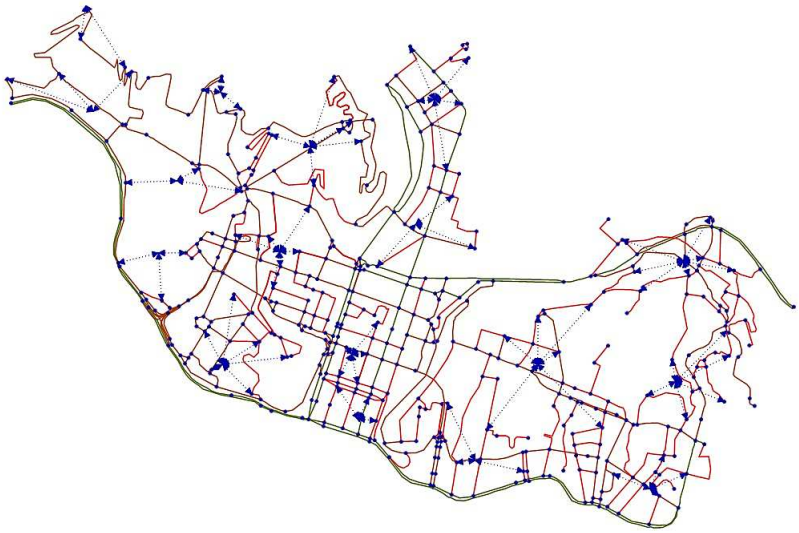

(B)

FIGURE 4.1: (A) Area considered for application (B) Network of the considered area

The considered network is represented by a synchronic graph; divided into 17 zones with 502 nodes and 1464 links covering an area of 8km^2. All zones in the network are origin and destination zones simultaneously with an initial fixed demand as shown in Table 4.1 obtained from Comune di Genova (the city municipality). The zones are numbered based on the data obtained and the numbers are edited to avoid any confusion during the analysis. Furthermore, while visualizing results; it's easier to refer to the zone

number instead of zone names when the results are a lot. The term maximum production refers to the maximum amount of trips or demand that can be on the network from a certain zone whereas the term maximum accommodating volume on the other hand reflects the number of inbound trips that a certain zone can handle without being saturated resulting in a halt situation. Considering that, these two values act as bounds and constraints for the two levels of the optimization model which resultantly tries to maximise the trip growth while keeping the inequities to the lowest. The maximum possible growth of newly generated demand for each zone is strongly dependent on the quantified penetration rate of the AVs in respective zones calculated as per the methodology defined in Chapter 3. Now when we say the generated demand is maximum; two things must be pointed out. First that the demand data obtained for the analysis was a real data set of the trips generated from the zones thus considered to be the maximum demand being generated. Second, the amount of AVs added to that demand is the maximum amount of AVs quantified for the said time according to the formulated indices. These both combine to give a sense of maximum possible growth of newly generated demand in particular. For that socio-economic and user demographical data for the area deemed is extracted from the ISTAT (Italian National Institute of Statistics) whereas, the transportation infrastructure data is retrieved from Eurostat. Information about trips is mined from *Statista* and *Odyssee-Mure* used for the quantification of the penetration rate of AVs.This data is utilized to quantify the penetration rate for AVs according to Scenario 0 (the present time scenario) and Scenario A (futuristic heterogeneous traffic stream scenario after 15 years) as well as for the sensitivity analysis in the form of maximum bounds. The population is categorized into four groups $(15-24, 25-44, 45-64 \; and \; \geq \; 65 \; years \; of \; age)$. For synthesizing social inclusion and opportunity indices the activities set ACT is defined with six

activities namely; Work, shopping, leisure, recreational, health, and education.

TABLE 4.1: Network data

Zone	Name	Originating Volume	Attraction Volume	Maximum production	Maximum accommodating volume
33	Prè	1145	1134	1545	1488
34	MADDALENA	657	659	886	822
35	MOLO	2079	2409	2806	3172
38	MANIN	1216	1188	1641	1463
39	S.VINCENZO	4272	4043	5767	5260
40	CARIGNANO	1363	1197	1840	1275
41	FOCE	579	605	781	747
42	BRIGNOLE	2927	2875	3951	3825
43	S.AGATA	1272	1167	1717	1333
47	MARASSI	1393	1388	1880	1643
61	S.MARTINO	2927	2875	3951	3725
62	ALBARO	2656	2394	3585	3052
63	S.GIULIANO	1311	1777	1770	2187
64	LIDO	1146	1129	1547	1280
65	PUGGIA	917	898	1237	1057
66	Oregina	1535	1489	2072	1884
67	Castelleto	1261	1319	1702	1646

All seven indices are calculated for the extracted data and based on the methodology mentioned in Chapter 3; a penetration rate for AVs is obtained.

4.2.1 Quantification of penetration rate

In Scenario 0, all seven indices are calculated based on extracted data for the year 2021 and subsequently considered as a base scenario with no AVs available to the general public. The values for the different indices are shown in Table 4.2. For Scenario *A*, the related growth rates are utilized to predict the socio-economic, demographical, trips, and transportation infrastructural conditions in fifteen years to be used in calculating all the indices. The growth rates are extracted based on the analysis of the projections of land usage and user demographics for the period of 2020-2040 presented by ISTAT. For the indicator classes of the road network, the relative growth rates are calculated based on past 15-year trends for included indicators as mentioned in Chapter 3. The growth rate for maintenance cost, population size, land unit rentals household size, household income, age group, transportation

expenditure, and travel time are computed (they are 19.41%, -1.4%, 6.23%, 3.13%, 10.47%, 9.23%, 3.14%, and 4% respectively). It must be noted that the growth rates for household size and age group are computed according to the division of age groups mentioned earlier. These new values are then used to quantify the penetration rate of AVs in fifteen years keeping in view the base year penetration rate is zero. Table 4.2 shows the values for indices and quantified index values for both scenarios. It must be noted that the quantified penetration index QE_{AV} index as in Chapter 3 formulated is not a simple summation of all the indices instead its value is based on the weights given to each of the seven indices through regression. The highest weights are given to the mobility index and activity accessibility index (they are 1.2 and 1.5, respectively), under the proposition of usage of AVs by the group of society who were previously unable to mobilize themselves on their own. From the fractiles approach discussed in Chapter 3, the penetration rate in Scenario A results at 35%, following the values reported in Table 4.2.

TABLE 4.2: Quantification of Penetration rate

Index	Scenario 0	Scenario A
$DLP_{u,t}$	12.55	50.28
TI	47.83	64.86
LC	14.48	38.03
UI	29.60	49.60
HBI_t	5.72	34.93
SI_p	15.89	21.72
OI	76.44	48.83
QE_{AV}	158.59	232.72

4.2.2 Senstivity analysis for quantified penetration rate

To identify the model uncertainties one of the best tools is sensitivity analysis. To keep things simple we assume the profit of land usage and infrastructure

usage is kept constant over the analysis period. Whereas, all other 5 indices are tested over the range of values to evaluate the impact of their variation on the QE_{AV} and consequently on the final penetration rate of AVs. Considering the trends of growth for the involved indicators the maximum possible bounds of each of the indices is tested to see the effect on penetration rate thus giving us a range of penetration rate instead of a single value.

TABLE 4.3: Senstivity analysis results on the penetration rate of AVs

Index	Scenario 0	Scenario A	OI	SI	HBI	TI	UI	All
DLP	12.55	50.28	50.28	50.28	50.28	50.28	50.28	50.28
TI	47.83	64.86	64.86	64.86	64.86	51.42	64.86	51.42
LC	14.48	38.03	38.03	38.03	38.03	38.03	38.03	38.03
UI	29.60	49.60	49.60	49.60	49.60	49.60	58.72	58.72
HBI	5.72	34.93	34.93	34.93	29.1	34.93	34.93	29.1
SI	15.89	21.725	21.725	18.12	21.725	21.725	21.725	18.12
OI	76.44	48.83	26.32	48.83	48.83	48.83	48.83	26.32
QE_{AV}	158.59	232.72	202.67	224.27	223.85	216.24	220.56	168.87
PR_z	25	35	30	35	35	35	35	25

In terms of the transportation land usage index (TI), the QE_{AV} is computed for a range of 20% to 26% for the road network of the considered area. All things kept constant this index has a moderate impact on the quantified penetration rate for its maximum possible bounds. For the user mobility condition index (UI), the model is tested for the bounds from 18% to 40% however the variation in QE_{AV} is a mere 6%. In the case of the household transportation budget index (HBI), social inclusion index (SI), and opportunity index (OI) the change in QE_{AV} is 4%, 4%, and 13% respectively for the sensitivity bounds of 16-83%, 23-55%, and 36-47% respectively. However, the collective change for all the indices has an appreciable variation in the value of QE_{AV} that is up to 29% for all the sensitivity bounds included as shown in Table 4.3. Now considering the fractiles approach as discussed in Chapter 3, the penetration rate according to the sensitivity analysis gives us a range

from 25% to 35% following the values reported in the quantiles approach in Table 3.1. This range is incorporated in further fundamental relationships for explicitly revealing the impacts of AVs on the traffic network fundamentals.

4.3 Macroscopic fundamental characteristics

After the quantification process of AVs, this penetration rate range (25-35%) is used as a percentage of AVs on an urban road network to generate a heterogeneous traffic stream. For the generation and initial accuracy testing of fundamental relationships, a representative link is used from the network. After which the derived fundamental relationships are applied to the network shown in Figure 4.1. To represent the prevailing traffic conditions in both scenarios, a speed-density relationship is obtained using equation 3.18 as shown in Figure 4.2 revealing the decrement in traffic stream speeds as the density is increased. Eventually, traffic will reach a block flow situation at jam density when the speed reaches zero.

However, for the same densities of traffic on the link, the heterogeneous stream is showing a range of higher speeds (area between the blue and green curves) as compared to the only TVs scenario that's where the effective time to hurdle in the case of AVs comes into play. The corresponding range of capacity of an urban road link is calculated from the speed-flow relationship from equation 3.19 as shown in Figure 4.3. It is evident that in a heterogeneous traffic stream the capacity of an urban road link increases efficiently with most of the parts yielding un-saturated traffic conditions in range areas of blue and green curves. Gains in flow rate are significant as long as the traffic state is un-saturated i.e. before the critical density is reached in both scenarios.

It would be prudent to obtain the traffic stream conditions with higher flows by increasing the free-flow speed however, the traffic stream will be

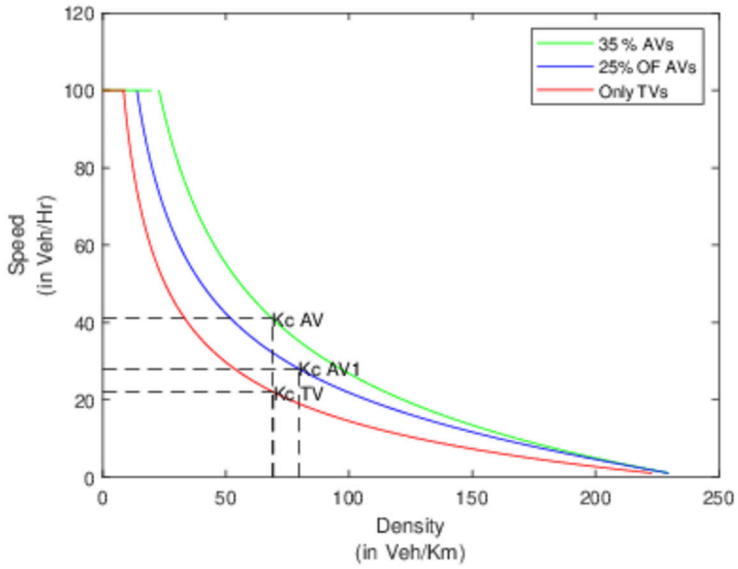

FIGURE 4.2: Speed-density relationship for Scenario 0 and scenario A under sensitivity range of AVs

more saturated and unstable. Also, the urban link congestion can be dealt with by keeping the topology intact and making it a heterogeneous stream with the inclusion of the desired percentage of AVs remaining under acceptable and realistic limits. Albeit safety and driving behavior will be the question that is out of the scope of this research. It is interesting to see that the range of AVs quantified when injected into the traffic stream of the heterogeneous stream has better performance in terms of macroscopic parameters whether its speed, flow, and speeds at the same critical densities which advocates favorability to AVs to be the part of the network casting positive impacts on network capacity.

The trend of saturation grade is also shown in Figure 4.4 which is again

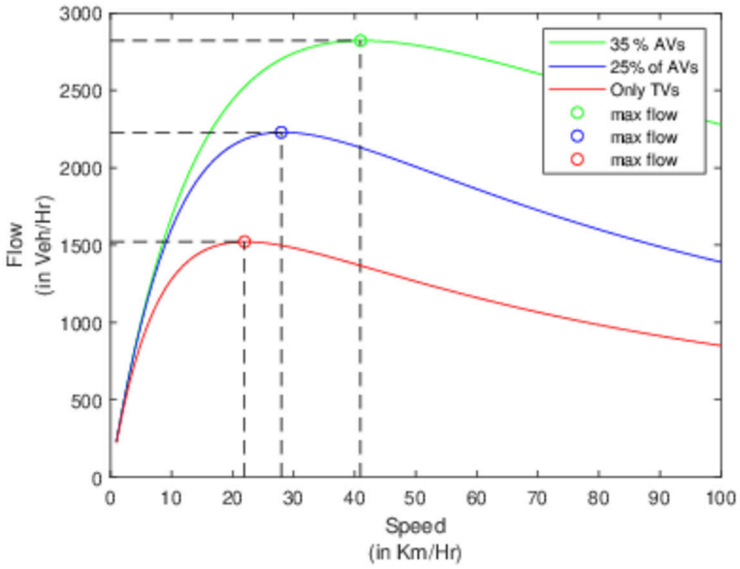

FIGURE 4.3: Speed-flow relationship for Scenario 0 and scenario A under sensitivity range of AVs

yielding higher speeds of the stream for the same saturation level as compared to the only TVs traffic stream against the critical densities obtained. Although the trend for saturation grade at a lower penetration range of 25% is quite closer to the TVs scenario yet giving an improvement in the speed at which saturation achieves. For evidence this saturation grade is 1 at a point where the network reaches it maximum allowed capacity, past this, the network starts to choke.

The travel-time flow relationships are plotted in Figures 4.5 4.6 following the defined equations in Section 3.2.4 using equations 3.20 and 3.21. It is clear from Figures 4.5 4.6 that opposite-direction flow has an impact on the travel times of an urban link. The increase in travel time is in the range of 7%-10%

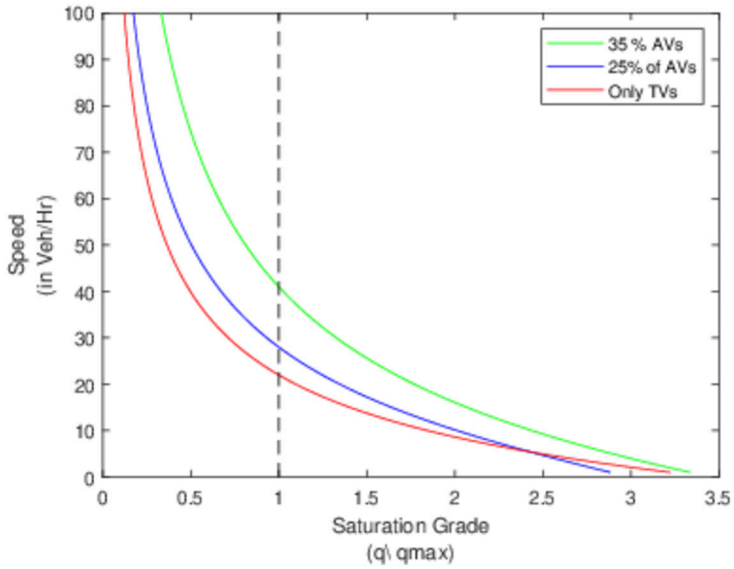

FIGURE 4.4: Decrement in vehicle speed with respect to Saturation grade

if no physical median is present between opposite links as seen in the area between blue and green curves which are common in urban street networks of the considered realistic network of Genoa. It is important to mention that 60% of the links in our considered network were consisting of a physical median between opposite directions. Although, it looks to the naked eye that the presence of a physical median has no impact but it has a small yet appreciable impact on the travel time for the flows in the heterogeneous traffic stream.

Moreover, to attain the stated objective in Chapter 1, the travel-time flow relationship is plotted as shown in Figure 4.7 by using equation 3.22 with the influence of the urban link's physical and functional characteristics. The

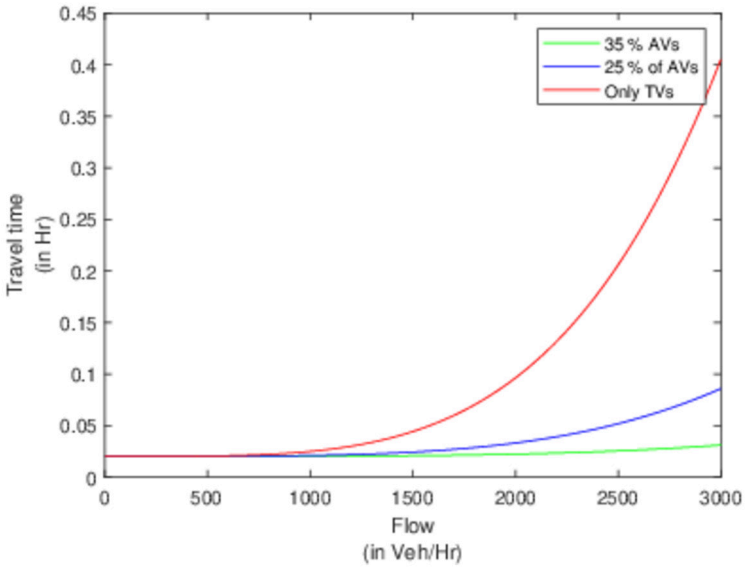

FIGURE 4.5: Travel-time flow relationship with a link having physical median and no influence of opposite direction flow under sensitivity range of AVs

increase in capacity of an urban link as deduced from the speed-flow relationship in Figure 4.3 by introducing AVs has an appreciable impact on the travel times as can be seen in Figure 4.7. The large area between the two penetration curves is revealing the fact of improved traffic conditions with the inclusion of AVs. In the considered network, useful road link width and the percentage of links occupied by parallel parking had a direct impact on the flow relationship. With an increment in parallel parking and decrement in useful road length, the travel time increased for both TVs and AVs. However, the increment was higher in TVs as compared to the heterogenous stream with AVs. Given the topography of the considered area tortuosity and the non-negative slope were very less except for the southern part of Corso Italia,

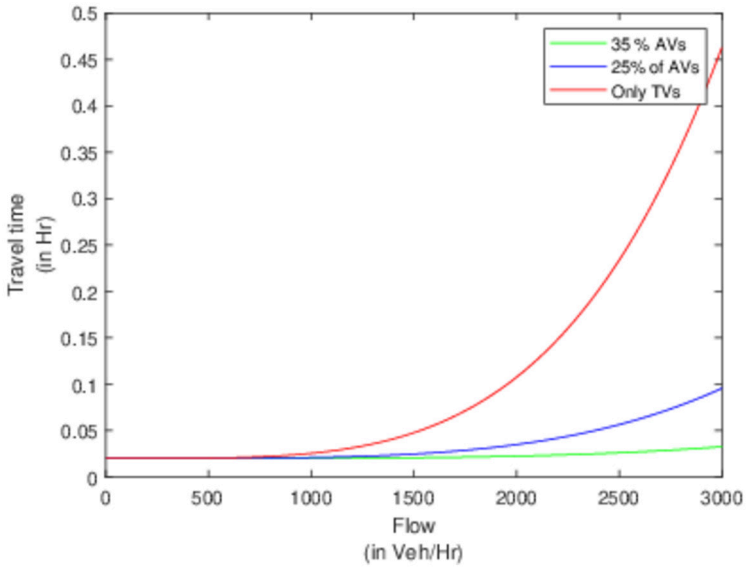

FIGURE 4.6: Travel-time flow relationship without a link having physical median and influence of opposite direction flow under sensitivity range of AVs

thus not affecting the results as much. Whereas the pavement type was the same for all the roads in our considered network. Another factor affecting the travel time and flow characteristics was the number of uncontrolled pedestrian crossings and side entries which again was mainly inducing an impact on the southern part of the considered area on Corso Italia.

4.4 Inequity analysis

Using the methodology stated in Chapter 3, the objective of inequity analysis is attained. Utilizing the data obtained from the above-mentioned sources for the city of Genoa, values for each of the seven indices are calculated as shown

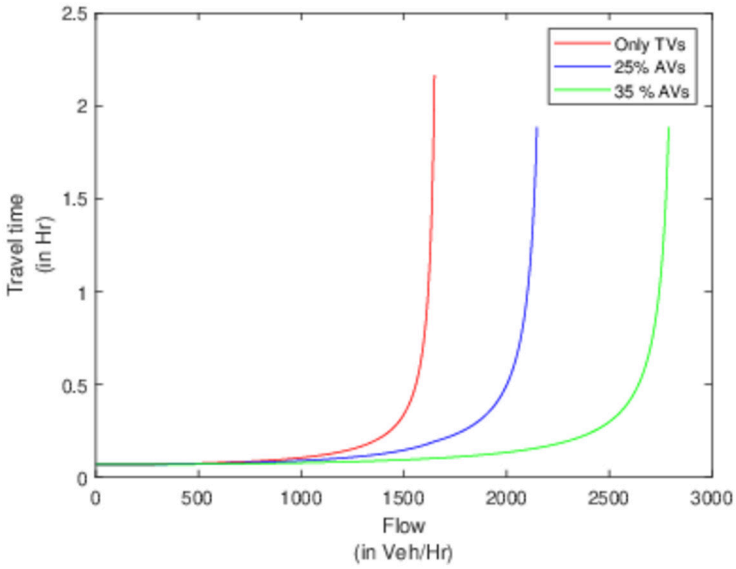

FIGURE 4.7: Travel-time flow relationship with physical and functional characteristics of links affecting travel time under sensitivity range of AVs

in Table 4.2; consequently giving an integrated index from the quantification equation (QE_{AV}) as in equation 3.12. Value of the integrated index is used and the final penetration rate to be used in the model is obtained from Table **??**. The quantified value range comes out to be 25-35% in light of the sensitivity analysis but for analyzing the inequity we opted for the maximum bound of penetration of AVs i.e. 35%. AVs are introduced into the network and are evaluated based on the projected growth of the defined indices for the next 15 years.

Given the assumptions in Chapter 3 as well as keeping in view the statement of (Bilal and Giglio, 2021) and (Lee, Wu, and Meng, 2006) that trip growth generally causes an increment in travel cost and consequently yields

a positive travel equilibrium ratio; the lower bound (θ_L) is kept equal to 1 whereas the upper bound (θ_u) is sensitively tested against different values (1.05, 1.07, 1.09 and 1.10). The aim of using close intervals for the upper bound value is to closely monitor the change in the respective optimal values for the upper and lower level of the problem as well as the fitness function.

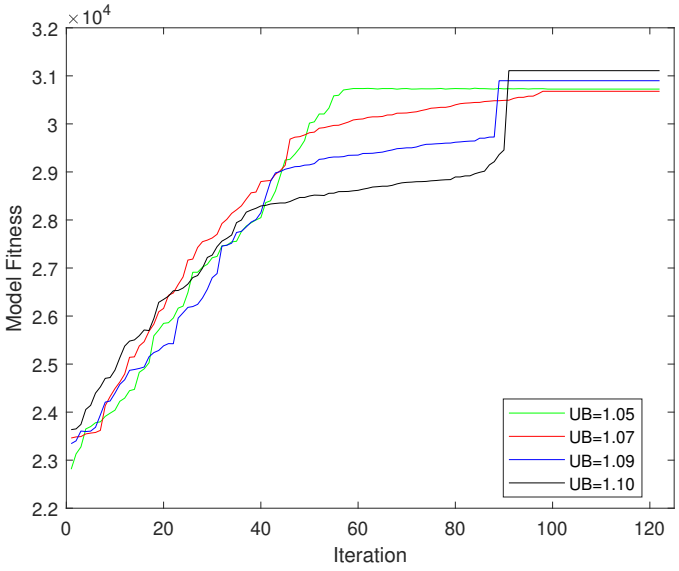

FIGURE 4.8: Fitness curves for GA with Upper inequity bound of 1.05, 1.07, 1.09 and 1.10

Looking at the fitness curves in Figure 4.8 it is apparent that for all the upper bounds the fitness of GA continues to increase. However, for the upper bound of 1.09 and 1.10, the fitness sharply increases after 80 iterations of the algorithm and finally becomes stable with a relatively higher value of fitness as compared to the earlier upper bounds i.e. 1.05 and 1.07. This depicts that almost all the newly generated demand under these bounds satisfies the model thus the fitness continues to increase. An interesting thing to note is that the fitness value for the upper bound of 1.07 took the longest to get stable yet it has the lowest fitness value. In contrast, the algorithm becomes stable only after 58 iterations in the case of an upper bound of 1.05.

For consistency check of the proposed assignment model based on SUE, results are compared with those of system optimum (SO) assignment having

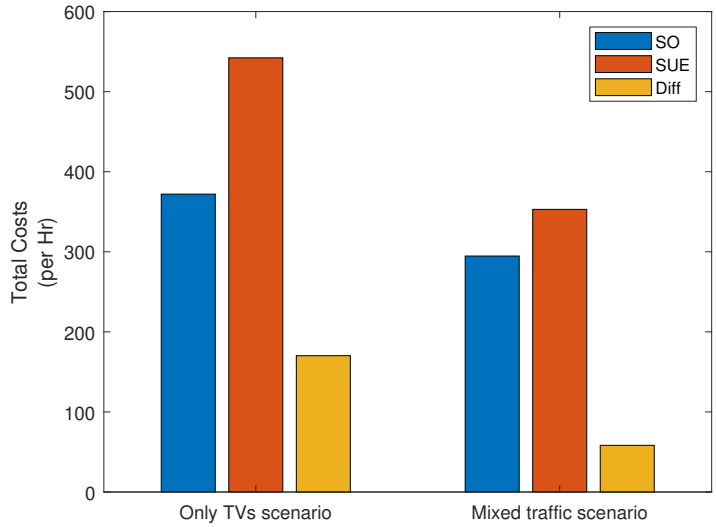

FIGURE 4.9: Total costs for SUE and SO assignment (Source: (Bilal and Giglio, 2022))

an ideal state of the considered network with a minimized total cost in absence of AVs. The assignment according to the MSA-FW algorithm as in the lower level of the Bi-level model gives us the total equilibrium cost as well as the network optimum costs in heterogeneous traffic stream scenarios with 35% AVs. It is evident in Figure 4.9 that on the inclusion of AVs both the SUE assignment and SO assignment shows a decrement in total equilibrium costs. Not only this but the total travel equilibrium cost is lesser than the total optimum cost when AVs are present in the traffic stream. This depicts the potential of AVs for improved network capacity.

Witnessing Figure 4.10, we can see the reduction in mean excess cost for heterogeneous traffic stream as compared to only the TVs scenario. As the number of iterations goes on to attain the equilibrium, the decrement in mean excess cost in the case of mixed traffic is more evident.

Comfort comes with a cost not only to individuals but also a mutual social cost. This can be verified by diving deep into the inequity analysis results. It is evident from Table 4.4 and Table 4.5 that the inequity values for the newly generated demand do not increase rapidly for the increased fitness values.

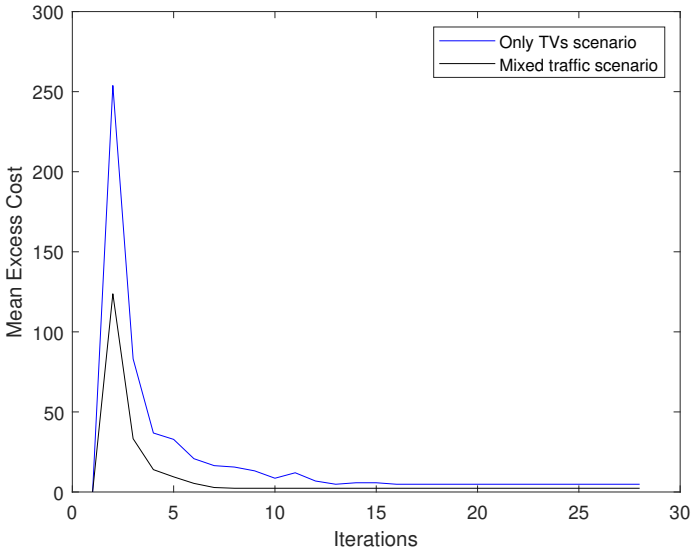

FIGURE 4.10: Mean excess costs comparisons for only TVs and heterogeneous traffic stream scenario (Source: (Bilal and Giglio, 2022))

As we witness in 4.8, the fitness consistently increases for an upper bound of 1.05 and 1.07 yet the detailed values of inequity for the upper bound of 1.05 from 4.4 suggest a slower increment specifically for zone 34, 43, and 63. Similarly, in 4.5 for the upper bound of 1.07, the inequity values for zone 34, 35, 39, and 62 do not depict as much change in inequity as the fitness suggests. the reason for the lower impact on inequity for these areas is the type of topography and land usage. These zones consist of the areas of downtown with the least car traffic moreover served by a single truck road thus the heterogeneous stream casting the lowest possible impacts both positive and negative. In contrast to that, zones 39, 40, 41-47, 61, and 62 depict balanced positive impacts in terms of maximizing volumes and negative impacts in terms of inequity with increasing fitness values for the upper bounds of 1.05 and 1.07. The impacts are more evident in the upper bound of 1.07 as evident from 4.5. But as we saw in the fitness curves in Figure 4.8 there is a rapid increase in the fitness values for the upper bounds of 1.09 and 1.10 after an intermediate drop and then a sudden steep surge after the 85th iteration, this is certified by the inequity values as we can see in Table 4.6 and Table 4.7. Again, the

zones most under influence are quite similar to those in the upper bound of 1.07. Although the new demand generated is being easily served by the network evident from the fitness curve with sharp increment in fitness; it also increases the inequity within the network thus increasing the overall equilibrium travel cost.

TABLE 4.4: Inequity model results for 1.05 upper bound.

	$\theta_U = 1.05$																					
Zones	**33**	**34**	**35**	**38**	**39**	**40**	**41**	**42**	**43**	**47**	**61**	**62**	**63**	**64**	**65**	**66**	**67**
33	—	1.0294	1.0494	1.0487	1.0476	—	—	1.0461	1.0493	—	1.0379	1.0426	—	—	1.0494	1.050	1.0433
34	1.045	—	1.049	1.045	1.049	1.041	—	1.025	—	—	1.042	1.047	1.029	1.047	—	1.049	—
35	1.0488	1.0471	—	1.0472	1.0477	1.0462	—	1.0424	1.0443	1.0464	1.0195	1.0443	1.0449	1.0482	1.0426	1.0490	1.0493
38	1.0468	1.0432	1.0479	—	1.0489	1.0397	—	1.041	—	1.0435	1.0491	1.0486	1.0463	1.0478	—	1.0475	1.0481
39	1.0259	1.0373	1.0253	1.0482	—	1.0498	1.0438	1.0429	1.0418	1.0376	1.0364	1.0322	1.0413	1.0364	1.0418	1.0478	1.0492
40	—	1.0473	1.0494	1.0461	1.0499	—	1.0457	1.0477	1.0466	—	1.0352	1.0473	1.0471	1.0494	—	1.0476	1.0353
41	—	—	—	—	1.0498	1.0499	—	1.0424	—	1.0398	1.0496	1.0497	1.0472	—	1.0472	1.0484	—
42	1.0494	1.0475	1.0362	1.0303	1.050	1.0454	1.0492	—	1.0381	1.0343	1.0478	1.0397	1.0460	1.0461	1.0480	1.0438	1.0493
43	1.0498	—	1.0178	—	1.0364	1.0438	—	1.0481	—	1.0455	1.0493	1.0433	1.0440	—	1.0419	1.0406	1.0421
47	—	—	1.0469	1.0314	1.038	—	1.0494	1.0493	1.0430	—	1.0412	1.1423	—	1.0257	—	1.0414	1.0383
61	1.0352	1.046	1.002	1.033	1.046	1.0480	1.0489	1.0422	1.037	1.016	—	1.030	1.0343	1.0297	1.046	1.0148	1.0145
62	1.0493	1.0450	1.0480	1.035	1.0478	1.049	1.046	1.043	1.040	1.046	1.047	—	1.0466	1.0121	1.043	1.0370	—
63	—	1.039	1.003	1.048	1	1.0415	1.001	1.0471	1.0448	—	1.0313	1.048	—	—	1.022	—	—
64	—	1.0482	1.035	1.0180	1.030	1	—	1.003	—	1.002	1.043	1.004	—	—	1.041	—	1.049
65	1.0275	—	1.0341	—	1.003	—	1.023	1.002	1.013	—	1.0412	1.024	1.0493	—	—	—	—
66	1.0160	1.046	1.040	1	1.048	1.0462	1.049	1.002	1.040	1.030	1.045	1.001	—	—	—	—	1
67	1.016	—	1.050	1.008	1.049	1.0421	—	1.049	1.001	1.002	1.043	—	—	1.0139	—	1.05	—

TABLE 4.5: Inequity model results for 1.07 upper bound.

	$\theta_U = 1.07$																
Zones	**33**	**34**	**35**	**38**	**39**	**40**	**41**	**42**	**43**	**47**	**61**	**62**	**63**	**64**	**65**	**66**	**67**
33	—	1.0294	1.0617	1.0690	1.0699	—	—	1.0661	1.0494	—	1.0671	1.0676	—	—	1.0613	1.0699	1.0671
34	1.0693	—	1.0643	1.0531	1.0665	1.0695	—	1.0681	—	—	1.0595	1.0606	1.0299	1.0646	—	1.0698	—
35	1.0648	1.0581	—	1.0636	1.0587	1.0537	—	1.0630	1.0591	1.0614	1.0680	1.0584	1.0450	1.0584	1.0635	1.0567	1.0633
38	1.0468	1.0627	1.0677	—	1.0696	1.0678	—	1.0611	—	1.0668	1.0592	1.0683	1.0688	1.0479	—	1.0526	1.0661
39	1.060	1.0541	1.0552	1.0694	—	1.0679	1.0665	1.0652	1.0611	1.0673	1.0619	1.0322	1.0587	1.0660	1.0601	1.0667	1.0686
40	—	1.0685	1.0694	1.0688	1.0645	—	1.0657	1.0676	1.0531	—	1.0353	1.0601	1.0695	1.0494	—	1.0593	1.0612
41	—	—	—	—	1.0686	1.0686	—	1.0425	–	1.0635	1.0679	1.0682	1.0582	—	1.0473	1.0485	—
42	1.0637	1.0613	1.0654	1.0682	1.0659	1.0649	1.0677	—	1.0614	1.0676	1.0684	1.0398	1.0647	1.0620	1.0507	1.0668	1.0550
43	1.0679	—	1.0178	—	1.0365	1.0690	—	1.0622	—	1.0543	1.0658	1.0562	1.0692	—	1.0622	1.0407	1.0672
47	—	—	1.0596	1.0520	1.0666	—	1.0495	1.0607	1.0632	—	1.0412	1.1424	—	1.0257	—	1.0549	1.0383
61	1.0679	1.0655	1.0697	1.0673	1.0580	1.0508	1.0694	1.0527	1.0634	1.0560	—	1.0302	1.0343	1.0298	1.0466	1.0148	1.0536
62	1.0682	1.0451	1.0683	1.0636	1.0616	1.0691	1.0652	1.0507	1.0579	1.0463	1.0536	—	1.0690	1.0121	1.0431	1.0370	—
63	—	1.0692	1.0584	1.0664	1.0686	1.0501	1.003	1.0472	1.0553	—	1.0313	1.0646	—	—	1.0230	—	—
64	—	1.0482	1.0503	1.0613	1.024	1.002	—	1.006	—	1.002	1.0512	1.0043	—	—	1.041	—	1.0496
65	1.0688	—	1.0342	—	1.060	—	1.0672	1.0685	1.055	—	1.0412	1.0247	1.0561	—	—	—	—
66	1.0695	1.0537	1.0404	1.048	1.0555	1.0695	1.0556	1.028	1.0407	1.0517	1.0686	1.0547	—	—	—	—	1
67	1.0695	—	1.0585	1.0089	1.0610	1.0618	—	1.0561	1.068	1.058	1.0537	—	—	1.0642	—	1.0524	—

TABLE 4.6: Inequity model results for 1.09 upper bound.

	$\theta_U = 1.09$																							
Zones	**33**	**34**	**35**	**38**	**39**	**40**	**41**	**42**	**43**	**47**	**61**	**62**	**63**	**64**	**65**	**66**	**67**
33	—	1.0294	1.0617	1.0896	1.0699	—	—	1.0893	1.0779	—	1.0842	1.0676	—	—	1.0754	1.0800	1.0850
34	1.0859	—	1.0887	1.0531	1.0881	1.0834	—	1.0891	—	—	1.0752	1.0780	1.0771	1.0898	—	1.0795	—
35	1.0752	1.0891	—	1.0824	1.0897	1.0886	—	1.0868	1.0870	1.0892	1.0863	1.0731	1.0900	1.0892	1.0786	1.0860	1.0860
38	1.0468	1.0789	1.0776	—	1.0872	1.0878	—	1.0877	—	1.0832	1.0895	1.0898	1.0883	1.0479	—	1.0526	1.0867
39	1.0873	1.0762	1.0870	1.0806	—	1.0679	1.0796	1.0776	1.0783	1.0817	1.0619	1.0854	1.0716	1.0805	1.0861	1.0830	1.0820
40	—	1.0892	1.0884	1.0886	1.0890	—	1.0884	1.0898	1.0531	—	1.0353	1.0814	1.0892	1.0863	—	1.0593	1.0791
41	—	—	—	—	1.0799	1.0870	—	1.0425	-	1.0764	1.0861	1.0863	1.0890	—	1.0473	1.0862	—
42	1.0859	1.0787	1.0654	1.0882	1.0865	1.0871	1.0769	—	1.0837	1.0840	1.0816	1.0841	1.0828	1.0880	1.0880	1.0809	1.0550
43	1.0842	—	1.0178	—	1.0880	1.0690	—	1.0868	—	1.0882	1.0847	1.0807	1.0692	—	1.0758	1.0838	1.0848
47	—	—	1.0596	1.0892	1.0666	—	1.0706	1.0769	1.0873	—	1.0813	1.1424	—	1.0831	—	1.0735	1.0383
61	1.0892	1.0655	1.0872	1.0797	1.0580	1.0508	1.0882	1.0894	1.0899	1.0560	—	1.0302	1.0343	1.0298	1.0466	1.0148	1.0536
62	1.0876	1.0890	1.0871	1.0636	1.0616	1.0816	1.0886	1.0507	1.0579	1.0866	1.0536	—	1.0866	1.0121	1.0431	1.0857	—
63	—	1.0846	1.0894	1.0898	1.0868	1.0782	1.0896	1.0472	1.0553	—	1.0313	1.0853	—	—	1.0230	—	—
64	—	1.0884	1.0703	1.0847	1	1.0896	—	1.0878	—	1.074	1.0512	1.0043	—	—	1.041	—	1.0496
65	1.0881	—	1.0706	—	1.063	—	1.0882	1.0881	1.044	—	1.0412	1.0247	1.0746	—	—	—	—
66	1.0879	1.0537	1.0886	1.075	1.0822	1.0890	1.0556	1.0783	1.0892	1.0878	1.0703	1.0859	—	—	—	—	1
67	1.0879	—	1.0803	1.0089	1.0842	1.0796	—	1.0561	1.049	1.058	1.0734	—	—	1.0642	—	1.0524	—

TABLE 4.7: Inequity model results for 1.10 upper bound.

	$\theta_U = 1.10$																
Zones	**33**	**34**	**35**	**38**	**39**	**40**	**41**	**42**	**43**	**47**	**61**	**62**	**63**	**64**	**65**	**66**	**67**
33	—	1.0294	1.0617	1.0997	1.0966	—	—	1.0893	1.0975	—	1.0994	1.0676	—	—	1.0754	1.0800	1.0978
34	1.0999	—	1.0887	1.0946	1.0960	1.0956	—	1.0991	—	—	1.0752	1.0983	1.0771	1.0919	—	1.0905	—
35	1.0985	1.0990	—	1.0824	1.0897	1.0993	—	1.0976	1.0902	1.0992	1.0965	1.1000	1.0900	1.0968	1.0957	1.0989	1.0927
38	1.0468	1.0981	1.0945	—	1.0968	1.0984	—	1.0997	—	1.0832	1.0982	1.0898	1.0883	1.0908	—	1.0526	1.0867
39	1.0873	1.0762	1.0991	1.0934	—	1.0679	1.0943	1.0915	1.0783	1.0989	1.0977	1.0958	1.0941	1.0976	1.0861	1.0830	1.0820
40	—	1.0972	1.0994	1.0990	1.0982	—	1.0951	1.0930	1.0531	—	1.0353	1.0814	1.0999	1.0863	—	1.0984	1.0944
41	—	—	—	—	1.0990	1.0961	—	1.0425	–	1.0981	1.0911	1.0996	1.0890	—	1.0473	1.0999	—
42	1.0980	1.0903	1.0901	1.0908	1.0960	1.0970	1.0769	—	1.0938	1.0840	1.0816	1.0841	1.0971	1.0973	1.0999	1.0910	1.0550
43	1.0921	—	1.0178	—	1.0995	1.0938	—	1.0868	—	1.0989	1.0946	1.0976	1.0940	—	1.0953	1.0978	1.0954
47	—	—	1.0596	1.0929	1.0965	—	1.0953	1.0769	1.0941	—	1.0813	1.1424	—	1.0995	—	1.0735	1.0383
61	1.0960	1.0942	1.0964	1.0797	1.0580	1.0508	1.0882	1.0985	1.0998	1.0560	—	1.0302	1.0986	1.0298	1.0466	1.0148	1.0536
62	1.0980	1.0984	1.0984	1.0936	1.0999	1.0816	1.0952	1.0507	1.0579	1.0866	1.0536	—	1.0973	1.0121	1.0431	1.0917	—
63	—	1.0908	1.0953	1.0938	1.0868	1.0952	1.0971	1.0472	1.0553	—	1.0956	1.0991	—	—	1.0230	—	—
64	—	1.0991	1.0703	1.0847	1.084	1.0915	—	1.0950	—	1.079	1.0512	1.0043	—	—	1.041	—	1.0496
65	1.0992	—	1.0706	—	1.0953	—	1.0990	1.0978	1.088	—	1.0412	1.0247	1.0746	—	—	—	—
66	1.0993	1.0537	1.0977	1.091	1.0980	1.0997	1.0556	1.0783	1.0925	1.0993	1.0703	1.0978	—	—	—	—	1
67	1.0993	—	1.0803	1.0089	1.0945	1.0796	—	1.0561	1.074	1.078	1.0734	—	—	1.0642	—	1.0524	—

Similarly, the change for inequity ratios for an upper bound of 1.10 is very less than the previous interval yet the fitness values increases sharply. This reveals that with higher upper bound values the inequity constraint as in equation 3.34 starts to become inactive because this excessive inequity upper bound will allow the newly generated demand to already reach the maximum values bounded by the constraint in equation 3.37 as well as the attraction constraint in equation 3.38. That also was one of the reasons to use close interval upper-bound values for inequity constraint. In the considered network three types of roads are used; highway, primary urban street, and tertiary urban street with a capacity of 2700, 1600, and 900 vehicles per hour respectively. The capacity is large enough to accommodate the maximum possible flows on the network. It must be noted that if the capacity is reduced then the inequity constraint becomes inactive for increasing iterations and the capacity constraint as in equation 3.35 will control the algorithm which certainly is not the motive here.

4.4.1 Travel equilibrium impacts

Now to help understand better the situation of inequity analysis for travel equilibrium costs, a side-by-side comparison is shown for all the zones and all the inequity upper bounds.

We can observe from the comparison of Figures 4.11, 4.12 depicts that despite the increase in inequity ratio due to a slight increment in the travel equilibrium costs for the zones the increase in volume is appreciable which is also revealed by the fitness function except for the zones 33 and 34 which shows a minimum change. This also stands true for our discussion in Section 4.4 where we identified the zones.

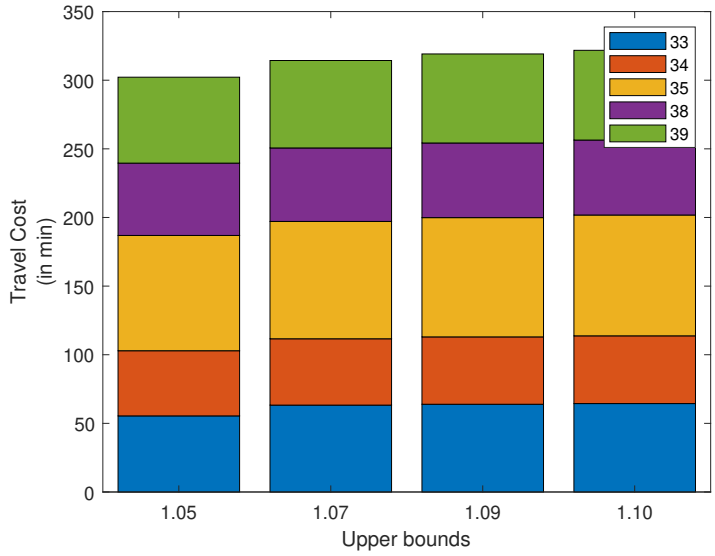

FIGURE 4.11: Change in travel equilibrium costs for different Upper bounds for Zone 33, 34, 35,38, and 39

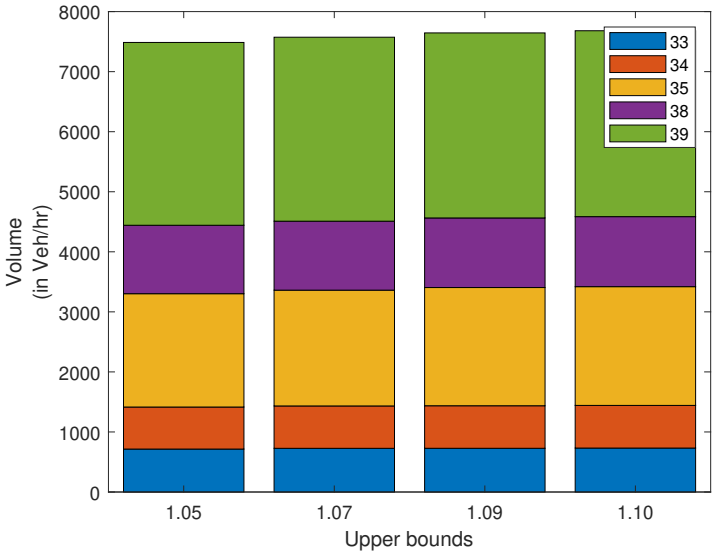

FIGURE 4.12: Change in volume for different upper bounds for zone 33, 34, 35,38, and 39

Similarly, the comparison of Figures 4.13, 4.14 shows that the higher allowance of inequity bound doesn't have any evident impact on travel equilibrium costs as well as volume for zone 40 and 41. Now, this trend wasn't evolved in our previous discussion revealing the importance of this comparison. If we look closely, the increase in travel equilibrium costs for the upper bound of 1.10 in the case of zone 42 makes a negative impact on volumes.

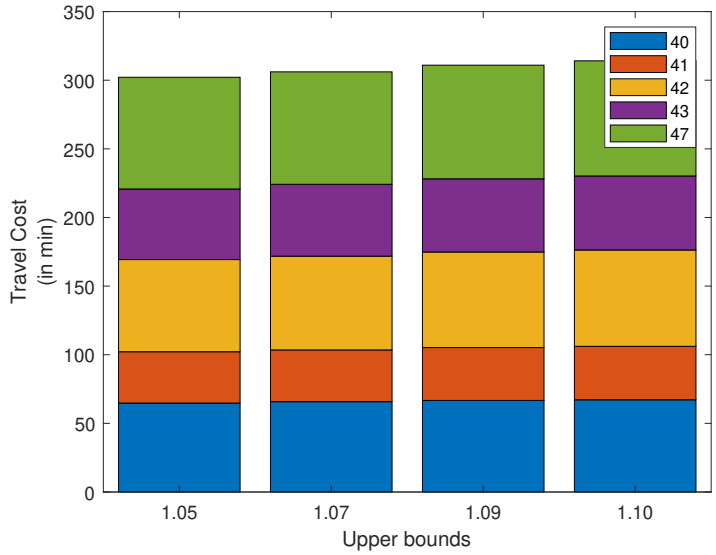

FIGURE 4.13: Change in travel equilibrium costs for different Upper bounds for Zone 40, 41, 42, 43, and 47

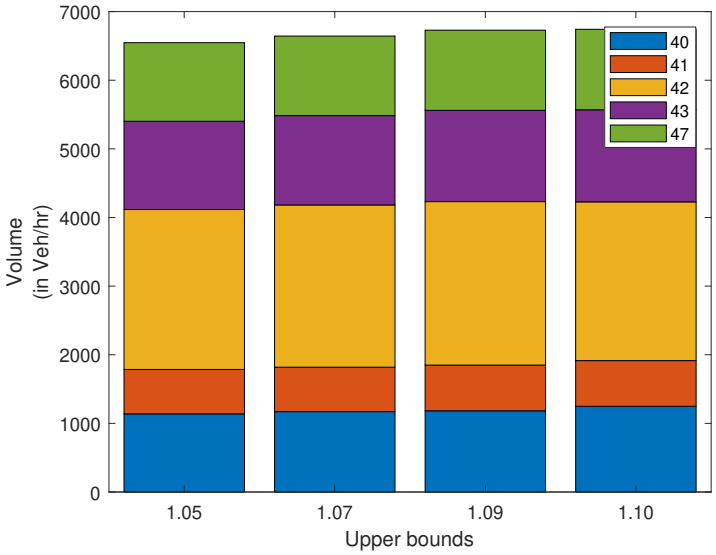

FIGURE 4.14: Change in volume for different upper bounds for zone 40, 41, 42, 43, and 47

Overall for other zones, the slight increase in travel equilibrium costs produces an appreciable volume increment. This does not mean that increasing cost increases the volume but it reflects the importance of capacity increment against minor social cost in the form of inequity.

Also, if we look into Figures 4.15, 4.16 we can identify the gains in volume for a slight change in travel cost for the upper bound interval of 1.07 to 1.09

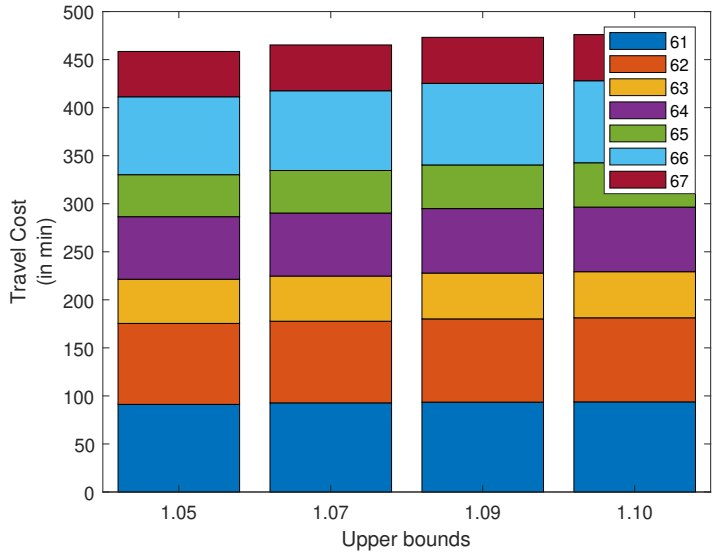

FIGURE 4.15: Change in travel equilibrium costs for different Upper bounds for Zone 61, 62, 63, 64, 65, 66, and 67

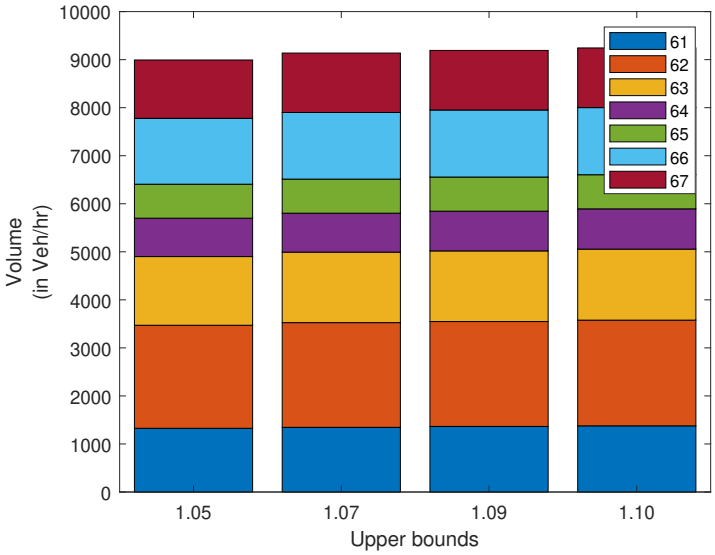

FIGURE 4.16: Change in volume for different upper bounds for zone 61, 62, 63, 64, 65, 66, and 67

except for zone 61. This makes us choose the upper bound of 1.09 as the best possible inequity policy as above that bound the change in decision variable is very less and the bound becomes ineffective as explained earlier.

Figures through 4.17 to 4.19 show the optimal results for the lower-level problem of the bi-level optimization model. We can witness the change in costs for all the network zones for all the possible OD pairs for which the

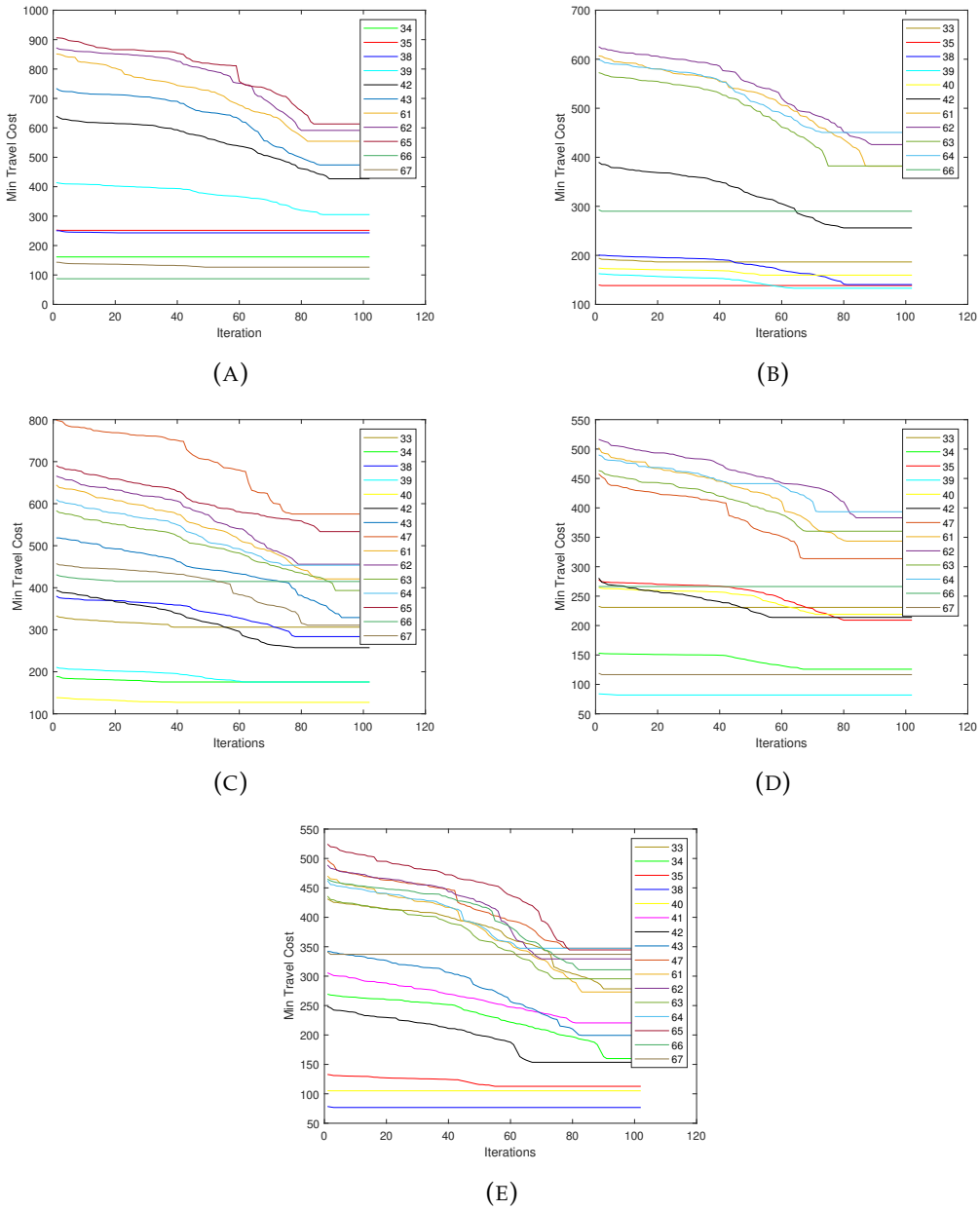

FIGURE 4.17: (A) Optimal minimized travel equilibrium costs for Origin zone 33; (B)Optimal minimized travel equilibrium costs for Origin zone 34 (C) Optimal minimized travel equilibrium costs for Origin zone 35 (D) Optimal minimized travel equilibrium costs for Origin zone 38 (E) Optimal minimized travel equilibrium costs for Origin zone 39

demand exists. Since, in the formulated bi-level optimization model, two agents are trying to simultaneously optimize their values; it gives a chance to visualize the effect of various upper bounds and the amount of compromise in travel costs and volumes.

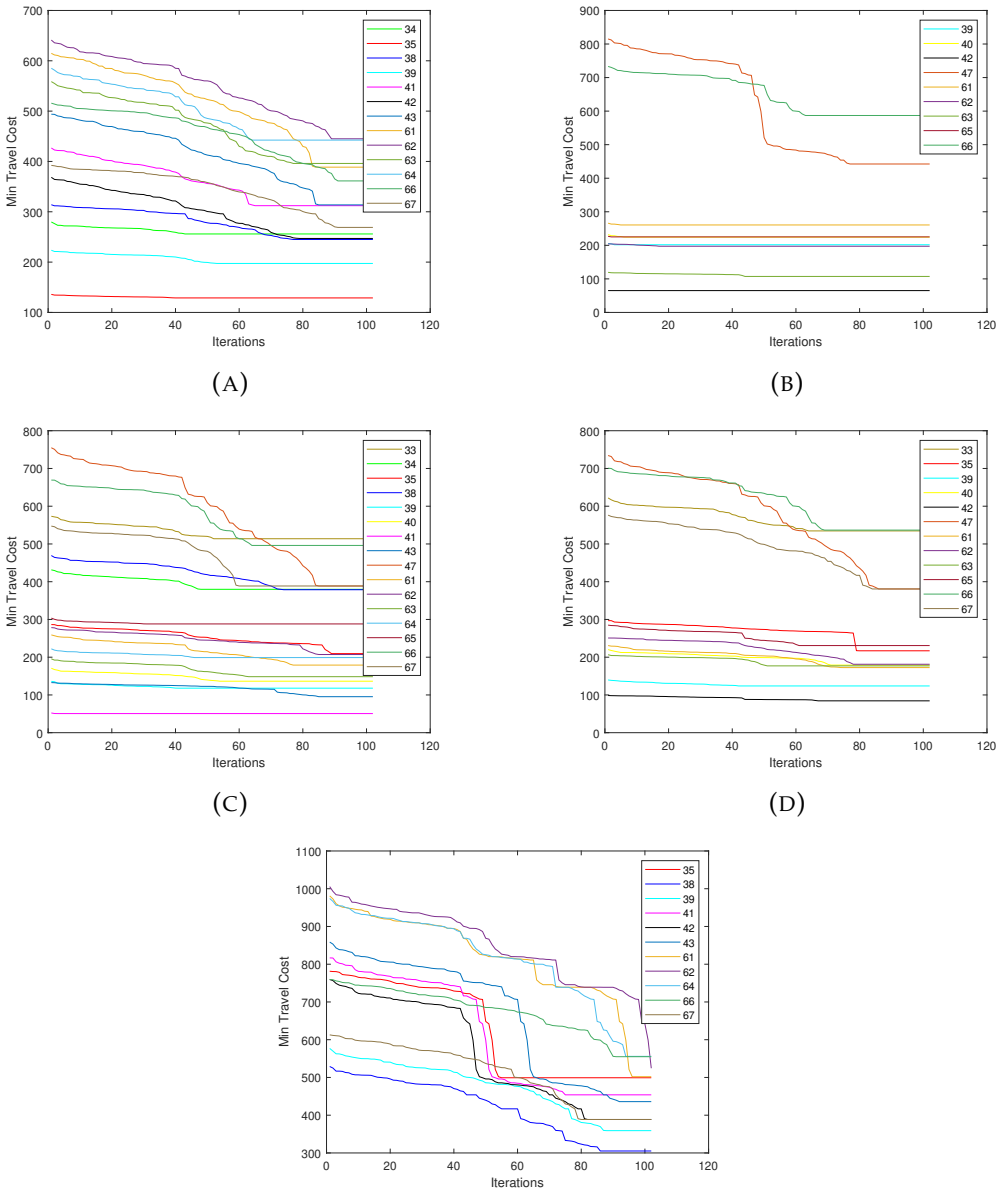

FIGURE 4.18: (A) Optimal minimized travel equilibrium costs for Origin zone 40; (B)Optimal minimized travel equilibrium costs for Origin zone 41 (C) Optimal minimized travel equilibrium costs for Origin zone 42 (D) Optimal minimized travel equilibrium costs for Origin zone 43 (E) Optimal minimized travel equilibrium costs for Origin zone 47

The minimized costs are the results of the maximized volumes. The fact for certain zones the inequity upper bound of 1.09 does not give appreciable results instead upper bound of 1.07 does. Looking closely at the optimal curves, the detailed potential of each origin zone towards each attraction

zone depicts the amount of equitable development in form of the introduction of AVs.

Whereas, Figures, 4.20 to 4.22, show the optimal results for the upper-level problem of the bi-level optimization model. We can witness the change in trip generation for all the network zones for all the possible OD pairs against the minimized equilibrium costs. Since, in the formulated bi-level optimization model, two agents are trying to simultaneously optimize their values; it gives a chance to visualize the effect of various upper bounds and the number of trips being generated while restricting the inequity allowed.

The fact for certain zones the inequity upper bound of 1.09 does not give appreciable results instead upper bound of 1.07 does. Looking closely at the optimal curves, the detailed potential of each origin zone towards each attraction zone depicts the amount of equitable development in form of the introduction of AVs.

The variations in the optimization behavior of the two decision variables at the lower and upper levels of the problem can be observed. The sharp decrement in travel equilibrium cost for trips from zone 41 to attraction zones particularly zone 63 and zone 47 do not come at any compromise of volume as can be seen in Figure 4.21 (B). In fact, for zone 63 the newly generated demand continues to maximize itself with decreasing and later steady travel equilibrium cost. Similar trends are noted for origin zone 47 in which newly generated demand is increasing steadily as in Figure 4.21 (E) whereas, the cost continues to minimize as in Figure 4.18 (E). This shows the strong behavior of constraints at the lower level of the formulated model which in turn is acting as a constraint for the upper level thus providing a balance in the production of new demand for each OD pair. The important takeaway from these optimal curves is that the increasing trips do not always increase the travel equilibrium costs yet for some OD pairs it is also decreasing the total costs.

Moreover, as we mentioned earlier for some origin zones the upper bound of 1.07 performed well depicting the importance of micro-level transportation and land use planning revealing the possible direction of urban development. This enlightens the possibilities for different zones of the bigger network to be micro-planned for development in terms of the inclusion of new forms of mobility with variable inequity allowance. This can also open doors for the micro-mobility options to serve the needs of the user group of zones where inequity is more.

4.5 Conclusions

Concerning the stated objectives in Chapter 1, this chapter applies the formulated methodology to a real transportation network of the city of Genoa, Italy. A quantified penetration rate of AVs is derived from a multiple indices system to synthesize seven different indices using user demographical, land usage, and socio-economic characteristics. Then by the quantile approach and sensitivity analysis, the range realistic value of AVs is determined which comes out to be 25 - 35% keeping in view 0% AVs in the current year and projection for the indices for the next 15 years. Later, this quantified penetration rate of AVs is used to determine the impact on macroscopic fundamental network parameters followed by the convex minimization problem which is a lower level of the bi-level optimization model. The lower-level problem distributed the trips onto the network following the SUE approach using the Frank-Wolfe algorithm. This lower-level problem itself acts as a constraint for the upper level of the bi-model. The presented bi-level optimization model is solved using a genetic algorithm that evidently addresses the inequity among the travel zones on the introduction of AVs into the network by sensing the deviation in travel equilibrium costs for each OD pair. Also, governs the maximum amount of new demand that can be produced

by each origin zone. Under different upper bounds for inequity, it was found that the most optimal travel equilibrium costs and newly generated demand are for the upper bound of 1.09. The proposed methods highlight the importance of planning for each zone to the extent that it grows to its maximum potential without causing an imbalance in the travel equilibrium costs when AVs are introduced into the network.

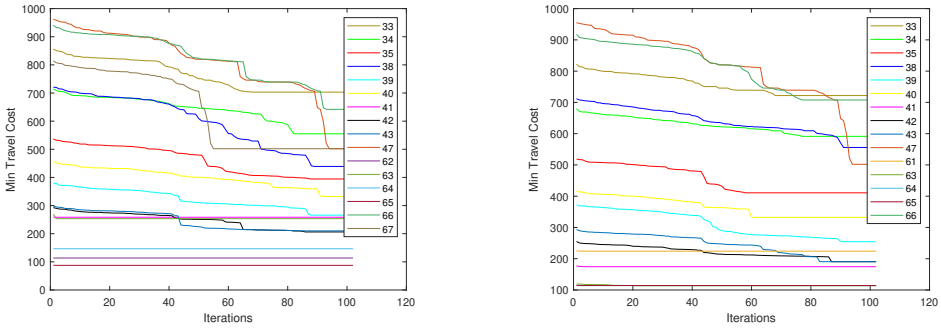

(A)

(B)

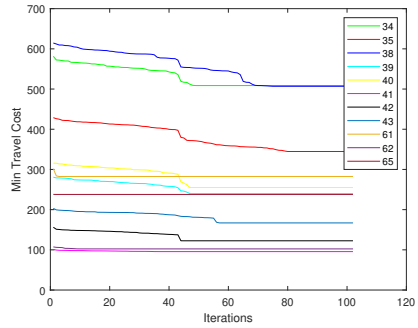

(C)

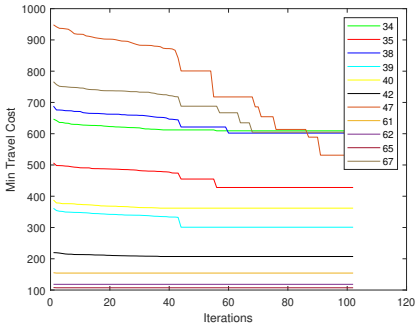

(D)

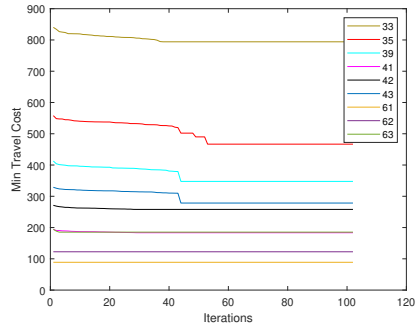

(E)

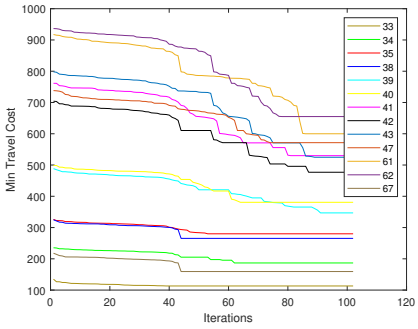

(F)

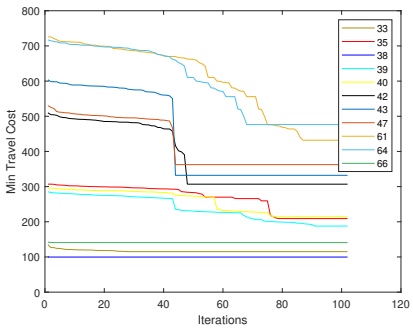

(G)

FIGURE 4.19: (A) Optimal minimized travel equilibrium costs for Origin zone 61; (B)Optimal minimized travel equilibrium costs for Origin zone 62 (C) Optimal minimized travel equilibrium costs for Origin zone 63 (D) Optimal minimized travel equilibrium costs for Origin zone 64 (E) Optimal minimized travel equilibrium costs for Origin zone 65 (F) Optimal minimized travel equilibrium costs for Origin zone 66 (G) Optimal minimized travel equilibrium costs for Origin zone 67

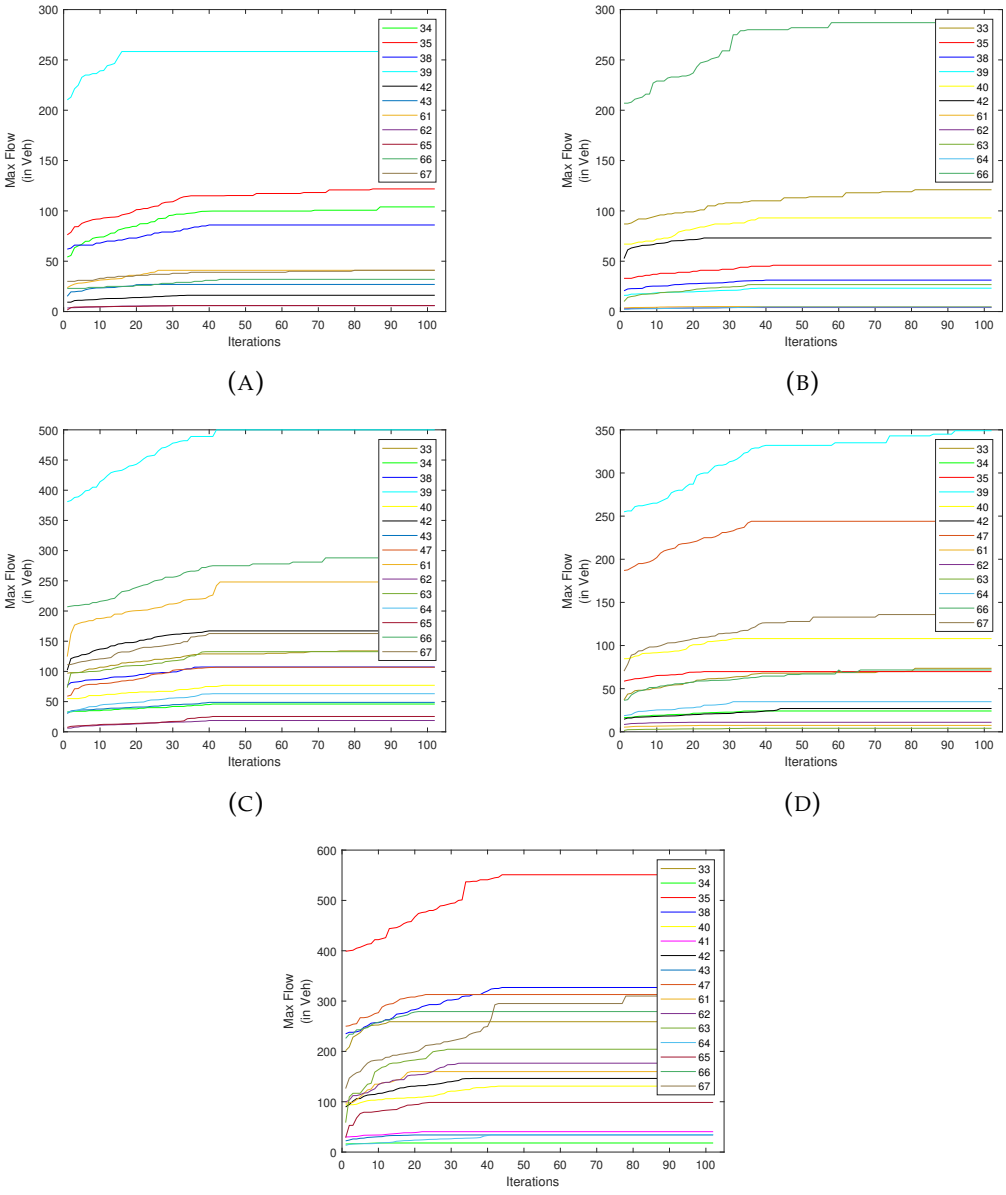

FIGURE 4.20: (A) Optimal maximized trip generation for Origin zone 33; (B)Optimal maximized trip generation for Origin zone 34 (C) Optimal maximized trip generation for Origin zone 35 (D) Optimal maximized trip generation for Origin zone 38 (E) Optimal maximized trip generation for Origin zone 39

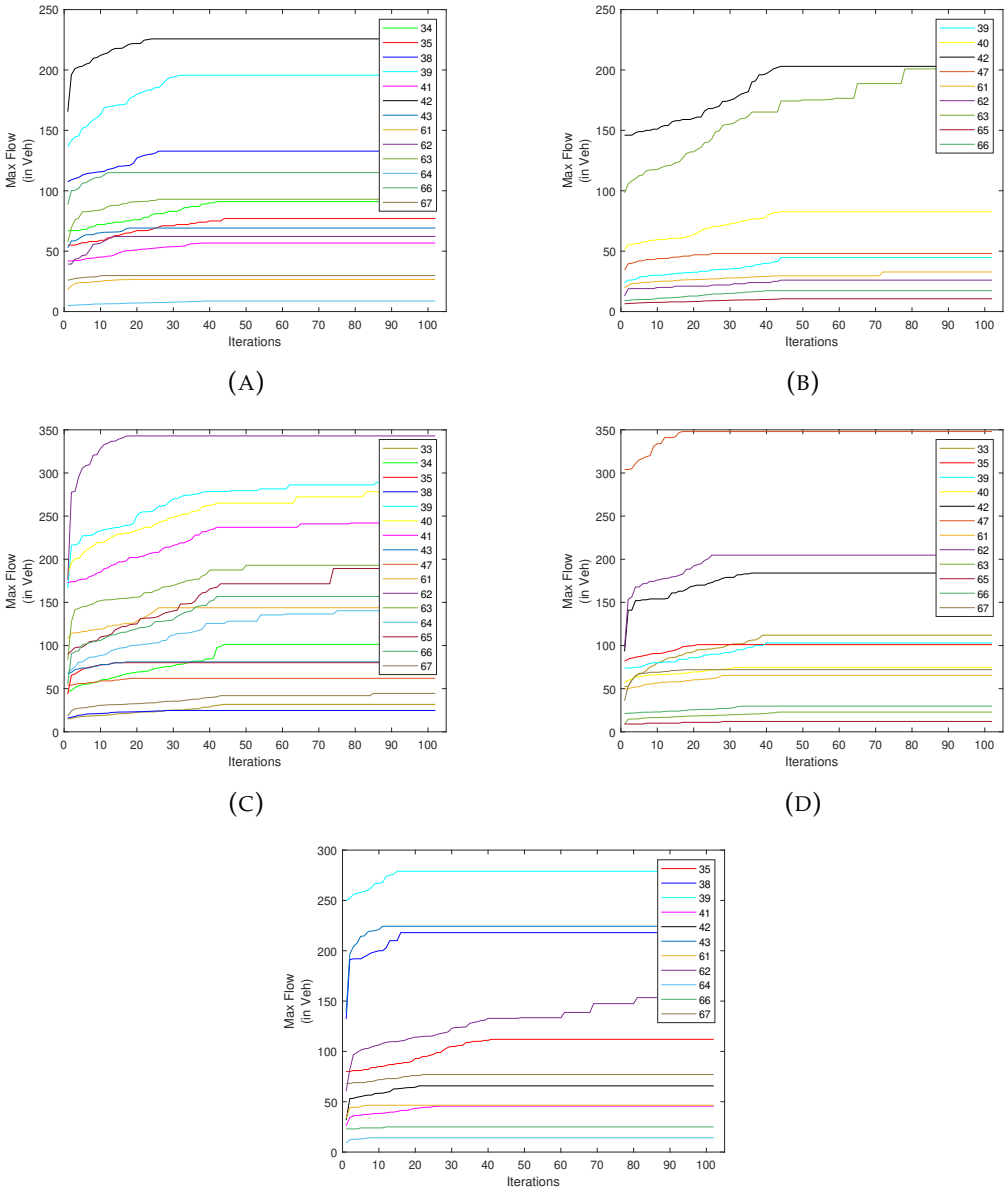

FIGURE 4.21: (A) Optimal maximized trip generation for Origin zone 40; (B)Optimal maximized trip generation for Origin zone 41 (C) Optimal maximized trip generation for Origin zone 42 (D) Optimal maximized trip generation for Origin zone 43 (E) Optimal maximized trip generation for Origin zone 47

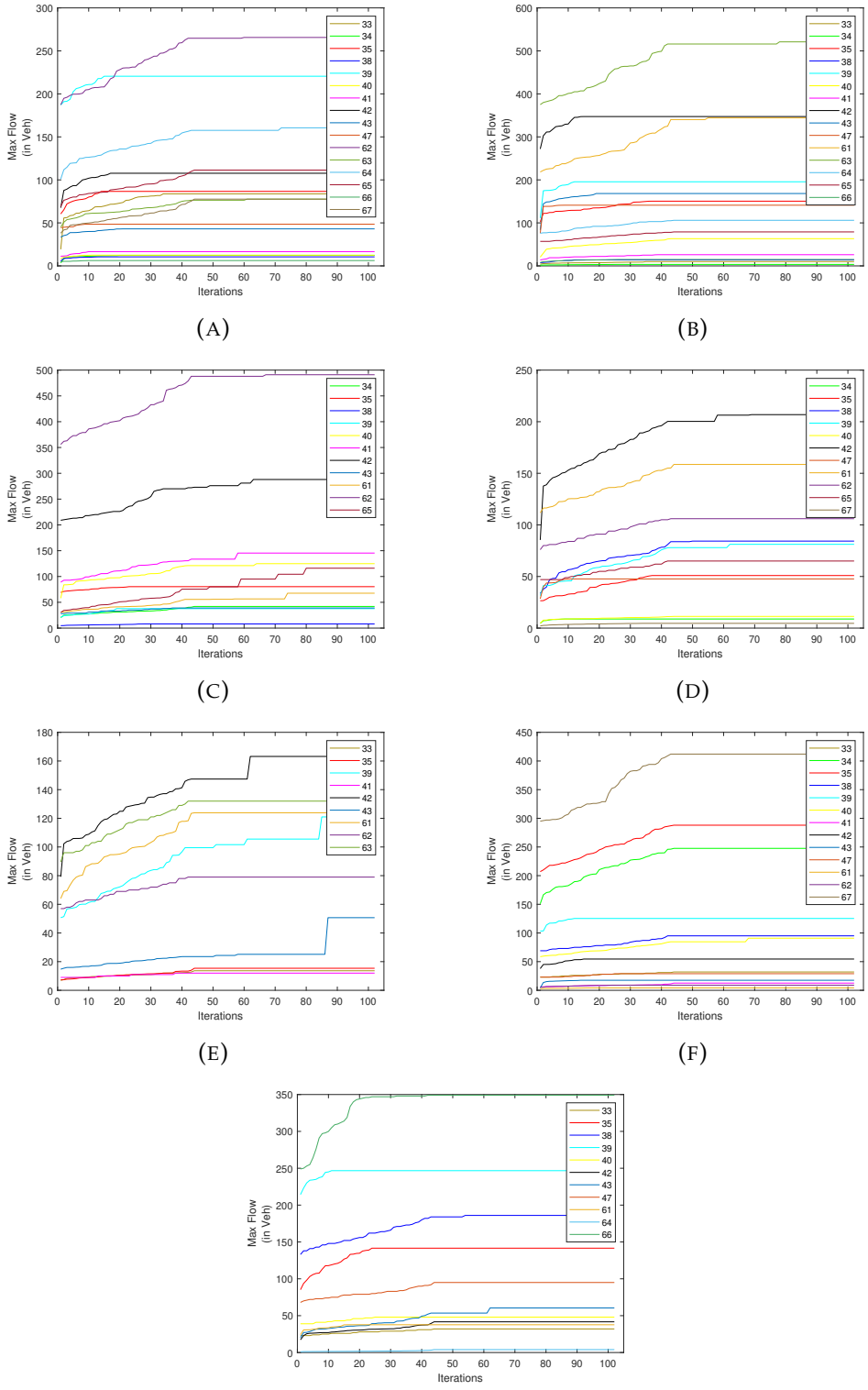

FIGURE 4.22: (A) Optimal maximized trip generation for Origin zone 61; (B)Optimal maximized trip generation for Origin zone 62 (C) Optimal maximized trip generation for Origin zone 63 (D) Optimal maximized trip generation for Origin zone 64 (E) Optimal maximized trip generation for Origin zone 65 (F) Optimal maximized trip generation for Origin zone 66 (G) Optimal maximized trip generation for Origin zone 67

Chapter 5

Public transport vulnerability analysis

5.1 Model implementation

This chapter includes the application of the extensive methodology formulated in Chapter 3 on Public transportation networks (PuT) for the city of Genoa, Italy, and Barcelona, Spain. Section 5.2 involves the definition of the study area and the resources used for extracting the data to be adopted for the analysis. The structural evaluation of the two networks is penned down in Section 5.3 whereas the vulnerable components in the PuT networks of Genoa and Barcelona are identified in Section 5.3.1. Section 5.4 involves the impact of disruptions both with and without the inclusion of shared micro-mobility services.

5.2 Real network application

The public transport network for the two cities is modeled in PTV Visum and coded in MATLAB with real-world timetables. The transit network for Barcelona follows a diagonal, horizontal, and vertical structural distribution expanding on an area of 173km^2. It covers the complete area of the metropolitan city of Barcelona as shown in Figure 5.1, serving the demand (i.e. 3857856

trips per day) via a transit system of 224 bus line routes and 6 tram lines out of which the majority of bus lines are operated by TMB (Transports Metropolitans de Barcelona) whereas some by Tusgsal, Monbus i Julia and Rosanbus. The tram lines are operated by a joint venture TRAM. The considered network of Barcelona consists of 8326 nodes, 22034 links, and 350 zones served by 3164 transit stops and effective operational schedules around the year for which the data is retrieved from (ATM) Autoritat del Transport Metropolita Barcelona and TRAM. The metro lines for the city of Barcelona are not considered for the analysis. The bicycle sharing system considered for Barcelona is known as Bicing, consisting of 509 sharing stations with a fleet of 7000 bicycles including a mix of electric and non-electric bicycles. The optimal occupancy value for each sharing station at any time of the analysis period is set to be 5. The analysis period is a normal working day from June for Barcelona.

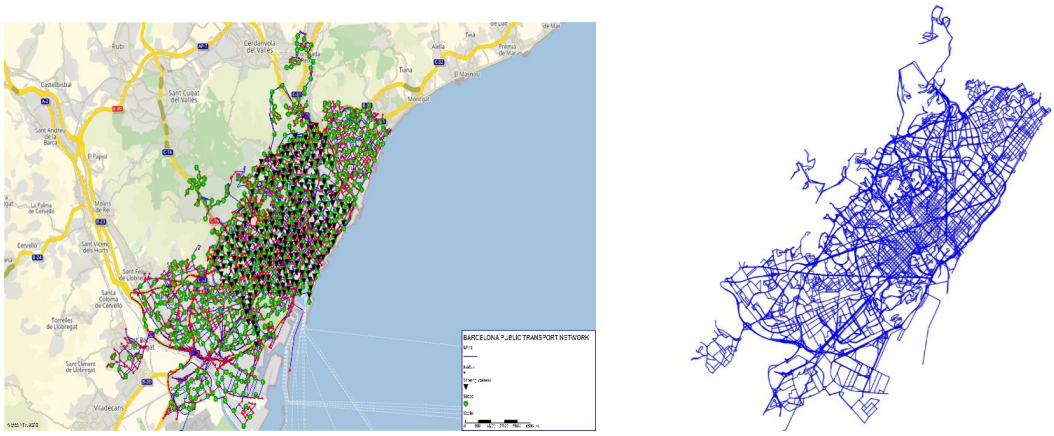

(A) (B)

FIGURE 5.1: (A) Barcelona PuT network in Visum (B) Line network coded in MATLAB for Barcelona PuT

Similarly, The transit network for Genoa follows a more horizontal and vertical structural distribution expanding on an area of 243km^2. It covers the complete area of the metropolitan city of Genoa as shown in Figure 5.2, serving the demand (i.e. 199848 trips per day) via a transit system of 244 bus line routes and 1 metro line. The transit system of Genoa is operated

by Azienda Mobilita e Trasporti (AMT). The considered network of Genoa consists of 2494 nodes, 5898 links, and 72 zones served by 2463 transit stops and operational schedules around the year for which the data is retrieved from AMT. The bicycle sharing system considered is a pilot project known as Zena managed by Genova Parcheggi, consisting of 16 sharing stations with a fleet of 100 bicycles (74 electric and 26 pedal assisted) to traverse a total of 50km of cycle paths around the city. The optimal occupancy value for each sharing station at any time of the analysis period is different depending upon the maximum occupancy of each station. The analysis period is a normal working day from August for Genoa.

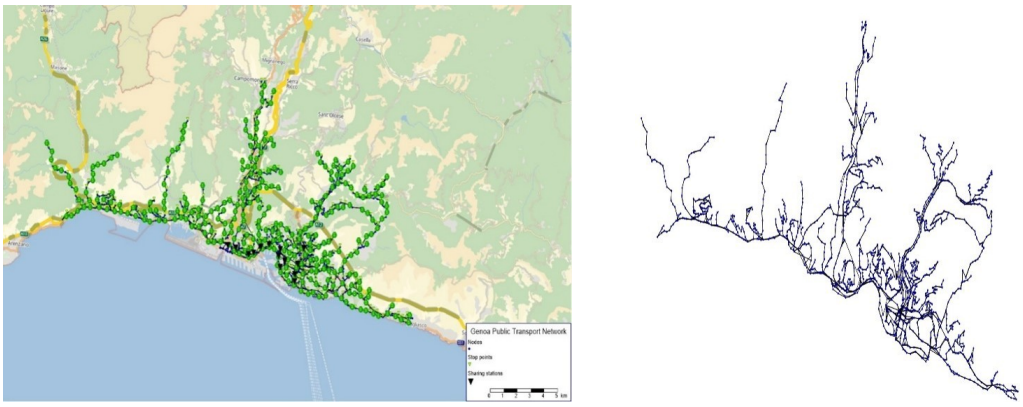

(A) (B)

FIGURE 5.2: (A) Genoa PuT network in Visum (B) Line network coded in MATLAB for Genoa PuT

The time-dependent dynamic demand matrix for all OD pairs is connected to the public transit network via access nodes /stops. Initially, the demand is simulated for a warm-up period of the morning peak hour $(8:00\ am \tilde{} 9:00\ am)$ based on the dynamic share of 8.68% and 8.34% of demand for Barcelona and Genoa respectively as mentioned in Table 5.1 & 5.2. Later, a stop-based passenger demand matrix is deduced using a relational trip distribution procedure for the original zonal passenger demand matrices. The aim of deducing such a detailed stop-to-stop matrix is to precisely calculate the usage of micro-mobility at the top level in case of random disruptions

thus revealing precise and realistic results for network performance in terms of vulnerabilities.

TABLE 5.1: Dynamic time series-based demand for Barcelona

Start time	End time	Weightage	Demand share	Accumulated share
05:00:00	06:00:00	0.951212	0.90%	0.90%
06:00:00	07:00:00	3.09911	2.94%	3.85%
07:00:00	08:00:00	8.131329	7.72%	11.57%
08:00:00	09:00:00	9.143909	8.68%	20.25%
09:00:00	10:00:00	5.492482	5.22%	25.47%
10:00:00	11:00:00	4.510586	4.28%	29.75%
11:00:00	12:00:00	4.510586	4.28%	34.03%
12:00:00	13:00:00	5.523167	5.24%	39.28%
13:00:00	14:00:00	6.597116	6.26%	45.54%
14:00:00	15:00:00	7.517643	7.14%	52.68%
15:00:00	16:00:00	9.5	9.02%	61.70%
16:00:00	17:00:00	8.5	8.07%	69.77%
17:00:00	18:00:00	7.1	6.74%	76.52%
18:00:00	19:00:00	7.456275	7.08%	83.60%
19:00:00	20:00:00	6.535747	6.21%	89.80%
20:00:00	21:00:00	5.308377	5.04%	94.84%
21:00:00	22:00:00	3.221847	3.06%	97.90%
22:00:00	23:00:00	1.411476	1.34%	99.24%
23:00:00	00:00:00	0.797791	0.76%	100.00%

5.3 Network structural evaluation

In the case of normal operations without any disruptions, a base scenario $(S0)$ is set up. Commuter demand is extracted from the origin-destination matrices for both cities courtesy of ATM di Barcelona and Comune di Genova. Later, this demand is assigned to the network following a time-table-based assignment as explained in Chapter 3 yielding commuter load across the network and perceived journey time relations. The branching resulted in

TABLE 5.2: Dynamic time series-based demand for Genoa

Start time	End time	Weightage	Demand share	Accumulated share
00:00:00	01:00:00	0	0.00%	0.00%
01:00:00	02:00:00	0	0.00%	0.00%
02:00:00	03:00:00	0	0.00%	0.00%
03:00:00	04:00:00	0.245	0.22%	0.22%
04:00:00	05:00:00	1.2	1.09%	1.32%
05:00:00	06:00:00	1.9	1.73%	3.05%
06:00:00	07:00:00	3.09911	2.83%	5.88%
07:00:00	08:00:00	8.131329	7.42%	13.29%
08:00:00	09:00:00	9.143909	8.34%	21.63%
09:00:00	10:00:00	6.5	5.93%	27.56%
10:00:00	11:00:00	5.42	4.94%	32.50%
11:00:00	12:00:00	4.510586	4.11%	36.62%
12:00:00	13:00:00	5.523167	5.04%	41.65%
13:00:00	14:00:00	6.597116	6.02%	47.67%
14:00:00	15:00:00	7.517643	6.86%	54.53%
15:00:00	16:00:00	7.7	7.02%	61.55%
16:00:00	17:00:00	9.5	8.66%	70.21%
17:00:00	18:00:00	9	8.21%	78.42%
18:00:00	19:00:00	7.456275	6.80%	85.22%
19:00:00	20:00:00	6.535747	5.96%	91.18%
20:00:00	21:00:00	4.24	3.87%	95.05%
21:00:00	22:00:00	3.221847	2.94%	97.99%
22:00:00	23:00:00	1.411476	1.29%	99.27%
23:00:00	00:00:00	0.797791	0.73%	100.00%

349,977 alternative paths for the entire network of Barcelona whereas 31,906 for that of Genoa. The huge change is due to the major topographical difference between the two cities. Based on Bounding methods, favorable paths are chosen to which the demand is assigned.

For the base scenario of normal operation, the mean perceived journey time including the ride time, origin and transfer wait times and walk time comes out to be 45 minutes for Barcelona whereas 60 minutes for Genoa. The commuter flow characteristics are passed to the coded network for structural

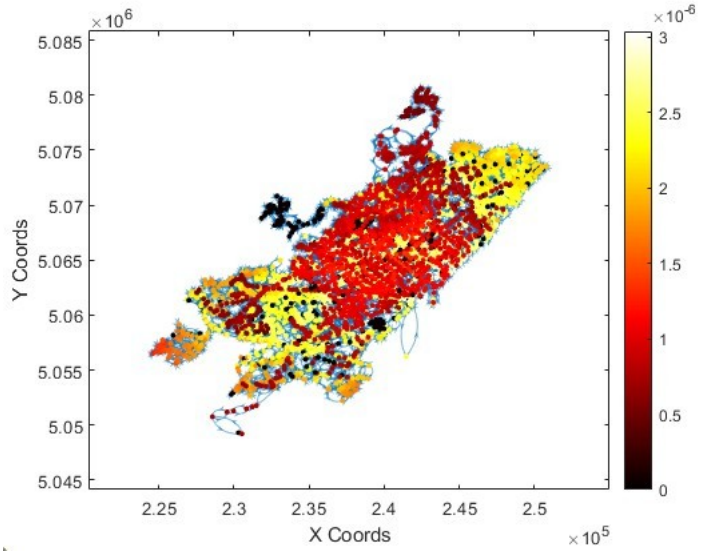

(A)

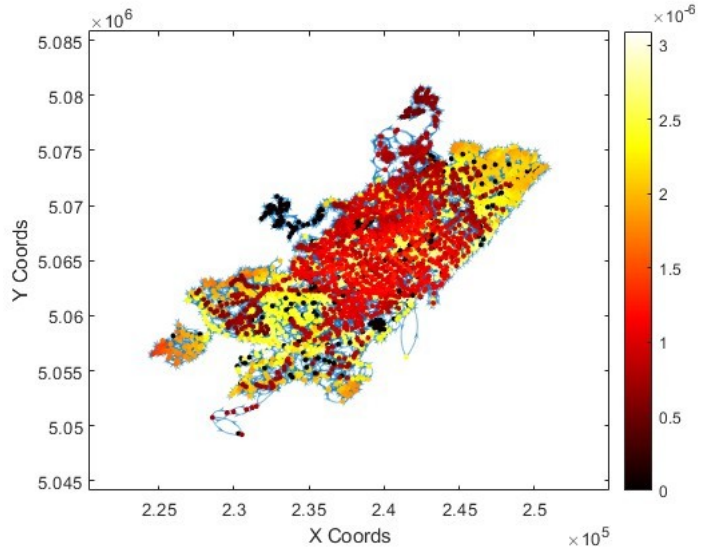

(B)

FIGURE 5.3: (A) Nodes hierarchy based on inward closeness from other nodes for Barcelona (B) Nodes hierarchy based on outward closeness from other nodes for Barcelona

evaluation of the network by using dynamic closeness and betweenness relationships for both nodes and links as explained earlier in Chapter 3. The evaluation of dynamic centrality for the network also takes into account vehicle journeys. Since we have a directed line-based graph for the transit network the collective identification of the vulnerable nodes is based on the weighted in and out the closeness of the nodes as well as the betweenness for nodes and links. As evident from Figure 5.3, the inward and outward closeness

for nodal components are quite similar with high density towards the elevated demand central areas of Barcelona whereas lower ranks towards the outer city. Some high-rank patches in the middle are due to the commuter trips around tourist attractions and shopping districts. Some of the well-connected areas in the outskirts of the city are also shown to be with moderate centrality rankings. Since the heat map is scaled in negative powers of 10, so the components with the highest centrality are in the middle of the heat scale with red color whereas the extremes (black and yellow) are with the zero or lowest centrality respectively. Moreover, as in 5.4 (B), high rankings of dynamic betweenness are observed for the links serving more than 5 transit lines for morning and evening peaks of commuter demand. This also reflects the vehicle capacities as high commuter links are being served by the articulated category of buses and tram lines. Again the high betweenness links are marked with red on a grayscale map.

For the network of Genoa, given its horizontal network structure, the high-ranking centrality components are along major arterials towards the west-central and eastern sides of the city. However, the two major northern arterials show moderate rankings of centrality even serving high demand of commuters as can be visualized in Figure 5.5. The outward centrality of nodes as in 5.5 (B) and betweenness centrality in 5.6 (A) describes a similar trend where high-demand nodes depict higher centrality. Looking into the dynamic betweenness of links, we can witness from the pictorial representation that the dynamic relation segregates high-ranking components of the transit network along the two busiest rail stations of the city (Piazza Principe and Brignole) as evident in Figure 5.6(B). Also, some of the higher centrality links are towards the two major arterials connecting the south and north parts of the city. A collective picture reveals that in all the centrality measures most of the central components are present around the two major rail stations and some around the airport area of Sestri Ponente.

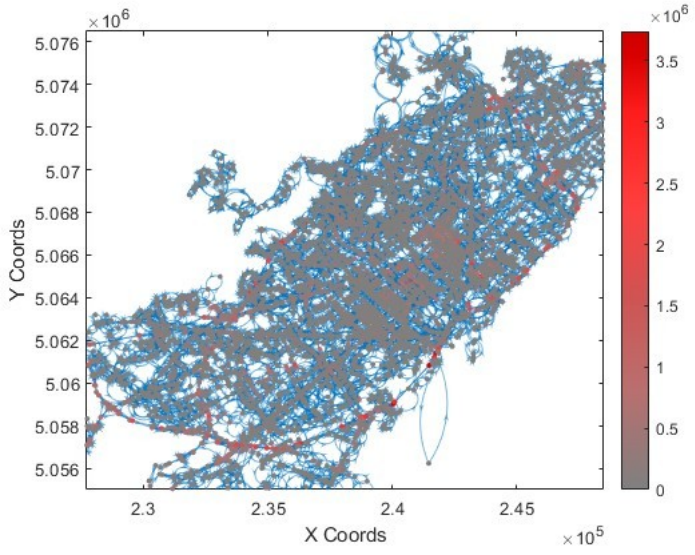

(A)

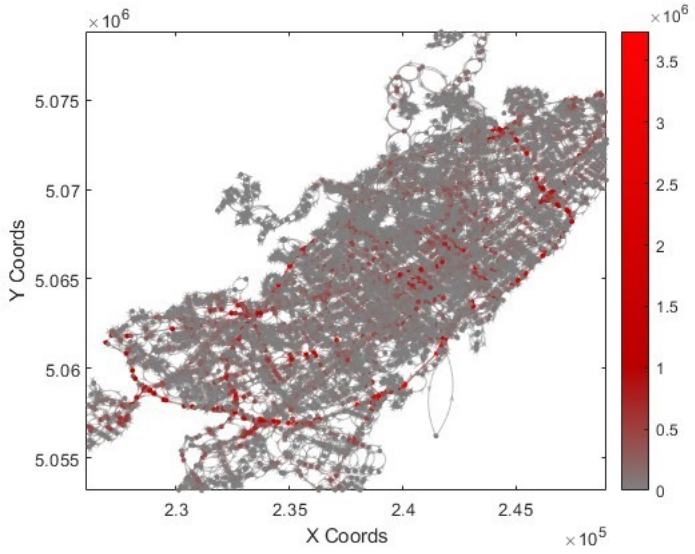

(B)

FIGURE 5.4: (A) Nodes hierarchy based on Betweenness for Barcelona (B) Link hierarchy based on dynamic betweenness

5.3.1 Vulnerable components identification

Before skimming out the high-ranking central components of the network, it is clusterized based on the evaluated centralities. As mentioned earlier, the whole network does not retain the same characteristics therefore it is required to cluster the network from the lowest to the highest rank. The centrality spread for nodes in the network of Barcelona is visualized in Figure 5.7(A) and the centrality spread for the links involved can be seen in Figure

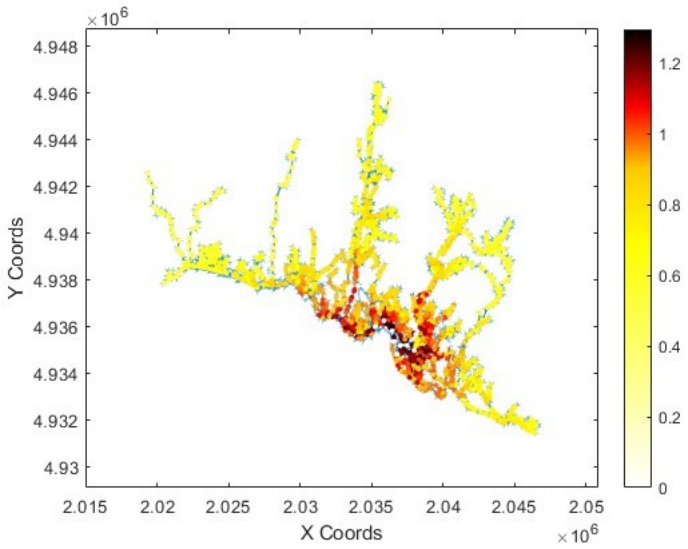

(A)

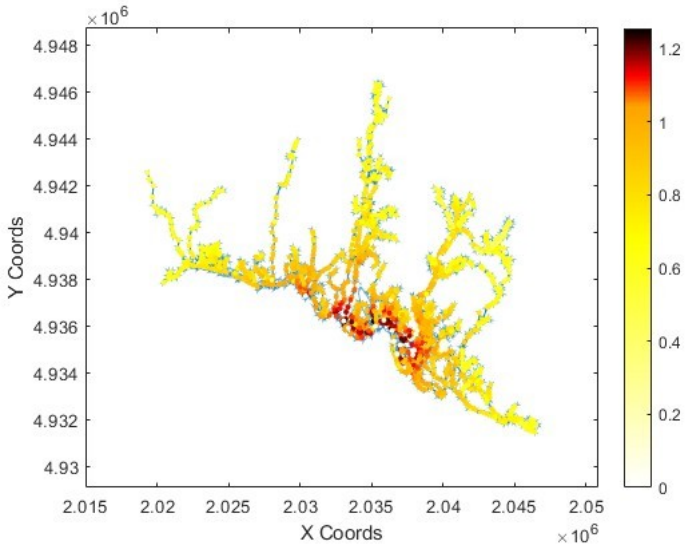

(B)

FIGURE 5.5: (A) Nodes hierarchy based on inward closeness from other nodes for Genoa (B) Nodes hierarchy based on outward closeness from other nodes for Genoa

5.8(A). It can be seen that there are some outliers, particularly in the centrality values of the nodes in the PuT network of Barcelona. These nodes are part of the suburban PuT network which was not considered in this study thus showing outlying values. Later, the validation is done for the most central components to see whether they are part of high-rank central clusters of the transit network or not. Following the K-means clustering method, separate clustering is done based on the centrality of nodes and links. The network

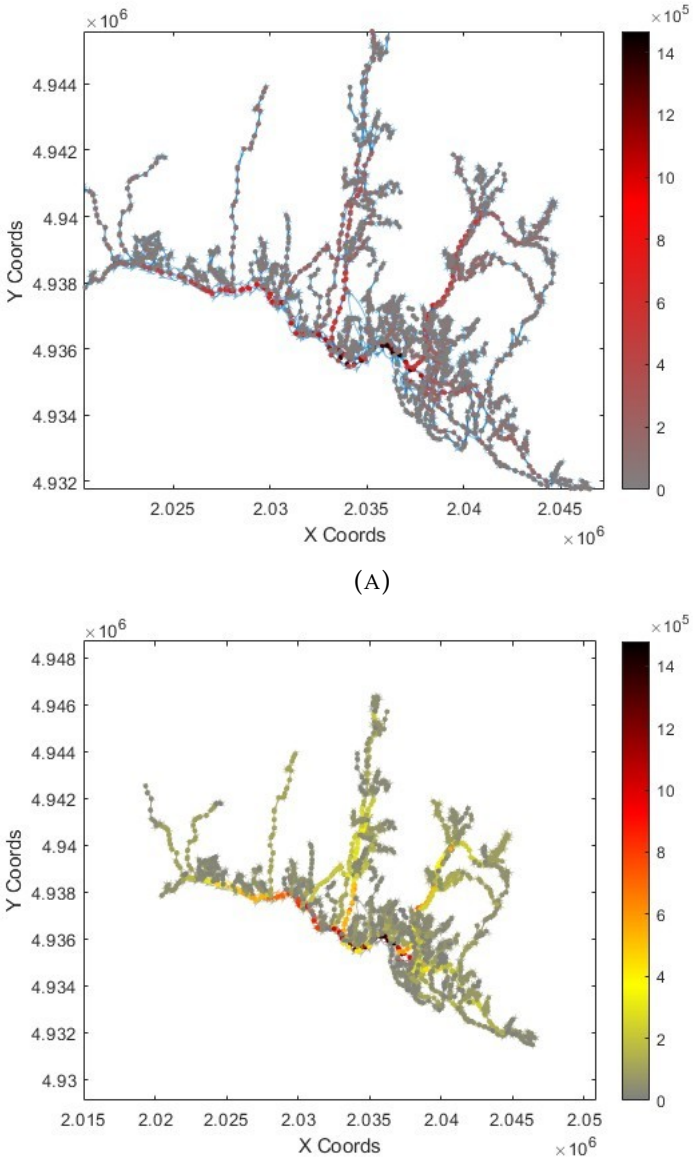

FIGURE 5.6: (A) Nodes hierarchy based on Betweenness for Genoa (B) Link hierarchy based on dynamic betweenness

is divided into two clusters for the centrality values of nodes and into three clusters based on the links' centrality for the case of Barcelona as visualized in Figure 5.7(B) & 5.8(B). The reason for considering the two and three clusters for nodes and links respectively is due to the silhouette plot validation that will be shown later.

In the case of Genoa, the centrality spread for nodes in the network is visualized in Figure 5.9(A) and the centrality spread for the links involved

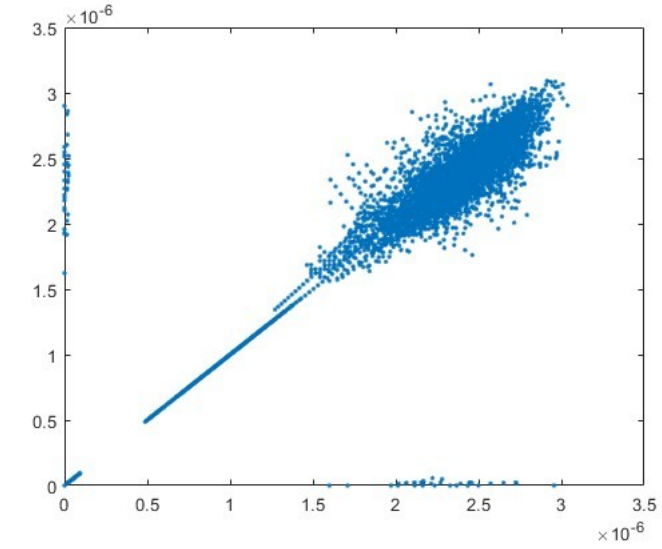

(A)

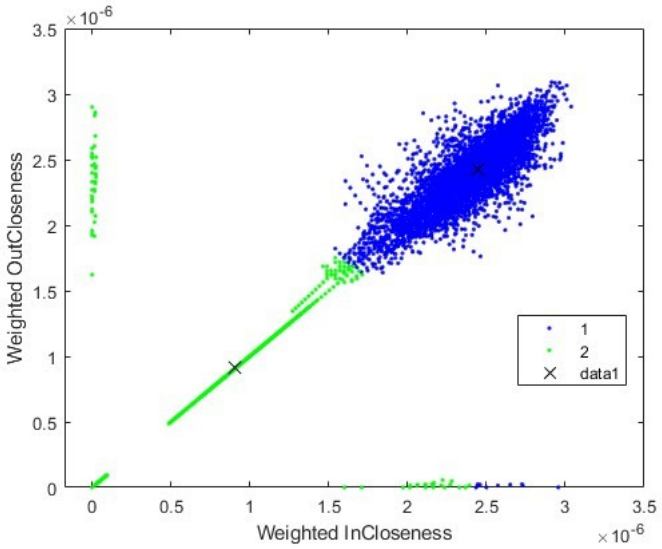

(B)

FIGURE 5.7: (A) Weighted dynamic closeness nodal centrality spread for Barcelona (B) Nodes grouped in 2 clusters

can be seen in Figure 5.10(A). It can be seen that there are some outliers, particularly in the centrality values of the nodes in the PuT network of Genova. These nodes are particularly served by demand responsive PuT system which was not considered in this study thus showing outlying values. Also, a couple of outliers exist for the link's centrality. The whole transit network is divided into two clusters based on nodes centrality and five clusters based on links centrality following the structural evaluation weighted by dynamic

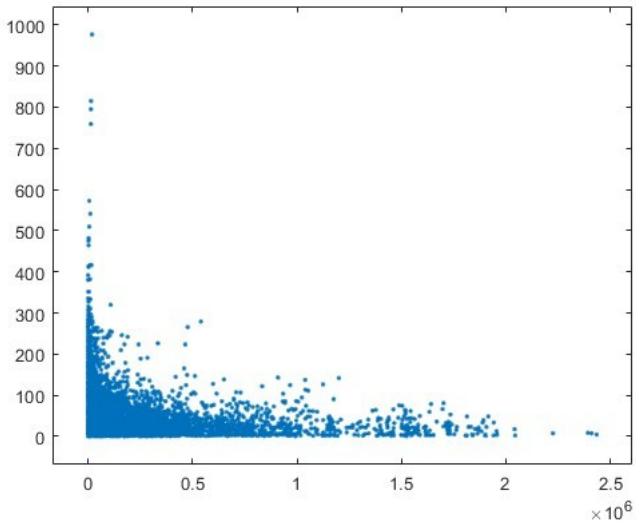

(A)

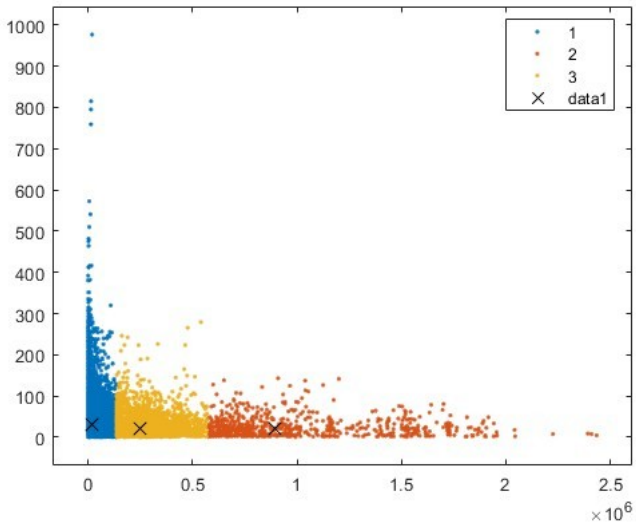

(B)

FIGURE 5.8: (A) Weighted dynamic betweenness link centrality spread for Barcelona (B) Links grouped in 3 clusters

commuter demand as shown below in Figure 5.9(B) & 5.10(B). The best-fit clusters for both nodes and links are identified based on their Silhouette values extracted from Silhouette plots shown below in Figures 5.11 and 5.12. The favorable mean Silhouette value for nodes and links clusters in Barcelona is 0.7644 and 0.7598 whereas that for Genoa comes out to be 0.4717 and 0.5934 respectively. It can be seen in Figure 5.11(A) and 5.12(A) that some Silhouette values are falling in the negative plane due to the outliers present in

centrality values as explained previously. The reason for considering a particular number of clusters is this validation through Silhouette plots. Any number of clusters above or below those we selected showed lower mean silhouette values and a high amount of negativity.

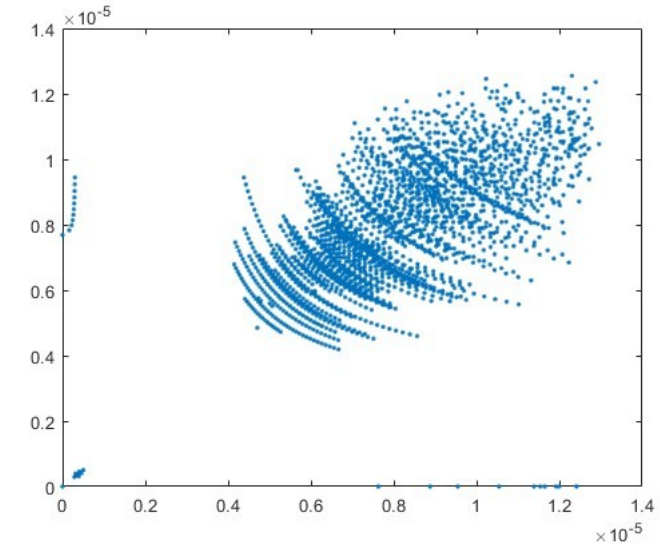

(A)

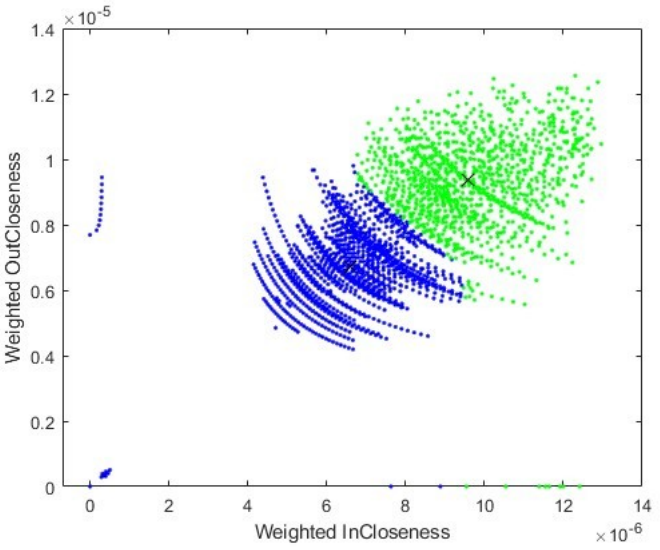

(B)

FIGURE 5.9: (A) Weighted dynamic closeness nodal centrality spread for Genoa (B) Nodes grouped in 2 clusters

The structural examination of the network of Barcelona reveals 5 central nodes and 6 central links. The nodes belong to cluster 2 in the segmented Barcelona network whereas the links belong to cluster 3. For Genoa, the

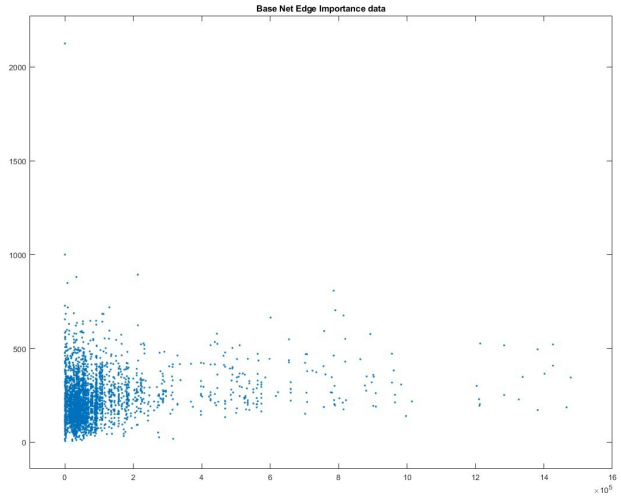

(A)

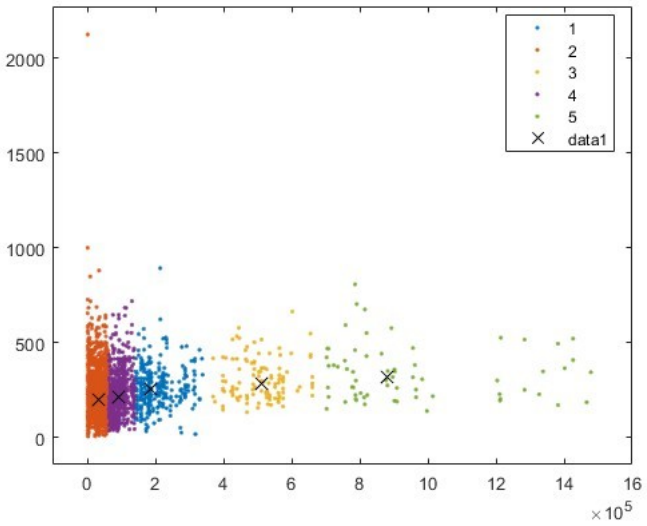

(B)

FIGURE 5.10: (A) Weighted dynamic betweenness link centrality spread for Genoa (B) Links grouped in 5 clusters

number of central nodes comes out to be 6 and 4 central links with the highest centrality rankings. The nodes fall in cluster 2 whereas the links fall in cluster 5 for the clustered transit network of Genoa. this again reveals that the clusterization of the networks is a good fit. All the central components come out to be at key locations with high demand and transfers available for commuters. However, the complexity of alternative paths makes them highly vulnerable. Also in the case of Genoa, some central links are present

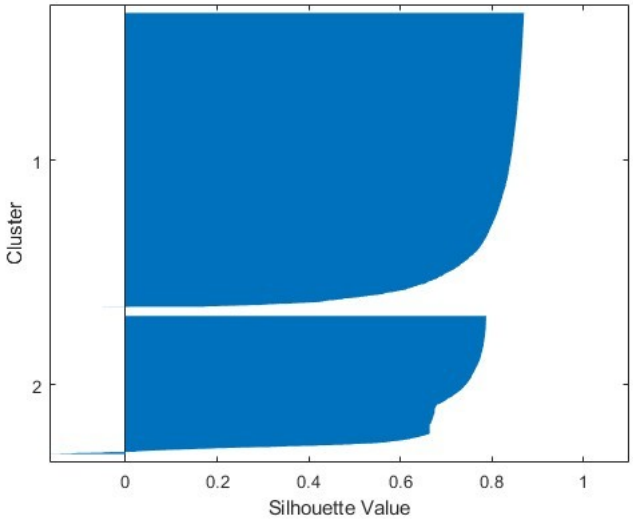

(A)

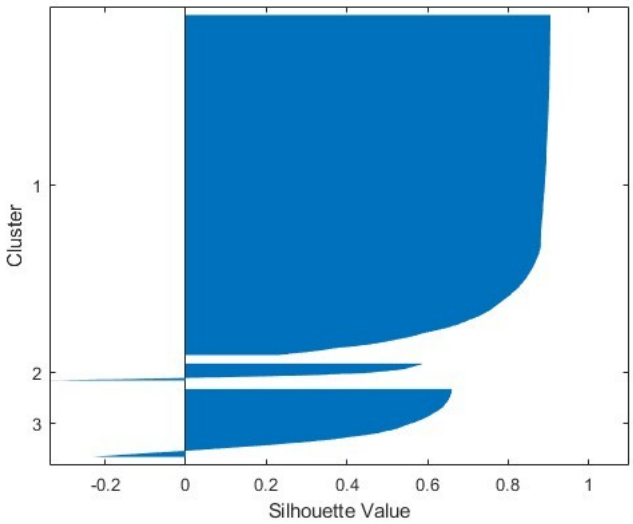

(B)

FIGURE 5.11: (A)Silhouette plot for k-mean clustering of nodes of Barcelona (B) Silhouette plot for k-mean clustering of Links of Barcelona

in such a topographic location that no alternative route for transit lines is possible thus creating a complete halt situation. All the central components for PuT networks of Barcelona and Genoa are penned down in Table 5.3. Once highly central components of both transit networks are identified, the k-nearest-neighbor method as defined in Chapter 3 is implied to identify the neighboring components that are at risk of failure i.e. most critical not relying on proximity but the commuter load and spillover demand effect in case

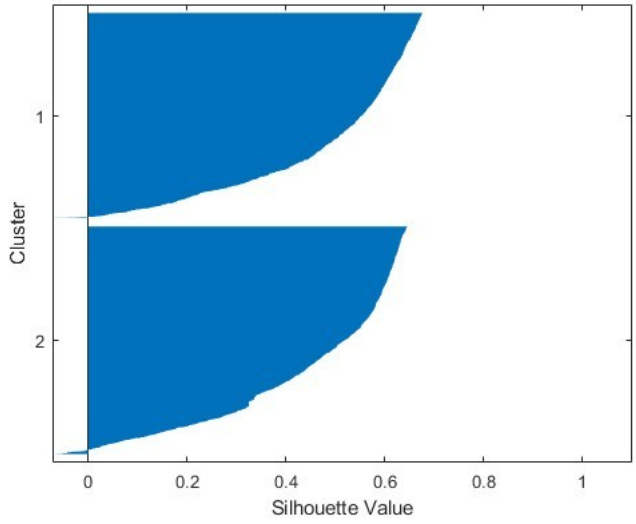

(A)

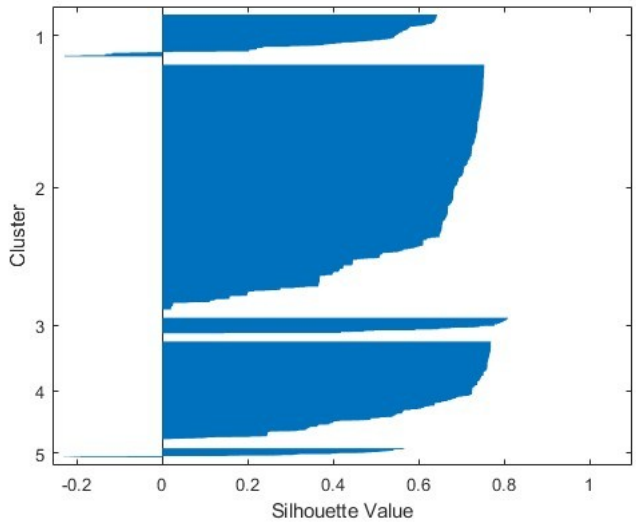

(B)

FIGURE 5.12: (A)Silhouette plot for k-mean clustering of nodes of Genoa (B) Silhouette plot for k-mean clustering of Links of Genoa

of disruptions on the vulnerable components. This reveals a complete picture of the most vulnerable components of the Barcelona transit network as seen in Figure 5.13(A) for nodes and 5.13(B) for links. Similarly, the highly vulnerable components in the transit network of Genoa are shown in Figure 5.14(A) for nodes and 5.14(B) for links.

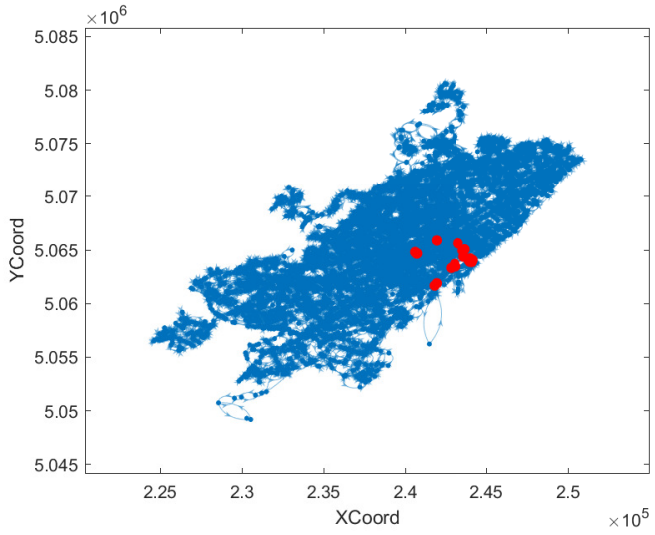

(A)

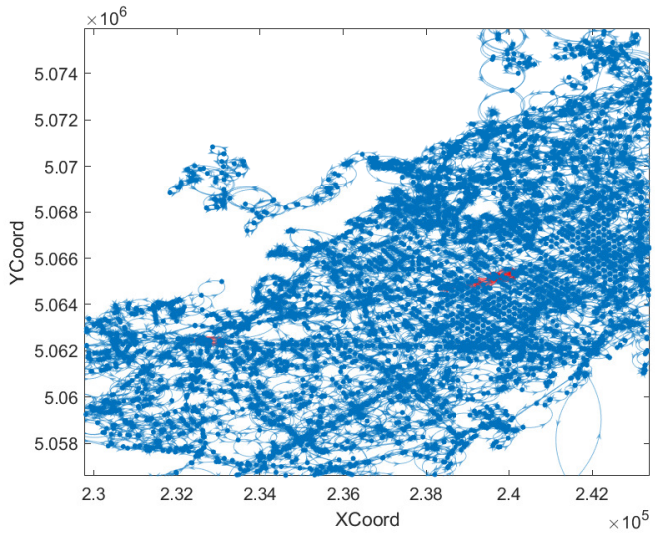

(B)

FIGURE 5.13: (A) High-ranked central nodes marked in red for the Barcelona transit network (B) High-ranked central links marked in red for the Barcelona transit network

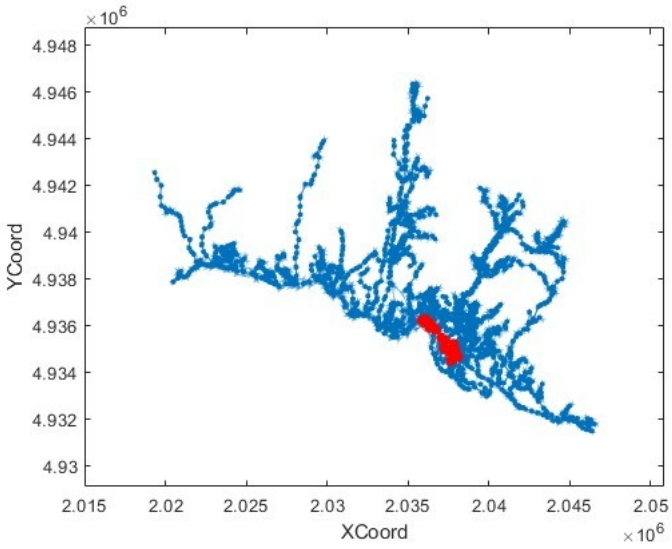

(A)

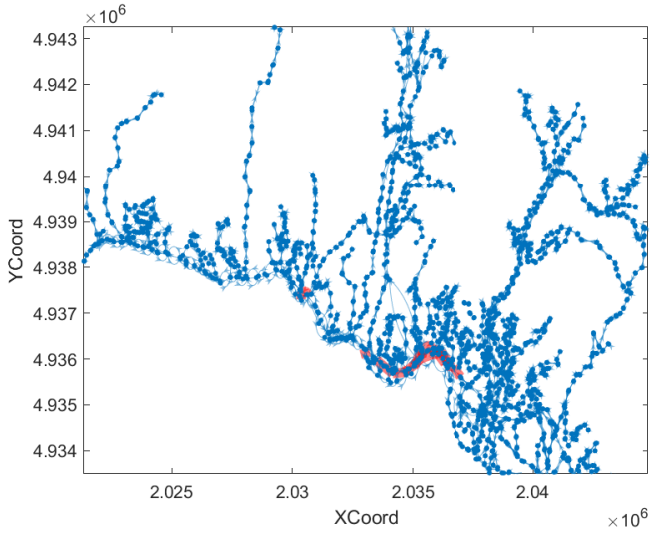

(B)

FIGURE 5.14: (A) High-ranked central nodes marked in red for the Genoa transit network (B) High-ranked central links marked in red for the Genoa transit network

TABLE 5.3: High-ranked candidate central components of the two transit networks selected for vulnerability analysis

BARCELONA				
RANKING	**STOP POINT**	**CENTRALITY** (10^{-6})	**LINK SEGMENT**	**CENTRALITY** (10^{6})
1	Placa Espanya	0.104	Carrer de la Constitucio	4.173
2	Vila Olímpica	0.27	Avinguda Diagonal	2.415
3	Estació de França	0.707	Granvia del Les Corts	3.90
4	Pau Claris - Mallorca	1.23	La Bordeta	1.248
5	Portal de la Pau	1.354	Carrer de Sants (Badal)	0.971
6	Pl Catalunya - Portal de l'Àngel	1.577	—	—
GENOVA				
RANKING	**STOP POINT**	**CENTRALITY**	**LINK SEGMENT**	**CENTRALITY** (10^{5})
1	Brignole FS Capolinea	1.8712	Via Antonio Gramsci	9.216
2	Gramsci 1/ Commenda	1.713	Via Balbi	7.781
3	Gramsci 2/ Darsena	1.697	Via Bruno Bouzzi/ Piazza Dinegro	7.081
4	Buenos Aires 2/ Lambruschini	1.569	Via Aurelia	5.231
5	Gastaldi 3/ Ponte di Terralba	1.149	—	—
6	Principe FS / Fanti di Italia	0.946	—	—

5.4 Impacts of disruptions

Following the final objective of this research laid down in Chapter 1, after identification of the central components of the public transit network in Barcelona and Genoa, the next step is to analyze the impacts of disruptions and assessment of vulnerability in presence of shared bicycle service as a micro-mobility option.

According to the assumptions, the disruptions are short-term without any replacement services by the operator. The details of random service disruption scenarios are mentioned in Chapter 3. A shared bicycle system option at the disrupted segment could prove to be mitigation by allowing commuters to reach their destination or the next nearest alternative. The simulative transit model considers a combination of various possibilities as mentioned in Chapter 3 compared to the base scenario (S0). For each scenario 13 simulative iterations were executed taking 55 minutes each scenario on a system of Core i7-8565U CPU @ 1.80GHz and 8GB RAM. This yielded a maximum divergence of the solution down to 0.001.

The disruptions impose longer wait times increasing the disutility of commuters in the case of Barcelona. In only the S1 scenario where there is no re-routing of the disrupted lines, the commuter's disutility $CD_{r(t,t+1)}$ (S1,0) increased by 3.93 %. However, when disrupted segments force the public transit lines to re-route their course skipping the stops, the rise in $CD_{r(t,t+1)}$ (S2,0) is 4.94% as compared to normal operations. The provision of the micro-mobility option cast a positive impact on $CD_{r(t,t+1)}$. It can be seen from Table 5.4 that for S0, the provision of micro-mobility in three different patterns $(B1, B2, B3)$ the CD is reduced to -2.9 with perceived journey time decreased by 7.14%.

For disruptive scenario S1, the perceived journey time increase from 1.4 to 6.7% in case of disruptions whereas the provision of the micro-mobility

option reduces the disutility from 1.48 to an improvement of -1.87%, this negative sign shows that the provision of micro-mobility even improved the commuter's utility as compared to normal operations by reducing the disutility. For the disruptive scenario of S2, the perceived journey time increase from 1.7 to 9.4% whereas the commuter's disutility increases from 2.7 to a hefty 50.3%. Similarly, the mean journey distance in S1 increased from 1.42 to 3.3% in all combinations (S, B) whereas, in the case of S2, the mean journey distance in S1 increased from 1.26 to 9.5% in all combinations (S, B). it is interesting to note that in S2 the provision combination of micro-mobility is worsening the situation as the commuter's disutility increases from 3..98 to 5.822.

As shown in Table 5.4 the spillover effects are also interesting to note in all the combinations of disruptions and micro-mobility usage scenarios. As compared to normal operations for S1, the spillover effect in the surrounding network ranges from 7.8 to 28.8% whereas, for S2, the spillover effect has a higher range from 19.1 to 37%. This justifies the commuter's disutility increase in S2 as seen earlier. To be precise with impacts on commuters and the system itself, it can be seen that the average journey time in the base scenario under normal conditions in the case of Barcelona is around 45 minutes including the stop access, waiting, and ride times together with the walking time at the transfer stop. The provision and usage of shared bicycle systems under normal operations improve the average journey time to 42 minutes yielding an improvement of almost 7%. As anticipated, the random disruptions in service and operations result in extended journey times either due to alighting to/ boarding from non-actual origin/destination stop. The disruptions without any mitigation increase the travel time to 49 minutes for the same OD pair in a standard rush hour generating additional commuter hours. This forces them to divert from their original planned path creating a

spillover effect by induced demand on neighboring central components resulting in increased complexity. Again this depends on the OD pair for each passenger. In the case of S1, the average journey times increase to 48 minutes with partial mitigation whereas reduced to 45 minutes in presence of a fully available shared bicycle system thus the share of commuters taking trips between 40min and 60 min increased from 7% to 11.2% for Barcelona, 1% of trips correspond to 2,971 commuters. Also, in the case of S1, a group of commuters benefits from disruptions in the form of fewer crowds and high reliability in the arrival times of transit.

In the case of Genoa, the random service disruptions impose extended wait times increasing the disutility of commuters. In scenario S1 where there is no re-routing of the disrupted lines, the commuter's disutility $CD_{r(t,t+1)}$ (S1,0) increased by 5.3%. However, when disrupted segments force the public transit lines to re-route their course skipping the stops, the rise in $CD_{r(t,t+1)}$ (S2,0) is 5.38% as compared to normal operations. The provision of the micro-mobility option cast a positive impact on $CD_{r(t,t+1)}$. It can be seen from Table 5.5 that for S0, the provision of micro-mobility in three different patterns $(B1, B2, B3)$ the CD is reduced to 3.21% with perceived journey time decreased by 4.41%.

For disruptive scenario S1, the perceived journey time increase from 0.33 to 12.2% in case of disruptions whereas the provision of the micro-mobility option reduces the disutility from 1.25 to an improvement of 0.1%, the negative sign shows that the provision of micro-mobility even improved the passenger's utility as compared to normal operations by reducing the disutility. For the disruptive scenario of S2, the perceived journey time increase from 0.58 to 9.8% whereas the relative change in commuter's disutility increases from 0.03 to 1.2%. Similarly, the mean journey distance in S1 increased from 2.1 to 2.8% in all combinations (S, B) whereas, in the case of S2, the mean journey distance in S1 increased from 1.9 to 7.7% in all combinations (S, B).

it is interesting to note that in all scenario combinations that the provision of partial micro-mobility is worsening the situation as the commuter's disutility increases. Another important thing to note is that this provision is not significantly affecting the disutility of commuters.

As compared to normal operations for S1, the spillover effect as witnessed in Table 5.5 in the surrounding network ranges from 4.3 to 28.3% whereas, for S2, the spillover effect has a higher range from 12.5 to 31.4%. To be precise with impacts on commuters and the system itself, it can be seen that the average journey time in the base scenario under normal conditions in the case of Genoa is around 59 minutes including the stop access, waiting, and ride times together with the walking time at the transfer stop. The provision and usage of shared bicycle systems under normal operations improve the average journey time to 57 minutes yielding an improvement of almost 4%. As anticipated, the random disruptions in service and operations result in extended journey times either due to alighting to/ boarding from non-actual origin/destination stop. The disruptions without any mitigation increase the travel time to 66 minutes for the same OD pair in a standard rush hour generating additional commuter hours. This forces them to divert from their original planned path creating a spill-over effect by induced demand on neighboring central components resulting in increased complexity. Again this depends on the OD pair for each passenger. In the case of S1, the average journey times increase to 67 minutes with partial mitigation whereas reduced to 60 minutes in presence of a fully available shared bicycle system thus the share of commuters taking trips between 55min to 75 min increased from 4% to 22%. for Genoa, 1% of trips correspond to 1059 commuters. Also, in the case of S1, a group of commuters benefits from disruptions in the form of fewer crowds and high reliability in the arrival times of transit.

TABLE 5.4: Relative perceived journey time and commuter's disutility variations in various scenario combinations for the transit network of Barcelona

SCENARIOS												
S0					**S1**				**S2**			
	B0	**B1**	**B2**	**B3**	**B0**	**B1**	**B2**	**B3**	**B0**	**B1**	**B2**	**B3**
Perceived Journey Time (PJT) (Sec)	2716	2695	2674	2524	2768	2898	2901	2755	2972	2936	2834	2762
Relative Change PJT (%)	—	- 0.77	- 1.54	- 7.14	1.91	6.7	6.8	1.4	9.4	8.1	4.3	1.7
$CD_{r(t,t+1)}$	3.87	- 0.86	- 1.22	- 2.9	3.93	3.89	3.81	3.8	4.94	3.98	4.85	5.822
Relative Change of $CD_{r(t,t+1)}$	—	2.9	2.9	5.79	1.48	0.45	- 1.61	- 1.87	27.56	2.77	25.24	50.34
Spillover effect (%)	—	—	—	—	28.8	21.3	15.7	7.8	37	19.1	31.3	23.8

TABLE 5.5: Relative perceived journey time and commuter's disutility variations in various scenario combinations for the transit network of Genoa

SCENARIOS												
S0					**S1**				**S2**			
	B0	**B1**	**B2**	**B3**	**B0**	**B1**	**B2**	**B3**	**B0**	**B1**	**B2**	**B3**
Perceived Journey Time (PJT) (Sec)	3538	3541	3572	3426	3763	3981	4015	3596	3935	3892	3781	3605
Relative Change PJT (%)	—	-1.12	-0.33	-4.41	4.99	11.07	12.02	0.33	9.8	8.6	5.5	0.58
$CD_{r(t,t+1)}$	4.28	4.32	6.28	3.21	5.3	5.53	5.347	4.19	5.38	3.37	4.35	4.31
Relative Change of $CD_{r(t,t+1)}$	—	0.04	2	-1.07	1.1	1.25	1.06	-0.1	1.02	-0.91	0.07	0.03
Spillover effect (%)	—	—	—	—	19.3	28.3	17.12	4.3	31.4	27.3	12.5	21.7

5.5 Conclusions

This detailed analysis and comparison of two completely different cities fulfill the purpose of attaining the objective laid in Chapter 1. The stochasticity of this proposed methodology reveals a realistic complete situation of the multi-modal transit networks of Barcelona and Genoa under different disruption scenarios with and without mitigation by the provision of a shared bicycle as a micro-mobility option. This also results in the most affected links, lines, and stops apart from the disrupted ones thus revealing the spillover effect too. The analysis of the obtained results shows appreciable results and decrement in the vulnerability of the transit network when micro-mobility is integrated. However, looking at the second scenario of disruption the complete combination of micro-mobility (S2, B3) for Barcelona and (S2, B1-3) for Genoa reveals that the commuter's disutility further worsens as compared to the previous combinations. This implies that the accurate provision of micro-mobility is also important. This further widens our research question what locations of the network do the sharing station occupancies need to be upgraded/downgraded? Moreover, how often should the relocation operations be done? The disturbance in the network is getting worse even with the inclusion of micro-mobility also suggests that not every journey can be mitigated via this method. With the revelation of this analysis, it is evident that research in this regard has high importance and relevance in the present time not only related to the impacts of micro-mobility on public transportation networks but also to attain the answer related to the optimal location and occupancy of the sharing stations.

Chapter 6

Conclusions

This chapter consists of the major conclusions drawn through this extensive research work. It also points out the answer to specific research questions raised in Chapter 1 and an explanation of how this research fills some of the skimmed gaps in Chapter 2. Finally, it composes and converges the compound impacts of the new forms of mobility on the transportation systems and limitations of this research leading to the recommendations for future work.

6.1 Potential impacts of the introduction of AVs

A pervasive review of the state-of-the-art in Chapter 2 revealed several stats on the impact of connected and automated vehicles on transportation network performances, traffic flow, and urban road network capacities. One way or another the stats are accepted and understood. Yet the limitation of those studies in terms of user-oriented evaluation, a realistic approach to quantify the amount of these new forms of vehicles to be introduced into the network and their consequent effects on travel equilibrium costs are missing. This research paved the way to explore and answer the maximum of possibility these questions related to the gaps identified relating to:

- Importance of demographic, road network, and land use factors in quantifying the penetration rate of AVs.

- Effect of physical and functional characteristics of urban road networks on capacity and travel time-flow relationships for heterogeneous traffic streams.
- The aftermath of inclusion of AVs into the network on inequity in terms of travel equilibrium costs.

Major conclusions were drawn and are reported below after applying the formulated methodology in Chapter 3 in the context of underlying assumptions.

6.1.1 Private transportation network performance and traffic flows

One of the first gaps identified in the current state-of-the-art is related to the realistic penetration rate of AVs used to evaluate their impacts on traffic flows and transportation network performances. The first question raised in Chapter 2 in this regard is:

- How do various demographic, road network, and land use factors govern the quantification of the penetration rate of AVs?

Concerning the first objective and question raised, an answer to the question is given following the methodology formulated in Chapter 3. A realistically quantified penetration rate of AVs is derived from a multiple indicators system to synthesize seven different indices using user socio-demographical, land usage, and road network characteristics. These indices relate to the adaptation of AVs in a system instead of including them as a random percentage. Then by sensitively analyzing each index for its impact on the penetration rate and comparing it using the quantile approach, the realistic value of AVs is determined which comes out to be a range of 25-35% keeping in view 0% AVs in the current year and projection for the indices for the next 15

years. Moreover, this value is based on vehicle ownership and readiness to buy a new vehicle.

The next objective laid is to interpret the impacts of AVs on the network performances under a quantified penetration rate. For that the question raised is:

- How do the physical and functional characteristics of urban road network influence the capacity and travel time flow relationship in presence of a realistically quantified amount of AVs?

Moving on to our second objective and question, the derived penetration rate is introduced into the network supply model set up to investigate the impacts. The increment in usage of AVs generates a heterogenous traffic stream increasing the capacity of an urban link by 35% to 59% as compared to the only TVs scenario. However, any induced demand to occupy that capacity will reduce the critical speed but prolong the un-saturated condition of the network. As can be seen from saturation grade in heterogeneous stream vehicles are moving with higher critical speed. This increment in capacity has a positive impact on the travel time of vehicles where the travel time to cover the urban road link is reduced in presence of a heterogeneous traffic stream. The presence of a physical median between opposite-direction traffic has an impact of 7-10% on travel times. Decrement in useful road width due to the presence of parallel parking has a direct impact on travel time yet heterogeneous traffic stream cast positive results as compared to the only TVs scenario. A similar, trend is witnessed for the number of pedestrian crossings, external disturbances, and tortuosity of the road network causing an increment in travel times.

6.1.2 Equillibrium shift in travel equilibrium costs

The third objective is to figure out the impressions of introducing AVs on inequity in terms of travel equilibrium costs. In this regard a question is raised:

- How the increased trip generation on the introduction of a quantified amount of AVs will result in inequity from the different equilibrium in travel costs among various travel zones?

The quantified penetration rate of AVs is used in the formulated convex minimization problem which is a lower level of the bi-level optimization model. The presented bi-level optimization model is solved using a genetic algorithm that addresses the inequity among the travel zones on the introduction of AVs into the network by sensing the deviation in travel equilibrium costs for each OD pair. Also, governs the maximum amount of new demand that can be produced by each origin zone. Under different upper bounds for inequity, it was found that the most optimal travel equilibrium costs and newly generated demand are for the upper bound of 1.09. Not only this but a detailed analysis of the optimal curves for each origin zone and every OD pair explicitly shows that with a steady growth of trips there is a possibility of decrement in travel equilibrium costs for some zones. Not every zone shows the optimal values for a single upper bound of inequity. This reveals the importance of micro-level planning for urban and transportation development.

6.1.3 Limitations and future recommendations

As an evolving area of study and constant technology development, there is scope for advancement and more detailed micro-research. Nothing is always perfect, and this is notably legitimate for the area of transport planning and operations. This research study also has limitations that open an invitation for recommendations to carry out future work in this regard.

The first limitation is related to the penetration rate. The devised penetration rate index QE_{AV} value for the current year corresponds to the penetration rate of 25%. But the current presence of AVs is much lesser than that yet not 0% because many manufacturers are providing some features that correspond to the Level 1 and 2 AVs in their high-end premium vehicles. However, this study is limited in incorporating the exact amount of vehicles being used by the general public as it must involve the relevant vehicle registration department. Nevertheless, future work can give more precise results thus validating the theoretical current value of QE_{AV} depending upon the data obtained from the concerned vehicle registration department.

Secondly, this research is limited in terms of considering the AVs-ready infrastructure e.g. signal controls and AVs-ready intersections. Also, data from user adaptation surveys can be incorporated to quantify the penetration rate in a more synchronized manner.

Another possibility to make the results more accurate is by incorporating the interaction of AVs with other AVs, vehicles, infrastructure as well as micro-mobility users, and pedestrians revealing a complete picture of their possible implications on the performances of private transportation networks.

6.2 Public transport network vulnerability

A detailed review of the state-of-the-art in Chapter 2 on interaction and impacts of micro-mobility services on the public transportation networks is penned. Since the pandemic, this new form of mobility attracted many governments to understand the view that this mobility method contributes to more inclusive, liveable, and sustainable cities. A huge amount of literature is reviewed analyzing the interactions of micro-mobility modes with public transportation networks yet, they were limited in terms of evaluating the impacts both positive and negative in the scenario of random disruptions in

services of public transportation systems. This research paved the way to explore and answer the maximum of possibility these questions related to the gaps identified relating to:

- The importance of dynamic centrality measures in identifying the most critical components of the PuT system as well as the nearest neighbors at risk of failure.
- The vulnerability of these critical components with and without the provision of micro-mobility services.
- The impact of cityscape, topography, and effective provision of shared micro-mobility services to enhance the performance of PuT systems.

Major conclusions were drawn and are reported below after applying the formulated methodology in Chapter 3 in the context of underlying assumptions.

6.2.1 Network evaluation

A detailed review of the existing literature in Chapter 2 leads us to formulate the fourth objective as well as the question to be answered related to the network's structural evaluation and identification of vulnerable components. The question raised:

- How do dynamic centrality measures help identify the most critical components of the network and most stressed neighbors?

An integrated public transport model is set up taking into account the dynamic and time-dependent commuter demand. The shared bicycle model is integrated into the public transport model considering the precision of renting or parking rejection. Dynamic OD demand is assigned to the network based on a timetable-based assignment method. This leads to identifying

critical components of the network following dynamic centrality relations fed into mixed unsupervised and supervised machine learning approaches. A total of 6 most critical nodes and 5 links are identified for the PuT network of Barcelona. Similarly, for Genoa, 6 critical nodes and 4 links are identified. later, *Knn* is used as explained in Chapter 3 to identify the most vulnerable neighbors giving us a complete picture of the most vulnerable components in the two PuT networks.

6.2.2 Vulnerability of components against random disruptions

Moving forward, the fifth objective of evaluating the performance of the PuT system under the occurrence of random service disruptions at the critical components to assess the vulnerability is attained. The question raised:

- How do electric/non-electric micro-mobility modes affect the public transport network vulnerability in a scenario of random disruptions?

Devising an answer to the raised question is an application of formulated methodology on two different PuT networks for the city of Genoa and Barcelona. Several short-term disruption scenarios were modeled at the critical components of the network revealing the vulnerability of the transit network in terms of commuters' disutility to travel with and without the provision of a shared micro-mobility system which in our case was a shared bicycle system. In various scenarios, the provision of a micro-mobility system decreased the perceived journey time by 7.14% for the case of Barcelona improving the commuter's disutility even more than the base scenario without disruption. Also, causing a massive spill-over effect on the nearest operational neighbors by 37%. In the case of Genoa, similar trends were observed. a decrement of 4.41% in perceived journey time while improving the disutility to 0.1%. The spill-over effect ranges from 12.5% to 31.4% in various scenarios.

Finally, the sixth question raised in lieu of the objective of this research is:

- How does cityscape and provision of effective shared micro-mobility systems improve the performance of public transport networks?

Looking at the second scenario of disruption the complete combination of micro-mobility (S2, B3) for Barcelona and (S2, B1-3) for Genoa reveals that the commuter's disutility further worsens as compared to the previous combinations. This implies that the accurate provision of micro-mobility is also important. Although the shared bicycle system of Barcelona is very vast with an enormous fleet, albeit, at some of the critical locations it failed to mitigate the vulnerable situations. This is mainly due to the inaccurate amount of infrastructure provision and planning of re-positioning of the fleet. In the case of Genoa, the system is in the pilot phase thus with a limited fleet but at the most critical point e.g. Via Gramsci, it is unable to mitigate the situation due to the lack of placement of shared stations, the nature of traffic, almost impossible availability of re-routing of the commuters trip to reach the destination. This clearly reveals the fact that planning the provision while keeping in view the topography and limitation of the network is highly important. Otherwise, instead of mitigation, the provision will start to generate a chaotic situation.

6.2.3 Limitations and future recommendations

Certainly, the integration of micro-mobility with public transport generates interesting facts and impacts overall user mobility but the absence of its impacts on the whole public transport network in terms of vulnerability assessment paves way for carrying out this research answering the important questions to fill the gap of current literature.

However, the facts revealed in attaining the last objective further widen the area to look at, what locations of the network do the sharing station occupancies need to be upgraded/downgraded. Moreover, how often should

the relocation operations be done? The disturbance in the network is getting worse even with the inclusion of micro-mobility also suggests that not every journey can be mitigated via this method. The research is limited in terms of the optimal location and occupancy of the sharing stations.

It would certainly be useful in future work where we need to identify the reasons as well as mitigation for the back flux effect of the micro-mobility provision in case of disruptions. On the other hand, for normal operation scenarios, the decreased disutility shows us that micro-mobility integration with public transportation services is certainly a fruitful option and cities should move towards this sustainable option. However, the planning should consider user preferences, topography and cityscape, and dynamic demand patterns.

Appendix A

List of Publications

A.1 Publications during the tenure of Ph.D.

1. M. T. Bilal, D. Giglio, S. Sarwar, and S. Sauri, “Appraisal of the dynamic vulnerability of multi-modal public transport network on the assimilation of shared micro-mobility services ”, [2022] Under review for the journal “Transportation Research Part C”.

2. S. Sarwar, S. Sauri, M.T. Bilal, and G. Majoral, “Analysis of Superblocks During Transition Phase from Manual Car to Fully Automated Vehicle Environment: A Case Study of Barcelona”, [2022] Under review for the journal “Transportation Research Part C”.

3. M.T. Bilal, D. Giglio, S. Sarwar, and S. Sauri, "Assessment of Dynamic Vulnerability of Public Transport Bus Network on the Integration of Micro-Mobility Services“, [2022] Accepted for presentation at "102nd Transportation Research Board Annual Meeting 2023".

4. M.T. Bilal and D. Giglio, "Analysing inequity in land use and transportation models by genetic algorithm for realistically quantified penetration rate of autonomous vehicles", [2022], Submitted on February 3, 2022, Awaiting decision from the Journal "Transport Research Interdisciplinary Perspectives".

5. M.T. Bilal and D. Giglio, "Evaluation of macroscopic fundamental diagram characteristics for a quantified penetration rate of autonomous vehicles", [2022] Provisionally Accepted for publication in the journal "European Transport Research Review".

6. M. T. Bilal and D. Giglio, "Realization of the penetration rate for autonomous vehicles in multi-vehicle assignment models," Transportation Research Procedia, [2022]
   URL= https://www.sciencedirect.com/science/article/pii/S2352146522001491

7. M. T. Bilal and D. Giglio, "Evaluation of macroscopic fundamental diagram characteristics for a quantified penetration rate of autonomous vehicles," [2021] European Transport Conference Online.
   URL = https://aetransport.org/past-etc-papers/conference-papers-2021?abstractId=7364&state=b

8. M. T. Bilal and D. Giglio, "Inequity evaluation for land use and transportation model on introduction of autonomous vehicles," [2021], 7th International Conference on Models and Technologies for Intelligent Transportation Systems (MT-ITS), 2021, pp. 1-7, doi: 10.1109/MTITS49943.2021.9529278. [2021]
   URL = https://ieeexplore.ieee.org/document/9529278

9. M. T. Bilal, S. Sarwar and D. Giglio, "Optimization of public transport route assignment via travel time reliability," 2021 7th International Conference on Models and Technologies for Intelligent Transportation Systems (MT-ITS), 2021, pp. 1-6, doi: 10.1109/MT-ITS49943.2021.9529303. [2021]
   URL=https://ieeexplore.ieee.org/document/9529303

Bibliography

A, Trivedi (2018). *Carmakers Throw Money at the Future of Driving - BNN Bloomberg*. https://www.bnnbloomberg.ca/carmakers-throw-money-at-the-future-of-driving-1.1147263. Accessed: 2022-10-22 06:24:13.

Abduljabbar, Rusul, Sohani Liyanage, and Hussein Dia (2021). "The role of micro-mobility in shaping sustainable cities: A systematic literature review". In: *Transportation Research Part D: Transport and Environment* 92, p. 102734. ISSN: 1361-9209. DOI: https://doi.org/10.1016/j.trd.2021.102734.

Adnan, Muhammad et al. (2019). "Last-mile travel and bicycle sharing system in small/medium sized cities: user's preferences investigation using hybrid choice model". In: *Journal of Ambient Intelligence and Humanized Computing* 10.12, pp. 4721–4731.

Albacete, X et al. (2017). "Measuring the accessibility of public transport: a critical comparison between methods in Helsinki". In: *Applied Spatial Analysis and Policy* 10.2, pp. 161–188.

Almeida Correia, Gonçalo Homem de and Bart van Arem (2016). "Solving the User Optimum Privately Owned Automated Vehicles Assignment Problem (UO-POAVAP): A model to explore the impacts of self-driving vehicles on urban mobility". In: *Transportation Research Part B: Methodological* 87, pp. 64–88. ISSN: 0191-2615. DOI: https://doi.org/10.1016/j.trb.2016.03.002. URL: https://www.sciencedirect.com/science/article/pii/S0191261515300692.

Anis, Summair and Csaba Csiszár (2019). "Management of Potential Conflicts between Pedestrians and Autonomous Vehicles". In: *2019 Smart City Symposium Prague (SCSP)*, pp. 1–6. DOI: 10.1109/SCSP.2019.8805678.

Ben-Haim, Gev, Reut Ben-Haim, and Yoram Shiftan (July 2018). "Penetration and impact of advanced car technologies". In: *MOJ Civil Engineering* 4, pp. 175–184. DOI: 10.15406/mojce.2018.04.00117.

Berche, Bertrand et al. (2009). "Resilience of public transport networks against attacks". In: *The European Physical Journal B* 71.1, pp. 125–137.

Bergström, A. and R. Magnusson (2003). "Potential of transferring car trips to bicycle during winter". In: *Transportation Research Part A: Policy and Practice* 37.8, pp. 649–666. ISSN: 0965-8564. DOI: https://doi.org/10.1016/S0965-8564(03)00012-0. URL: https://www.sciencedirect.com/science/article/pii/S0965856403000120.

Bilal, Muhammad Tabish and Davide Giglio (2021). "Inequity evaluation for land use and transportation model on introduction of autonomous vehicles". In: *2021 7th International Conference on Models and Technologies for Intelligent Transportation Systems (MT-ITS)*, pp. 1–7. DOI: 10.1109/MT-ITS49943.2021.9529278.

— (2022). "Realization of the penetration rate for autonomous vehicles in multi-vehicle assignment models". In: *Transportation research procedia* 62, pp. 171–180.

Bilal, Muhammad Tabish, Samra Sarwar, and Davide Giglio (2021). "Optimization of public transport route assignment via travel time reliability". In: *2021 7th International Conference on Models and Technologies for Intelligent Transportation Systems (MT-ITS)*. IEEE, pp. 1–6.

Buijtenweg, Abel et al. (2021). "Quantifying the hierarchy of public transport networks". In: *2021 7th International Conference on Models and Technologies for Intelligent Transportation Systems (MT-ITS)*. IEEE, pp. 1–6.

Cantarella, Giulio E. et al. (2019). "Solving stochastic assignment to transportation networks with TVs and AVs". In: *Transportation Research Procedia* 42. Modeling and Assessing Future Mobility ScenariosSelected Proceedings of the 46th European Transport Conference 2018, ETC 2018, pp. 7–18. ISSN: 2352-1465. DOI: https://doi.org/10.1016/j.trpro.2019.12.002. URL: https://www.sciencedirect.com/science/article/pii/S2352146519305691.

Car and Driver (2019). URL: https://www.caranddriver.com/features/a27116837/italy-autonomous-vehicle-testing/.

Carrese, Stefano et al. (2019). "A preliminary study of the potential impact of autonomous vehicles on residential location in Rome". In: *Research in Transportation Economics* 75, pp. 55–61.

Carroll, David L et al. (1996). "Genetic algorithms and optimizing chemical oxygen-iodine lasers". In: *Developments in theoretical and applied mechanics* 18.3, pp. 411–424.

Carteni, A and V Punzo (2007). "Travel time cost functions for urban roads: A case study in Italy". In: *WIT Transactions on the Built Environment* 96, pp. 233–243.

Cascetta, Ennio (2009). *Transportation systems analysis: models and applications*. Vol. 29. Springer Science & Business Media.

Castrillon, Felipe and Jorge Laval (2018). "Impact of buses on the macroscopic fundamental diagram of homogeneous arterial corridors". In: *Transportmetrica B: Transport Dynamics* 6.4, pp. 286–301. DOI: 10.1080/21680566.2017.1314203. eprint: https://doi.org/10.1080/21680566.2017.1314203. URL: https://doi.org/10.1080/21680566.2017.1314203.

Cats, Oded and Erik Jenelius (2012). "Vulnerability analysis of public transport networks: a dynamic approach and case study for Stockholm". In: *The 5th International Symposium on Transportation Network Reliability (INSTR2012), Hong Kong, 18-19 December, 2012*.

Cats, Oded and Erik Jenelius (2014). "Dynamic vulnerability analysis of public transport networks: mitigation effects of real-time information". In: *Networks and Spatial Economics* 14.3, pp. 435–463.

Chan, Kevin and Steven Farber (2020). "Factors underlying the connections between active transportation and public transit at commuter rail in the Greater Toronto and Hamilton Area". In: *Transportation* 47.5, pp. 2157–2178.

Chen, Anthony et al. (2007). "Network-based accessibility measures for vulnerability analysis of degradable transportation networks". In: *Networks and Spatial Economics* 7.3, pp. 241–256.

Cheng, Yung-Hsiang and Yi-Chun Lin (2018). "Expanding the effect of metro station service coverage by incorporating a public bicycle sharing system". In: *International Journal of Sustainable Transportation* 12.4, pp. 241–252.

Chowdhury, Debashish, Ludger Santen, and Andreas Schadschneider (2000). "Statistical physics of vehicular traffic and some related systems". In: *Physics Reports* 329.4, pp. 199–329. ISSN: 0370-1573. DOI: https://doi.org/10.1016/S0370-1573(99)00117-9. URL: https://www.sciencedirect.com/science/article/pii/S0370157399001179.

Christoforou, Zoi et al. (2021). "Who is using e-scooters and how? Evidence from Paris". In: *Transportation Research Part D: Transport and Environment* 92, p. 102708. ISSN: 1361-9209. DOI: https://doi.org/10.1016/j.trd.2021.102708.

Comi, Antonio, Antonio Polimenia, and Agostino Nuzzolo (2022). "An Innovative Methodology for Micro-Mobility Network Planning". In: *Transportation Research Procedia* 60. New scenarios for safe mobility in urban areasProceedings of the XXV International Conference Living and Walking in Cities (LWC 2021), September 9-10, 2021, Brescia, Italy, pp. 20–27. ISSN: 2352-1465. DOI: https://doi.org/10.1016/j.trpro.2021.12.004.

Cordera, Ruben et al. (2019). *Land Use-Transport Interaction Models*. Ed. by Ruben Cordera et al. London, England: CRC Press.

Crucitti, Paolo, Vito Latora, and Sergio Porta (2006). "Centrality measures in spatial networks of urban streets". In: *Physical Review E* 73.3, p. 036125.

Daganzo, Carlos F and Nikolas Geroliminis (2008). "An analytical approximation for the macroscopic fundamental diagram of urban traffic". In: *Transportation Research Part B: Methodological* 42.9, pp. 771–781.

Di Febbraro, Angela and Nicola Sacco (2016). "Open problems in transportation engineering with connected and autonomous vehicles". In: *Transportation Research Procedia* 14, pp. 2255–2264.

Dios Ortúzar, Juan de, Andrés Iacobelli, and Claudio Valeze (2000). "Estimating demand for a cycle-way network". In: *Transportation Research Part A: Policy and Practice* 34.5, pp. 353–373. ISSN: 0965-8564. DOI: https://doi.org/10.1016/S0965-8564(99)00040-3. URL: https://www.sciencedirect.com/science/article/pii/S0965856499000403.

Erlander, Sven (1977). "Accessibility, entropy and the distribution and assignment of traffic". In: *Transportation Research* 11.3, pp. 149–153. ISSN: 0041-1647. DOI: https://doi.org/10.1016/0041-1647(77)90012-0. URL: https://www.sciencedirect.com/science/article/pii/0041164777900120.

Fagnant, Daniel J. and Kara M. Kockelman (2014). "The travel and environmental implications of shared autonomous vehicles, using agent-based model scenarios". In: *Transportation Research Part C: Emerging Technologies* 40, pp. 1–13. ISSN: 0968-090X. DOI: https://doi.org/10.1016/j.trc.2013.12.001. URL: https://www.sciencedirect.com/science/article/pii/S0968090X13002581.

Fakhrmoosavi, Fatemeh et al. (2020). "Impacts of connected and autonomous vehicles on traffic flow with heterogeneous drivers spatially distributed

over large-scale networks". In: *Transportation research record* 2674.10, pp. 817–830.

Fan, Aihua, Xumei Chen, and Tao Wan (2019). "How have travelers changed mode choices for first/last mile trips after the introduction of bicycle-sharing systems: An empirical study in Beijing, China". In: *Journal of Advanced Transportation* 2019.

Fan, Yingling et al. (2019). "Advancing Transportation Equity: Research and Practice". In.

Fisk, Caroline (1979). "More paradoxes in the equilibrium assignment problem". In: *Transportation Research Part B: Methodological* 13.4, pp. 305–309. ISSN: 0191-2615. DOI: https://doi.org/10.1016/0191-2615(79)90023-7. URL: https://www.sciencedirect.com/science/article/pii/0191261579900237.

Freeman, Linton C, Stephen P Borgatti, and Douglas R White (1991). "Centrality in valued graphs: A measure of betweenness based on network flow". In: *Social networks* 13.2, pp. 141–154.

Frei, Fernando (2006). "Sampling mobility index: Case study in Assis—Brazil". In: *Transportation Research Part A: Policy and Practice* 40.9, pp. 792–799. ISSN: 0965-8564. DOI: https://doi.org/10.1016/j.tra.2005.12.004. URL: https://www.sciencedirect.com/science/article/pii/S0965856405001837.

Friedrich, Bernhard (2016). "The Effect of Autonomous Vehicles on Traffic". In: *Autonomous Driving: Technical, Legal and Social Aspects*. Ed. by Markus Maurer et al. Berlin, Heidelberg: Springer Berlin Heidelberg, pp. 317–334. ISBN: 978-3-662-48847-8. DOI: 10.1007/978-3-662-48847-8_16. URL: https://doi.org/10.1007/978-3-662-48847-8_16.

Geroliminis, Nikolas and Carlos F Daganzo (2008). "Existence of urban-scale macroscopic fundamental diagrams: Some experimental findings". In: *Transportation Research Part B: Methodological* 42.9, pp. 759–770.

Geurs, Karst T, Lissy La Paix, and Sander Van Weperen (2016). "A multi-modal network approach to model public transport accessibility impacts of bicycle-train integration policies". In: *European transport research review* 8.4, pp. 1–15.

Ghiasi, Amir, Xiaopeng Li, and Jiaqi Ma (2019). "A mixed traffic speed harmonization model with connected autonomous vehicles". In: *Transportation Research Part C: Emerging Technologies* 104, pp. 210–233.

Griffin, Greg Phillip and Ipek Nese Sener (2016). "Planning for bike share connectivity to rail transit". In: *Journal of public transportation* 19.2, p. 1.

Guo, Yuanyuan and Sylvia Y He (2020). "Built environment effects on the integration of dockless bike-sharing and the metro". In: *Transportation Research Part D: Transport and Environment* 83, p. 102335.

Hamidi, Zahra, Rosalia Camporeale, and Leonardo Caggiani (2019). "Inequalities in access to bike-and-ride opportunities: Findings for the city of Malmö". In: *Transportation Research Part A: Policy and Practice* 130, pp. 673–688.

He, Zhenggang, Jing-Ni Guo, and Jun-Xiang Xu (2019). "Cascade failure model in multimodal transport network risk propagation". In: *Mathematical Problems in Engineering* 2019.

Heinen, Eva and Wendy Bohte (2014). "Multimodal commuting to work by public transport and bicycle: Attitudes toward mode choice". In: *Transportation Research Record* 2468.1, pp. 111–122.

Hensher, David A., Peter Stopher, and Philip Bullock (2003). "Service quality—developing a service quality index in the provision of commercial bus contracts". In: *Transportation Research Part A: Policy and Practice* 37.6, pp. 499–517. ISSN: 0965-8564. DOI: https://doi.org/10.1016/S0965-8564(02)00075-7. URL: https://www.sciencedirect.com/science/article/pii/S0965856402000757.

Janasz, Tomasz (2017). *Paradigm shift in urban mobility: towards factor 10 of automobility*. Springer.

Ji, Yanjie et al. (2018). "Exploring spatially varying influences on metro-bikeshare transfer: A geographically weighted poisson regression approach". In: *Sustainability* 10.5, p. 1526.

Jiang, Yangsheng et al. (2021). "A cellular automata model for mixed traffic flow considering the driving behavior of connected automated vehicle platoons". In: *Physica A: Statistical Mechanics and its Applications* 582, p. 126262.

Kaparias, I, MGH Bell, and M Tomassini (2011). "Key performance indicators for traffic management and intelligent transport systems". In: *Isis* 14.06.

Karbasi, Amirhosein, Behzad Bamdad Mehrabani, and Mahmoud Saffarzadeh (2020). "Impact of Connected and Automated Vehicles on Capacity of single lane road based on macroscopic fundamental diagram". In: *2nd Conference on Environment, Civil, Architecture and Urban Development*.

Kassens-Noor, Eva et al. (2020). "Sociomobility of the 21st century: Autonomous vehicles, planning, and the future city". In: *Transport Policy* 99, pp. 329–335. ISSN: 0967-070X. DOI: https://doi.org/10.1016/j.tranpol.2020.08.022. URL: https://www.sciencedirect.com/science/article/pii/S0967070X20303292.

Keegan, Owen and Margaret O'Mahony (2003). "Modifying pedestrian behaviour". In: *Transportation Research Part A: Policy and Practice* 37.10, pp. 889–901. ISSN: 0965-8564. DOI: https://doi.org/10.1016/S0965-8564(03)00061-2. URL: https://www.sciencedirect.com/science/article/pii/S0965856403000612.

Kim, Kyung-Hwan and Donghyung Yook (2015). "AN ANALYSIS OF EXPECTED EFFECTS OF THE AUTONOMOUS VEHICLES ON TRANSPORT AND LAND USE IN KOREA". In.

Krizek, Kevin J and Eric W Stonebraker (2011). "Assessing options to enhance bicycle and transit integration". In: *Transportation Research Record* 2217.1, pp. 162–167.

Kröger, Fabian (2016). "Automated Driving in Its Social, Historical and Cultural Contexts". In: *Autonomous Driving: Technical, Legal and Social Aspects*. Ed. by Markus Maurer et al. Berlin, Heidelberg: Springer Berlin Heidelberg, pp. 41–68. ISBN: 978-3-662-48847-8. DOI: 10.1007/978-3-662-48847-8_3. URL: https://doi.org/10.1007/978-3-662-48847-8_3.

Kutgun, Hakan, Vivian Duc Pont, and Henry Janzen (2018). "Effects of Future Connected Autonomous Vehicles on Freeway Congestion using Fuzzy Cognitive Mapping". In: *2018 Portland International Conference on Management of Engineering and Technology (PICMET)*, pp. 1–7. DOI: 10.23919/PICMET.2018.8481991.

Lavasani, Mohammad, Xia Jin, and Yiman Du (2016). "Market penetration model for autonomous vehicles on the basis of earlier technology adoption experience". In: *Transportation Research Record* 2597.1, pp. 67–74.

Leclercq, Ludovic, Nicolas Chiabaut, and Béatrice Trinquier (2014). "Macroscopic fundamental diagrams: A cross-comparison of estimation methods". In: *Transportation Research Part B: Methodological* 62, pp. 1–12.

Lee, Der-Horng, Lan Wu, and Qiang Meng (2006). "Equity based land-use and transportation problem". In: *Journal of Advanced Transportation* 40.1, pp. 75–93.

Lee, Jaeyeong, Keechoo Choi, and Yountaik Leem (2016). "Bicycle-based transit-oriented development as an alternative to overcome the criticisms of the conventional transit-oriented development". In: *International Journal of Sustainable Transportation* 10.10, pp. 975–984.

Li, Xin et al. (2020). "An integrated approach for optimizing bi-modal transit networks fed by shared bikes". In: *Transportation research part E: logistics and transportation review* 141, p. 102016.

Lin, Diao et al. (2019). "The analysis of catchment areas of metro stations using trajectory data generated by dockless shared bikes". In: *Sustainable Cities and Society* 49, p. 101598.

Lin, Jingyi and Yifang Ban (2013). "Complex network topology of transportation systems". In: *Transport reviews* 33.6, pp. 658–685.

Litman, Todd (2020). "Autonomous vehicle implementation predictions: Implications for transport planning". In.

— (2021a). "Evaluating Transportation Equity: Guidance for Incorporating Distributional Impacts in Transport Planning". In: *Victoria Transport Policy Institute*.

— (2021b). *New Mobilities: Smart Planning for Emerging Transportation Technologies*. Island Press.

Little, Arthur (2019). *Capacity effect of autonomous vehicles | Arthur D. Little*. https://www.adlittle.com/en/insights/viewpoints/capacity-effect-autonomous-vehicles. Accessed: 2022-10-22 06:21:20.

Liu, Baoding (1998). "Stackelberg-Nash equilibrium for multilevel programming with multiple followers using genetic algorithms". In: *Computers & Mathematics with Applications* 36.7, pp. 79–89.

Liu, Yang et al. (2020). "Understanding the determinants of young commuters' metro-bikeshare usage frequency using big data". In: *Travel behaviour and society* 21, pp. 121–130.

Liu, Yangzexi et al. (2017). "Characteristic analysis of mixed traffic flow of regular and autonomous vehicles using cellular automata". In: *Journal of Advanced Transportation* 2017.

Loder, Allister et al. (2019). "Understanding traffic capacity of urban networks". In: *Scientific reports* 9.1, pp. 1–10.

Louf, Rémi and Marc Barthelemy (2013). "Modeling the polycentric transition of cities". In: *Physical review letters* 111.19, p. 198702.

Lu, Qing-Chang and Shan Lin (2019). "Vulnerability analysis of urban rail transit network within multi-modal public transport networks". In: *Sustainability* 11.7, p. 2109.

Luo, Ding, Oded Cats, and Hans van Lint (2020). "Can passenger flow distribution be estimated solely based on network properties in public transport systems?" In: *Transportation* 47.6, pp. 2757–2776.

Mahmassani, Hani S (2016). "50th anniversary invited article—Autonomous vehicles and connected vehicle systems: Flow and operations considerations". In: *Transportation Science* 50.4, pp. 1140–1162.

Marqués, Ricardo et al. (2015). "When cycle paths are not enough: Seville's bicycle-PT project". In: *Urban Transport* 21.146, pp. 79–91.

Martens, Karel (2007). "Promoting bike-and-ride: The Dutch experience". In: *Transportation Research Part A: Policy and Practice* 41.4, pp. 326–338.

Martin-Gasulla, Marilo, Peter Sukennik, and Jochen Lohmiller (2019). "Investigation of the Impact on Throughput of Connected Autonomous Vehicles with Headway Based on the Leading Vehicle Type". In: *Transportation Research Record* 2673.5, pp. 617–626. DOI: 10.1177/0361198119839989. eprint: https://doi.org/10.1177/0361198119839989. URL: https://doi.org/10.1177/0361198119839989.

Maximcsuk, Balázs, Qiong Lu, and Tamás Tettamanti (2019). "Determining Maximum Achievable Flows of Autonomous Vehicles Based on Macroscopic Fundamental Diagram". In: *Perner's Contacts, Special Issue:" 36th International Colloquium on Advanced Manufacturing and Repair Technologies in Vehicle Industry*, pp. 192–199.

Mena-Oreja, Jesús, Javier Gozalvez, and Miguel Sepulcre (2018). "Effect of the Configuration of Platooning Maneuvers on the Traffic Flow under Mixed Traffic Scenarios". In: *2018 IEEE Vehicular Networking Conference (VNC)*, pp. 1–4. DOI: 10.1109/VNC.2018.8628381.

Meng, Qiang and Hai Yang (2002). "Benefit distribution and equity in road network design". In: *Transportation Research Part B: Methodological* 36.1, pp. 19–35.

Milakis, Dimitris et al. (2017). "Development and transport implications of automated vehicles in the Netherlands: Scenarios for 2030 and 2050". In: *European Journal of Transport and Infrastructure Research* 17.1.

Miramontes, Montserrat et al. (2017). "Impacts of a multimodal mobility service on travel behavior and preferences: user insights from Munich's first Mobility Station". In: *Transportation* 44.6, pp. 1325–1342.

Mouronte-López, Mary Luz (2021). "Analysing the vulnerability of public transport networks". In: *Journal of Advanced Transportation* 2021.

Narayanan, Santhanakrishnan, Emmanouil Chaniotakis, and Constantinos Antoniou (2020). "Factors affecting traffic flow efficiency implications of connected and autonomous vehicles: A review and policy recommendations". In: *Advances in Transport Policy and Planning* 5, pp. 1–50.

Nicolas, J-P, Pascal Pochet, and Hélène Poimboeuf (2003). "Towards sustainable mobility indicators: application to the Lyons conurbation". In: *Transport policy* 10.3, pp. 197–208.

Nigro, Marialisa et al. (2022). "Exploiting floating car data to derive the shifting potential to electric micromobility". In: *Transportation Research Part A: Policy and Practice* 157, pp. 78–93. ISSN: 0965-8564. DOI: https://doi.org/10.1016/j.tra.2022.01.008.

O, V. (1936). *Robot Car to Thread Way in Traffic Today*. Schenectady Gazette, 24 October 1936, p. 7. Accessed: 2022-10-22 06:24:13.

Oppenheim, Nobert (1995). *Urban travel demand modeling*. en. Nashville, TN: John Wiley & Sons.

Patella, S. M., F. Aletta, and L. Mannini (2019). "Assessing the impact of Autonomous Vehicles on urban noise pollution". In: *Noise Mapp* 6, pp. 72–82. DOI: https://doi.org/10.1515/noise-2019-0006.

Payre, William, Julien Cestac, and Patricia Delhomme (2014). "Intention to use a fully automated car: Attitudes and a priori acceptability". In: *Transportation research part F: traffic psychology and behaviour* 27, pp. 252–263.

Pritchard, John P et al. (2019). "Potential impacts of bike-and-ride on job accessibility and spatial equity in São Paulo, Brazil". In: *Transportation research part A: policy and practice* 121, pp. 386–400.

Putman, Stephen (2013). *Integrated urban models volume 1: Policy analysis of transportation and land use (RLE: The City)*. Routledge.

Qin, Huanmei et al. (2018). "Effects of perception on public bike-and-ride: A survey under complex, multifactor mode-choice scenarios". In: *Transportation research part F: traffic psychology and behaviour* 54, pp. 264–275.

Qiu, Esta et al. (2022). "Recalibration of the BPR function for the strategic modelling of connected and autonomous vehicles". In: *Transportmetrica B: transport dynamics* 10.1, pp. 779–800.

Research, Precedence (2020). *Autonomous Vehicle Market Size, Share, Trends, Report 2022-2030*. https://www.precedenceresearch.com/autonomous-vehicle-market.

Rodier, C. et al. (2010). "Equity analysis of land use and transport plans using an integrated spatial model." In: *Proceedings of the Transportation Research Board Annual Meeting*. Accessed: 2022-10-22 06:15:58.

S, Bills T (2013). *Enhancing Transportation Equity Analysis for Long-Range Planning and Decision Making*.

SAE (2014). *J3016: Taxonomy and Definitions for Terms Related to Driving Automation Systems for On-Road Motor Vehicles SAE International*. Accessed: 2022-10-22 06:18:39.

Sagaris, Lake, Ignacio Tiznado-Aitken, and Stefan Steiniger (2017). "Exploring the social and spatial potential of an intermodal approach to transport planning". In: *International Journal of Sustainable Transportation* 11.10, pp. 721–736.

Sagir, Fasil and Satish V Ukkusuri (2018). "Mobility impacts of autonomous vehicle systems". In: *2018 21st International Conference on Intelligent Transportation Systems (ITSC)*. IEEE, pp. 485–490.

Schröder, Jörn-Ole et al. (2014). "Developing and evaluating intermodal e-sharing services–a multi-method approach". In: *Transportation Research Procedia* 4, pp. 199–212.

Sentinel, Milwaukee (1926). "Phantom Auto'will tour city". In: *The Milwaukee Sentinel* 4.

Shao, Yunli and Zongxuan Sun (2021). "Energy-Efficient connected and automated vehicles: real-time traffic prediction-enabled co-optimization of vehicle motion and powertrain operation". In: *IEEE Vehicular Technology Magazine* 16.3, pp. 47–56.

Staricco, Luca et al. (2018). "Toward Policies to Manage the Impacts of Autonomous Vehicles on the City: A Visioning Exercise". In: *Sustainability* 5222. DOI: https://doi.org/10.3390/su11195222.

Stern, Raphael E. et al. (2018). "Dissipation of stop-and-go waves via control of autonomous vehicles: Field experiments". In: *Transportation Research Part C: Emerging Technologies* 89, pp. 205–221. ISSN: 0968-090X. DOI: https://doi.org/10.1016/j.trc.2018.02.005. URL: https://www.sciencedirect.com/science/article/pii/S0968090X18301517.

Szeto, Wai Yuen et al. (2015). "A sustainable road network design problem with land use transportation interaction over time". In: *Networks and Spatial Economics* 15.3, pp. 791–822.

Talebpour, Alireza and Hani S Mahmassani (2015). *Influence of autonomous and connected vehicles on stability of traffic flow*. Tech. rep.

Tavassoli, Kayhan and Mohammad Tamannaei (2020). "Hub network design for integrated Bike-and-Ride services: A competitive approach to reducing automobile dependence". In: *Journal of Cleaner Production* 248, p. 119247.

Transportation, National Highway Department of and Traffic Safety Administration (2022). *Electronic codes of federal Regulations, Transportation: 571.121, Standard No. 121, Section 5.3.1*.

Wang, Ziyulong et al. (2020). "Unraveling the hierarchy of public transport networks". In: *2020 IEEE 23rd International Conference on Intelligent Transportation Systems (ITSC)*. IEEE, pp. 1–6.

Wegener, Michael and Franz Fürst (2004). "Land-use transport interaction: State of the art". In: *Available at SSRN 1434678*.

Wetmore (2003). "Driving the dream. The history and motivations behind 60 years of automated highway systems in America". In: *Automotive History Review* 7.2, pp. 4–19. DOI: 10.1016/0004-3702(84)90008-0.

Wilson, Alan Geoffrey (1998). "Land-use/transport interaction models: Past and future". In: *Journal of transport economics and policy*, pp. 3–26.

Wu, Xueying et al. (2019). "Measuring the destination accessibility of cycling transfer trips in metro station areas: A big data approach". In: *International journal of environmental research and public health* 16.15, p. 2641.

Xie, Hairuo et al. (2019). "Quantifying the impact of autonomous vehicles using microscopic simulations". In: *Proceedings of the 12th ACM SIGSPATIAL International Workshop on Computational Transportation Science*. Chicago IL USA: ACM.

Yap, Menno et al. (2019). "Where shall we sync? Clustering passenger flows to identify urban public transport hubs and their key synchronization priorities". en. In: *Transp. Res. Part C Emerg. Technol.* 98, pp. 433–448.

Ye, Lanhang, Toshiyuki Yamamoto, and Takayuki Morikawa (2018). "Heterogeneous traffic flow dynamics under various penetration rates of connected and autonomous vehicle". In: *2018 21st International Conference on Intelligent Transportation Systems (ITSC)*. IEEE, pp. 555–559.

Yoshioka, Naoki, Takashi Shimada, and Nobuyasu Ito (2017). "Macroscopic fundamental diagram in simple model of urban traffic". In: *Artificial Life and Robotics* 22.2, pp. 217–221.

Yoshioka, Naoki et al. (2019). "Macroscopic fundamental diagram in simple street networks". In: *Journal of Computational Social Science* 2.1, pp. 85–95.

Zhao, Pengjun and Shengxiao Li (2017). "Bicycle-metro integration in a growing city: The determinants of cycling as a transfer mode in metro station areas in Beijing". In: *Transportation research part A: policy and practice* 99, pp. 46–60.

Zhao, Yong and Kara M Kockelman (2018). "Anticipating the regional impacts of connected and automated vehicle travel in Austin, Texas". en. In: *J. Urban Plan. Dev.* 144.4.

Zheng, Fangfang et al. (2019). "Traffic oscillation using stochastic lagrangian dynamics: Simulation and mitigation via control of autonomous vehicles". In: *Transportation Research Record* 2673.7, pp. 1–11.

Zhong, Chen et al. (2014). "Detecting the dynamics of urban structure through spatial network analysis". In: *International Journal of Geographical Information Science* 28.11, pp. 2178–2199.

Zmud, Johanna et al. (2018). *Updating Regional Transportation Planning and Modeling Tools to Address Impacts of Connected and Automated Vehicles, Volume 2: Guidance*. Tech. rep.

Zuo, Ting et al. (2020). "First-and-last mile solution via bicycling to improving transit accessibility and advancing transportation equity". In: *Cities* 99, p. 102614.